A DYNAMIC LOAD SHEDDING SCHEME FOR MAINTAINING SYSTEM FREQUENCY STABILITY WITH THE INCREASING RENEWABLE ENERGY PENETRATION

B H M S T Herath

178612G

Degree of Master of Science

Department of Electrical Engineering

University of Moratuwa
Sri Lanka

August 2021

A DYNAMIC LOAD SHEDDING SCHEME FOR MAINTAINING SYSTEM FREQUENCY STABILITY WITH THE INCREASING RENEWABLE ENERGY PENETRATION

B H M S T Herath

178612G

Thesis/ Dissertation was submitted to the Department of Electrical Engineering of the University of Moratuwa in partial fulfillment of the requirements for the Degree of Master of Science in Electrical Installation

August 2021

Supervisor: Dr. L N W Arachchige

DECLARATION OF THE CANDIDATE AND SUPERVISORS

I declare that this is my own work and this thesis/dissertation does not incorporate without acknowledgement any material previously submitted for a Degree or Diploma in any other University or institute of higher learning and to the best of my knowledge and belief it does not contain any material previously published or written by another person except where the acknowledgement is made in the text.

Also, I hereby grant to University of Moratuwa the non-exclusive right to reproduce and distribute my thesis/dissertation, in whole or part in print, electronic or other medium. I retain the right to use this content in whole or part in future works (Such as articles or books).

Signature:

.Shamalka……. Date: 25-08-2021

B. H. M. S. T. Herath

The above candidate has carried out research for the Masters Dissertation under my supervision.

Signature of the supervisor:

……. Date: 25-08-2021

Dr. L. N. Widanagama Arachchige

ABSTRACT

Renewable energy power plants, especially grid connected solar and wind generation units are displacing the conventional generator stations with rotating machines with inertia. In Sri Lanka, renewable energy generation has begun to increase significantly. The total solar and wind energy penetration is 13% for 2020 and according to the least cost long term generation expansion plan 2018 – 2037 of Ceylon Electricity Board, this amount will be 47% by 2030. With the increased penetration of wind and solar energy generations units having no rotational inertia, there would be a variation in operational and dynamic characteristics in the power system. The power generation of solar power plants varies drastically with the cloud cover. The power output of solar and wind energy varies with their intermittent nature and as a result of it, the system frequency deviations becomes faster and risking the stability of power system as well. This study is focused on evaluating the frequency stability of Sri Lankan power system at major contingencies during the day-peak periods having maximum wind and solar generation.

In Sri Lanka, static under frequency load shedding scheme is used to restore the stability of power system after major disturbances. This load shedding scheme is initiated based on the rate of change of frequency and under frequency settings, which shed pre-determined load amounts at frequency set points in six stages. This thesis analyzes the frequency response of Sri Lankan power system with the maximum wind and solar generation for year 2030 to evaluate the performance of the present load shedding scheme in maintaining system stability. A dynamic load shedding scheme can provide quick and optimal solution by using real-time data of operating conditions. Therefore, this research is proposing a new load shedding scheme based on dynamic load shedding method to improve the frequency stability of Sri Lankan power system while absorbing maximum solar and wind power into the system.

Keywords: Static under frequency load shedding scheme, Renewable energy penetration, Solar power, Wind power, Dynamic load shedding scheme, Power system stability, Frequency stability

ACKNOWLEDGEMENT

First and foremost, I would like to express my sincere gratitude to my supervisor Dr. L. N. Widanagama Arachchige, for guiding me to develop this research concept and successful journey so far up to preparation of final thesis. And my heartfelt thanks for her motivation, enthusiasm and continuous support throughout my research. It is a great experience to having work with a supervisor who is having an immense knowledge related to my research work. If not for her blessings and excellent guidance, the research work would not success.

Also, I would like to express my sincere gratitude to Dr. H. M. Wijekoon Banda, Chief engineer, Transmission Planning Unit, Ceylon Electricity Board for having provided me the permission to use PSS/E software to do the project successfully and for spending his valuable time to sharing his knowledge and experience, all the electrical engineers of Transmission Planning Unit, Ceylon Electricity Board for their support and valuable instructions for successful completion of my research.

I take this opportunity to extend my sincere thanks to all Engineers of System Control Center, Ceylon Electricity Board, who supported me to collect all the data required for this research work.

Further, it is a great pleasure to remember my masters' coordinator Dr. Prasad and all of my lecturers of University of Moratuwa for providing useful suggestions and valuable advices in progress reviews.

Finally, I would like to thank and express my heartfelt gratitude to my loving husband and my parents for their unconditional support, sacrifice and understanding in supporting me always.

TABLE OF CONTENTS

DECLARATION OF THE CANDIDATE AND SUPERVISORS i

ABSTRACT ii

ACKNOWLEDGEMENT iii

TABLE OF CONTENTS iv

LIST OF FIGURES ix

CHAPTER 1 1

INTRODCUTION 1

1.1 Present Sri Lankan Power System 1

1.1.1 Energy Generation 1

1.1.2 Installed Capacity 2

1.1.3 Demand Growth 3

1.2 Problem Statement 3

1.3 Research Objectives 6

1.4 Thesis Overview 7

CHAPTER 2 8

LITERATURE REVIEW 8

2.1 Power System Stability 8

2.2 Frequency Control Basics 9

2.2.1 Primary Control 11

2.2.2 Secondary Control 11

2.2.3 Tertiary Control 11

2.3 Load Shedding Schemes 11

2.3.1 Methods of Load Shedding 12

2.3.2 Present Load Shedding Scheme in CEB 13

2.2.3 Disadvantages of Traditional Load Shedding Schemes 15

2.3.4 Dynamic Load shedding Schemes 17
2.4 Selection of Study Year 19
2.5 Effects of Renewable Energy on Power System Stability 25
CHAPTER 3 27
MODELING APPROACH 27
3.1 Power System Modeling 27
3.1.1 Overview of PSS/E 28
3.1.2 Steady State and Dynamic Analysis 28
3.2 Modeling of 2019 Power System 29
3.2.1 2019 Power System 30
3.3 PSS/E Models used for 2019 Power System Model 33
3.3.1 Power Flow Data Entry 33
3.3.2 Power System Dynamic Modeling 36
CHAPTER 4 62
MODEL VALIDATION 62
4.1 Validation of 2019 Power System Model 63
4.2 Modeling of 2030 Power System 69
4.2.1 Droop Settings, Active Power and Reactive Power Limits 70
4.2.2 Pumped Storage Power Plant Development 71
4.2.3 Frequency Limitation Settings 71
4.3 Simulation Scenarios of 2030 Power System 73
4.3.1 Generation Dispatch Scenarios 73
4.3.2 Demand Scenarios 74
4.3.3 Proposed Simulation Scenarios 79
CHAPTER 5 81
ANALYSIS OF PRESENT LOAD SHEDDING SCHEME 81
5.1 Scenario 1 - Hydro Maximum Day Peak (HMDP) 81

Case 1.1: Tripping 275 MW Loaded Lakvijaya 1 Unit (Loosing 6% Generation – Tripping Single Unit)....84

Case 1.2: Tripping 275 MW Loaded Lakvijaya 2 Units (Loosing 12% Generation – Tripping Two Units)....85

Case 1.3: Tripping 275 MW Lakvijaya 3 Units and 140 MW Sampoor 1 Unit (1,115 MW) (Loosing 24% Generation – Tripping Two Plants)....86

5.2 Scenario 2 - Thermal Maximum Day Peak (TMDP)....87

Case 2.1: Tripping 275 MW Loaded Lakvijaya 1 Unit (Loosing 6% Generation – Tripping Single Unit)....90

Case 2.2: Tripping 275 MW Loaded Lakvijaya 2 Units (Loosing 12% Generation – Tripping Two Units)....91

Case 2.3: Tripping 275 MW Loaded Lakvijaya 3 Units and 270 MW Loaded Sampoor 2 Units (1,365 MW) (Loosing 30% Generation – Tripping Two Plants)....92

Case 2.4: Tripping 275 MW Loaded Lakvijaya 5 Units (Loosing 31% Generation – Tripping Single Plant) (1375 MW)....93

5.3 Scenario 3 - Renewable Maximum Day Peak (RMDP)....95

Case 3.1: Tripping 200 MW Loaded 2 Units and 150 MW Loaded 1 Unit in Lakvijaya (Loosing 11.5% Generation – Tripping Three Units)....99

Case 3.2: Tripping 200 MW, 150 MW Loaded Lakvijaya 3 Units and 150 MW Loaded Sampoor 1 Unit (700 MW) (Loosing 15% Generation – Tripping Two Plants)....102

Case 3.3: Tripping 200 MW, 150 MW Lakvijaya 3 Units and 140 MW Sampoor 1 Unit and 45 MW Pumped Storage 3 Units (835 MW) (Loosing 18% Generation – Tripping Three Plants)....103

CHAPTER 6....105

PROPOSED LOAD SHEDDING SCHEME....105

6.1 Implementation of Proposed Load Shedding Scheme....108

6.2 Developing the Program Algorithm and Coding in PSS/E....112

CHAPTER 7....119

ANALYSIS OF PROPOSED LOAD SHEDDING SCHEME....119

7.1 Scenario 1 - Hydro Maximum Day Peak (HMDP) 119

Case 1.4: Tripping 275 MW Loaded Lakvijaya 3 Units (Loosing 17% Generation – Tripping Single Plant) 119

Case 1.5: Tripping 275 MW Loaded Lakvijaya 3 Units and 140 MW Loaded Sampoor 1 Unit (965 MW) (Loosing 21% Generation – Tripping Two Plants) 120

Case 1.6: Tripping Lakvijaya 3 Units, Sampoor 1 Unit and Upper Kothmale 2 Units and Samanalawewa 2 Units (1235 MW) (Loosing 27% Generation – Tripping Four Plants) .121

Case 1.7: Total Wind Power Plants Outage (976.9 MW) (Loosing 21% Generation – Tripping Single Plant) 123

Case 1.8: Tripping Lakvijaya 3 Units and 50% of All Solar Power Plants (1,140 MW) (Loosing 25% Generation – Tripping Two Plants) 123

Case 1.9: Tripping Lakvijaya 3 Units and 50% of All Wind Power Plants (1,375MW) (Loosing 29% Generation – Tripping Two Plants) 124

7.2 Scenario 2 - Thermal Maximum Day Peak (TMDP) 127

Case 2.5: Total Solar Power Plants Outage (1,018 MW) (Loosing 23% Generation – Tripping Single Plant) 127

Case 2.6: Tripping Lakvijaya 5 Units and 50% of All Wind Power Plants (1,375MW) (Loosing 29% Generation – Two Plants Trip) 127

Case 2.7: Tripping Lakvijaya 5 Units and Total Wind Power Plants Outage (1,933 MW) (Loosing 43% Generation – Two Plants Trip) 128

Case 2.8: Tripping Lakvijaya 5 Units and Total Solar Power Plants Outage (2,463 MW) (Loosing 43% Generation – Two Plants Trip) 129

7.3 Scenario 3 - Renewable Maximum Day Peak (RMDP) 132

Case 3.4: Tripping 200 MW and 150 MW Loaded Lakvijaya 3 Units (Loosing 11.5% Generation – Single Plant Trip) 132

Case 3.5: Tripping 200 MW, 150 MW Lakvijaya 3 Units and 140 MW Sampoor 1 Unit and 45 MW Pumped Storage 3 Units (835 MW) (Loosing 18% Generation – Three Plants Trip) 133

Case 3.6: Tripping Lakvijaya 3 Units and Total Wind Power Plants Outage (1,527 MW) (Loosing 33% Generation – Two Plants Trip) 134

Case 3.7: Tripping Lakvijaya 3 Units and Total Solar Power Plants Outage (1,628 MW) (Loosing 36% Generation – Two Plants Trip) 134
CHAPTER 8 137
CONCLUSION AND FUTURE WORKS 137
8.1 Conclusion 137
8.2 Future Works and Limitations 139
REFERENCE LIST 141
APPENDICS 144
APPENDIX B 145
APPENDIX C 146
APPENDIX D 150
APPENDIX E 151

LIST OF FIGURES

Figure 1: Electricity Generation Mix 2019 2
Figure 2: Variation of daily load curve for the years 2011 to 2018 [3] 3
Figure 3: Typical Activation Time of Frequency Control Reserves [7] 10
Figure 4: Total Renewable Energy Capacity Development [3] 21
Figure 5: Load Model in PSS/E [24] 34
Figure 6: Fixed Bus Shunt Model in PSS/E [24] 34
Figure 7: Generator Model in PSS/E [24] 34
Figure 8: Generator model used in load flow studies [24] 35
Figure 9: Transformer Model in PSS/E [24] 35
Figure 10: Generator model used for dynamic simulation [24] 37
Figure 11: Salient Pole Synchronous Generator Model – GENSAL [24] 38
Figure 12: Hydraulic and Governor Model – HYGOV [24] 40
Figure 13: Hydro Turbine and Governor – PIDGOV [24] 41
Figure 14: Simplified Excitation System [24] 42
Figure 15: Bus or Solid fed SCR bridge excitation system [24] 44
Figure 16: IEEE Type AC1A Excitation System [24] 44
Figure 17: IEEE Type ST1A Excitation System [24] 46
Figure 18: Round Rotor Synchronous Generator Model – GENROU [24] 48
Figure 19: Steam Turbine - Governor Model [24] 49
Figure 20: Gas Turbine-Governor Model – GAST [24] 50
Figure 21: Woodward Diesel Governor [24] 51
Figure 22: IEEE Type ST1 Excitation System [24] 52
Figure 23: Representation of WT4 Generator connected to the grid through the power converter [24] 53
Figure 24: WT4 Connectivity Diagram [24] 54
Figure 25: WT4G1 Wind Generator/Converter Model [24] 55
Figure 26: WT4E1 Electrical Control Model [24] 55
Figure 27: PV Connectivity Diagram [24] 57
Figure 28: PVGU1 Power Converter/Generator Model [24] 57

Figure 29: Block Diagram of PVEU1 Electrical Control Model [24] 58
Figure 30: Representation of Block Diagram of CLODAL Load Model [24] 60
Figure 31: BEN Recording of the tripping of Kelanitissa GT 07 generator 65
Figure 32: Frequency Response of 220kV Kelanitissa transmission line 1 as recorded in BEN Recorder 66
Figure 33: System frequency Variation of tripping of Kelanitissa GT 07 generator 67
Figure 34: Comparison of year 2019 and 2030 Transmission Networks of Sri Lanka .. 69
Figure 35: The total solar PV production of about 200 days in 2030 77
Figure 36: Active power generation of selected solar power plants in HMDP scenario 83
Figure 37: Frequency Response of Tripping 275 MW Loaded Lakvijaya 1 Unit in HMDP scenario 84
Figure 38: Frequency Response of Tripping 275 MW Loaded Lakvijaya 2 Units in HMDP scenario 85
Figure 39: Frequency Response of Tripping 275 MW Lakvijaya 3 Units and 140 MW Sampoor 1 Unit (1115 MW) in HMDP scenario 86
Figure 40: Active power generation of selected solar power plants in TMDP scenario. 90
Figure 41: Frequency Response of Tripping 275 MW Loaded Lakvijaya 1 Unit in TMDP scenario 91
Figure 42: Frequency Response of Tripping 275 MW Loaded Lakvijaya 2 Units in TMDP scenario 92
Figure 43: Frequency Response of Tripping 275 MW Loaded Lakvijaya 3 Units and 270 MW Loaded Sampoor 2 Units in TMDP scenario 93
Figure 44: Frequency Response Tripping 275 MW Loaded Lakvijaya 5 Units in TMDP scenario 94
Figure 45: Active power generation of all solar power plants in RMDP scenario 98
Figure 46: Active power generation of selected wind power plants in RMDP scenario 99
Figure 47: Frequency Response of Tripping 200 MW Loaded 2 Units and 150 MW Loaded 1 Unit in Lakvijaya at 50 s in RMDP scenario 100
Figure 48: Frequency Response of Tripping 200 MW Loaded 2 Units and 150 MW Loaded 1 Unit in Lakvijaya at 3 s in RMDP scenario 101

Figure 49: Frequency Response of Tripping 200 MW, 150 MW Loaded Lakvijaya 3 Units and 150 MW Loaded Sampoor 1 Unit at 50 s in RMDP scenario 102
Figure 50: Frequency Response of Tripping 200 MW, 150 MW Loaded Lakvijaya 3 Units and 150 MW Loaded Sampoor 1 Unit and 45 MW Pumped Storage 3 Units at 50 s in RMDP scenario 103
Figure 51: Basic implementation of proposed load shedding scheme 107
Figure 52: Algorithm of proposed load shedding scheme 111
Figure 53: Developed Python Code in PSS/E – Code Initialization 112
Figure 54: Developed Python Code in PSS/E – Adding Channels and Initialization... 113
Figure 55: Developed Python Code in PSS/E – Data Retrieval 114
Figure 56: Developed Python Code in PSS/E – Insert Retrieved Data into Lists 114
Figure 57: Developed Python Code in PSS/E – Power Difference Calculation 115
Figure 58: Developed Python Code in PSS/E –Frequency Deviation Calculation..... 115
Figure 59: Developed Python Code in PSS/E – Calculation Load generation is given 116
Figure 60: Developed Python Code in PSS/E – Calculation of Load amount to be shed 116
Figure 61: Developed Python Code in PSS/E – Load Shedding loop 118
Figure 62: Tripping 275 MW Loaded Lakvijaya 3 Units in HMDP scenario 119
Figure 63: Tripping 275 MW Loaded Lakvijaya 3 Units and 140 MW Loaded Sampoor 1 in HMDP scenario 120
Figure 64: Tripping Lakvijaya 3 Units, Sampoor 1 Unit and Upper Kothmale 2 Units and Samanalawewa 2 Units 121
Figure 65: Total Wind Power Plants Outage in HMDP scenario 123
Figure 66: Tripping Lakvijaya 3 Units and 50% of All Solar Power Plants in HMDP scenario 124
Figure 67: Tripping Lakvijaya 3 Units and 50% of All Wind Power Plants in HMDP scenario 125
Figure 68: Total Solar Power Plants Outage in TMDP scenario 127
Figure 69; Tripping Lakvijaya 5 Units and 50% of All Wind Power Plants in TMDP scenario 128

Figure 70: Tripping Lakvijaya 5 Units and Total Wind Power Plants Outage in TMDP scenario 129
Figure 71: Tripping Lakvijaya 5 Units and Total Solar Power Plants Outage in TMDP scenario 130
Figure 72: Tripping 200 MW and 150 MW Loaded Lakvijaya 3 Units in RMDP scenario 132
Figure 73: Tripping 200 MW, 150 MW Lakvijaya 3 Units and 140 MW Sampoor 1 Unit and 45 MW Pumped Storage 3 Units in RMDP scenario 133
Figure 74: Tripping Lakvijaya 3 Units and Total Wind Power Plants Outage in RMDP scenario 134
Figure 75: Tripping Lakvijaya 3 Units and Total Solar Power Plants Outage in RMDP scenario 135

LIST OF TABLES

Table 1: Allowable Maximum Frequency Variation [5] 8
Table 2: Under Frequency Load Shedding Scheme in CEB as of January 2020 14
Table 3: Projected Future Development of ORE [3] 22
Table 4: Large Scale Solar and Wind Power Plants in 2030 model 23
Table 5: Base Demand Forecast for the years 2020 – 2044 [3] 24
Table 6: Hydro and ORE Power Plants (Existing and Committed) [3] 31
Table 7: Thermal Power Plants (Existing and Committed) [3] 32
Table 8: Other Renewable Energy (ORE) Capacities (Existing) [3] 32
Table 9: Existing Wind Power Plants 33
Table 10: Existing Solar Power Plants 33
Table 11: Parameters of GENSAL Model [24] 38
Table 12: Parameters of HYGOV Model [24] 39
Table 13: Parameters of PIDGOV Model [24] 41
Table 14: Parameters of Simplified Excitation System Model [24] 43
Table 15: Parameters of Bus or Solid Fed SCR Bridge Excitation System Model [24]. 43
Table 16: Parameters of IEEE Type AC1A Excitation System Model [24] 45
Table 17: Parameters of the IEEE Type ST1A Excitation System Model [24] 46
Table 18: Parameters of GENROU Model [24] 47
Table 19: Parameters of Steam Turbine - Governor Model [24] 49
Table 20: Parameters of GAST Model [24] 50
Table 21: Parameters of Woodward Diesel Governor Model [24] 51
Table 22: Parameters of IEEE Type ST1 Excitation System Model [24] 52
Table 23: Parameters of WT4G1 Wind Generator/Converter Model [24] 54
Table 24: Parameters of WT4E1 Electrical Control Model [24] 56
Table 25: Parameters of PANELU1 (I-P characteristics) [24] 59
Table 26: Parameters of IRRADU1 (PV Irradiance profile) [24] 59
Table 27: Details of CLODAL model (Complex Load Model) 60
Table 28: Parameters of LDSHBL [24] 61
Table 29: Parameters of DLSHBL [24] 61

Table 30: Machine Governors used in Free Governor Mode 64
Table 31: Tabulated results of system frequency response of the event, Actual System vs. PSS/E Model 68
Table 32: Machine Governors used for Frequency Control 70
Table 33: Details of Pumped Storage Power Plant used in Free Governor Mode 71
Table 34: Trip settings of over frequency and under frequency used for FRQTPAT Model 71
Table 35: Generation and Loading Scenarios considered for the studies 76
Table 36: Demand used in each scenario 76
Table 37: Total Generation for each of the selected study scenarios 78
Table 38: Features of Selected Simulation Scenarios 78
Table 39: Typical average demand values Selected Simulation Scenarios in 2030 78
Table 40: Generation mix in HMDP Scenario 81
Table 41: Machine Governors used in Free Governor Mode in HMDP Scenario 81
Table 42: Major Hydro and Thermal Power Plants in operation in HMDP Scenario 82
Table 43: Tabulates results of HMDP Scenario with existing LSS 87
Table 44: Generation mix in TMDP Scenario 88
Table 45: Machine Governors used in Free Governor Mode in TMDP Scenario 88
Table 46: Major Hydro and Thermal Power Plants in operation in TMDP Scenario 89
Table 47: Tabulated results of TMDP Scenario with existing LSS 95
Table 48: Generation mix in RMDP Scenario 96
Table 49: Machine Governors used in Free Governor Mode in RMDP Scenario 96
Table 50: Major Hydro and Thermal Power Plants in operation in RMDP Scenario 97
Table 51: Tabulated results of RMDP Scenario with existing LSS 104
Table 52: Comparison of results of HMDP Scenario with both existing and new LSS 122
Table 53: Comparison of results of HMDP Scenario with both existing and new LSS 126
Table 54: Comparison of results of TMDP Scenario with both existing and new LSS 131
Table 55: Comparison of results of RMDP Scenario with both existing and new LSS 136

LIST OF ABBREVIATIONS

Abbreviation	Description
CEB	Ceylon Electricity Board
LECO	Lanka Electricity Company
LSS	Load Shedding Scheme
NCRE	Non-Conventional Renewable Energy
ORE	Other Renewable Energy
PPP	Private Power Producers
PUCSL	Public Utilities Commission of Sri Lanka
PV	Photo Voltaic
ROCOF	Rate of Change of Frequency
SCC	National System Control Center
UFLS	Under Frequency Load Shedding

LIST OF APPENDICES

Appendix	Description	Page
Appendix - A	Map of Transmission system of Sri Lanka in the year 2019	144
Appendix - B	Power flow data for PSS/E modeling	145
Appendix - C	Pre-fault system demand and system generation data of frequency failure event of 25th July 2019 at 11.09 am	146
Appendix - D	Schematic diagram of 2030-year transmission system of Sri Lanka in PSS/E	150
Appendix - E	Active power and reactive power limits of the Generators of 2030-year PSS/E model	151

CHAPTER 1

INTRODCUTION

1.1 Present Sri Lankan Power System

The electricity sector in Sri Lanka comprises the state utility provider, the Ceylon Electricity Board (CEB), the regulator, the Public Utilities Commission of Sri Lanka (PUCSL), and the Private Power Producers (PPP). The CEB and PPP generate electricity using hydropower, thermal (oil), thermal (coal) and Other Renewable Energy (ORE) sources consisting Mini Hydro, Solar, Wind, Dendro and Biomass. CEB is the owner of monopolistic market in the generation, transmission and distribution of electricity and both CEB and Lanka Electricity Company (LECO) distribute electricity energy. All power plants connected to the national grid at 220 kV and 132 kV operating voltage levels.

1.1.1 Energy Generation

According to Statistical Digest 2019 published by CEB, the total power generation of major hydro owned by CEB is registered a decline of 26% to 3,784 GWh, while the thermal oil-based power generation witnessed an increase of 38.2% to 5,016 GWh in 2019 in comparison with the year 2018. Also despite the breakdowns of the Lakvijaya coal power plant, the total coal power generation increased by 12.5% to 5,361 GWh in 2019. The generation of electricity through nonconventional renewable energy (NCRE) sources, except mini-hydro, increased 25.2% to 750 GWh in the year 2019 [1].

As illustrated in Figure 1, the electricity generation mix of Sri Lanka in 2019, respective electricity generation shares in total generation were 23.8% major hydro power, 11% ORE and 47.1% coal. Therefore, it is clear that the bulk electricity requirement is generated by the coal power plant.

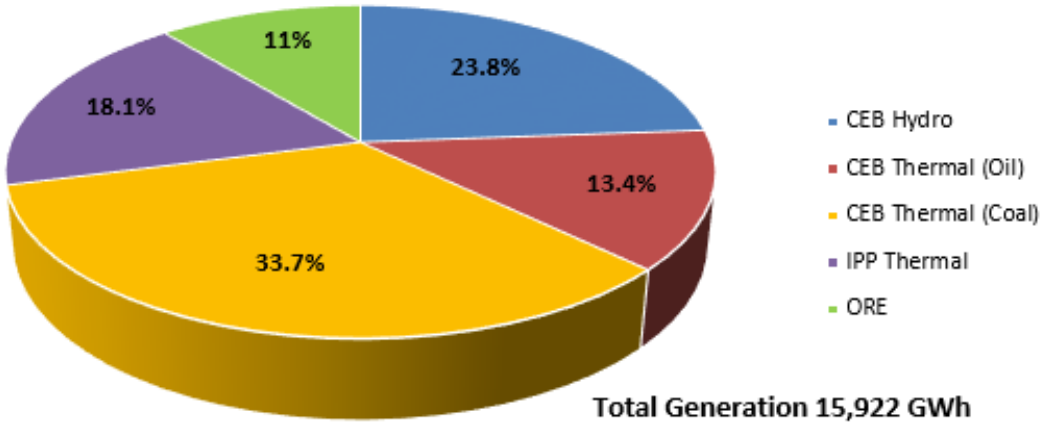

Figure 1: Electricity Generation Mix 2019

1.1.2 Installed Capacity

According to Statistical Digest 2019, published by CEB [1], the total installed capacity of all major hydro power stations owned and operated by CEB as of 31st December 2019 is 1,399 MW while the total installed capacity of all thermal power plants owned and operated by CEB is 1,554 MW. Private thermal (oil) power plants with 628 MW capacity connected to the national grid. Approximately, installed capacities of mini hydro 410 MW, wind 128 MW and ORE (solar, dendro, biomass) 97 MW owned by private sector are connected to the national grid while total installed capacity of the system is 4,217 MW.

By 2015, the total generation capacity of the Lakvijaya coal power station is 900 MW with the completion of Phase III. Even though full load running of the plant provides the high efficiency in energy generation, the plant is sometimes partly loaded, as it is operated in compliance with the recommended standards to maintain system stability. Considering the stability under ***n-1*** contingency, the running capacity of the largest generator is limited to 20-30 % of the demand at any given time [2]. Therefore, it is important to conduct detailed stability studies for verifying such capacity limitations.

1.1.3 Demand Growth

The daily load variation curve recorded on the day of annual peak for the years from 2011 to 2018 is presented in Figure 2. It illustrates that the variation of the demand curve has remained same for the previous eight years. However, compared to other years, the day peak shows a significant growth at a rate of 6.5 % in the day peak of the last three years of 2016, 2017 and 2018. The peak demand of the system has occurred from about 18.30 to 22.00 hours daily for a short period. It could be observed that the system peak is at its maximum of 2,523MW as recorded in 2017, while in 2018 it is 2,616 MW [3].

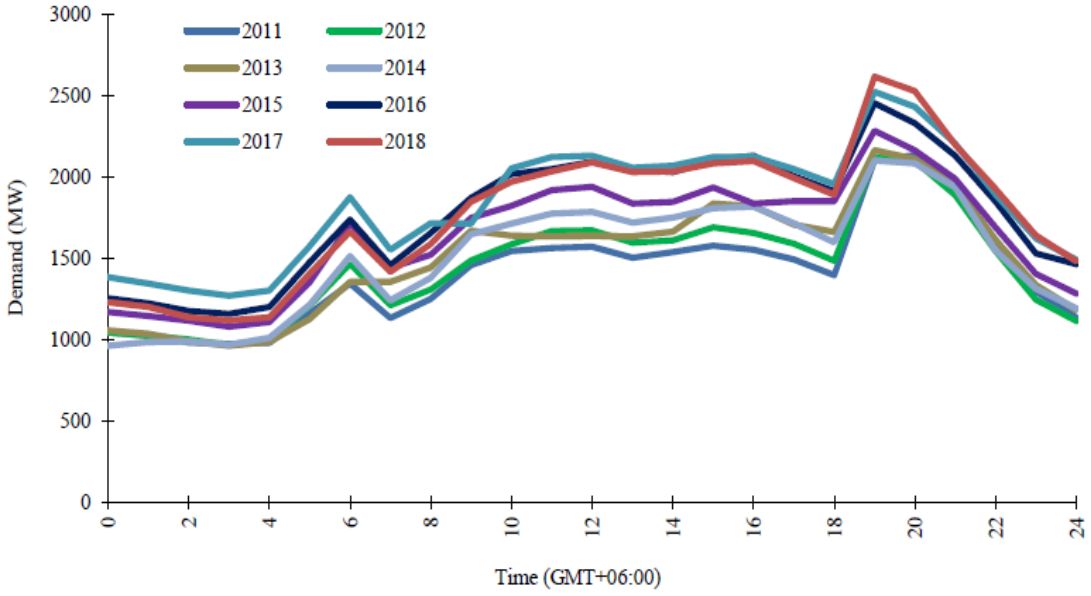

Figure 2: Variation of daily load curve for the years 2011 to 2018 [3]

1.2 Problem Statement

According to the least cost long term generation expansion plan proposed by CEB [4], a strong renewable energy development is expected for the next twenty years as compared to the past two decades. A total of 3,495 MW of ORE capacity has been identified to be developed during the next 20 years. In order to maintain renewable portfolio in the generation mix, and to facilitate the harnessing of indigenous natural resources, it has been proposed to integrate 1,218 MW of solar capacity and 976.9 MW wind capacity

into the Sri Lankan power network by year 2030. Among this, 1,018 MW solar capacity will be connected as 1 MW – 10 MW solar plants or solar parks to the medium and high voltage networks. The remaining 200 MW solar capacity will be connected to the low voltage network as rooftop solar plants. Since renewable energy has less operating cost, it is economical to integrate solar and wind capacity to the system. However, solar and wind power are non-dispatchable and contains no rotational inertia.

In Sri Lankan power grid, the single largest unit has the capacity of 300 MW since 2015, which remains true for year 2030. Lakvijaya coal power station will be generating 1,500 MW by year 2028, which consists of five super critical generators, each one generating 300 MW maximum, after the completion of 4^{th} and 5^{th} phases. These new 300 MW generators are proposed to be connected to the national grid by a separate bus while the existing three generators being connected to the Puttalam bus.

The balance between power generation and power consumption may be broken, due to a major disturbance or a tripping of a large generator unit in the power system. If the power consumption is greater than the power generation, or the power grid failed to supply sufficient generation to the consumers, the system frequency decreases drastically, even leading to frequency collapse. Thus some effective measures should be taken to prevent the dangerous situation. Load shedding to match the power imbalance is an effective solution to restore the system frequency. At present in Sri Lanka, a static Under Frequency Load Shedding (UFLS) scheme is used, which is initiated through the rate of change of frequency (ROCOF) value. In static load shedding, a pre-determined load amount is shed from pre-selected feeders at each stage according to the planned under-frequency settings and ROCOF value.

The irradiance level is severely affected by the cloud coverage and that affects the solar PV generation. Movement of clouds can reduce the irradiance level rapidly to its minimum value. The clouds moving out of the location of the solar power generation station can increase the irradiance level to its maximum value within few seconds.

During the day peak time, each generator in Lakvijaya coal power station is in high load condition. On the other hand, during daytime solar and wind penetration is high. Since solar and wind are both intermittent power sources, system may experience such

intermittent power variations as transients and with more inverter based generation in the system, system equivalent inertia will also be decreased. These may lead to stability issues in the system. During a power ramping due to intermittency of renewable power, if a larger disturbance such as tripping of a larger generator occurred in the system, it will affect the system stability. The utility in Sri Lanka, CEB has to operate thermal power plants throughout every season to maintain spinning reserve to overcome intermittency nature of solar and wind power generation. Therefore, as a base-load power plant, Lakvijaya coal power station will have to be de-loaded with high renewable penetration. It has more spinning in de-load condition and may be has enough capacity to support the system. However, this is inefficient and may not be good for the machine.

With increasing renewable penetration into the system, when renewable sources supply more energy, if a largest unit tripped, whether the system is strong enough to cater under contingency situation, is the research problem. At this kind of situation frequency will drop very steeply because of lower system inertia due to high penetration of inverter based generation with no inertia. During such a situation, the Static Load Shedding Scheme (LSS) might not be able to restore system frequency because it sheds pre-determined loads without considering the load and generation mismatch of the system after the contingency event. There are a few drawbacks of existing load shedding scheme used by CEB, which can be identified through simulation studies. If the loads were shed more than the required amount to match the generation, or in other words excessive load shedding occurred, there can be over shoot in the frequency. It leads to trip other generators and cascaded tripping of generators would create a worse situation. The existing load shedding scheme is designed to shed totally 60.5% of the total load. It is designed to shed loads for more than 100% overloading. The existing static load shedding method, which shed the load amount based on a pre-defined frequency with a pre-determined amount of load may not be adequate to match the power imbalance due to an event of tripping of a major generator or a severe disturbance, which can be characterized by a higher ROCOF value or a very sharp frequency decline. If such contingency is not properly handled, it can lead to system blackout.

System frequency stability is the focus area of the research, and as a solution to the aforementioned problem, a dynamic LSS is proposed. The dynamic LSSs are designed to shed a similar amount of load as the load generation mismatch, and identify which loads need to be shed without shedding critical loads. This research is thus is focused to keep the maximum solar and wind penetration into the national grid by proposing a dynamic load shedding scheme.

The total solar energy penetration will be 25.6% and total wind energy penetration will be 20.5% by year 2030 as proposed [3]. According to the draft grid code [5], the system frequency should be within the limit of ±1% of 50 Hz (i.e. 49.5 – 50.5 Hz) in steady state to maintain system frequency stability. During maximum hydro period or in wet season, in order to maintain system stability standards, while absorbing the maximum penetrations of solar and wind capacities in to the national grid, at least three generators in Lakvijaya coal power station out of five generators should operate violating the merit order. Due to this, available hydro power plants would be partially dispatched and this will cause spilling of larger reservoirs. Therefore, some portion of the total solar and wind absorption capacities are curtailed in every renewable integration planning study conducted by the state utility provider to meet the specific requirements.

1.3 Research Objectives

The main objective of this project is to design a dynamic load shedding scheme for maintaining system frequency stability with the increasing renewable energy penetration in an islanded power system.

The specific objectives are:

- To develop a model of the transmission system of Sri Lanka with the large scale renewable power plants consisting both solar and wind power plants using simulation software.
- To validate the developed model using an actual tripping event.

- To analyze the frequency response of Sri Lankan power system with present under frequency load shedding scheme for different contingency events and for different scenarios of system operation.
- To design a dynamic load shedding scheme and to evaluate the performance of proposed dynamic load shedding scheme.

1.4 Thesis Overview

- Perform detailed literature survey on available load shedding schemes in Sri Lanka as well as other countries.
- Study of stability of the Sri Lankan power system with the coal power plant and the large scale renewable power plants using present and future system forecasted data.
- Study of stability of the future Sri Lankan power system with forecasted data to determine system behavior with availability of generation, under contingency situation with low inertia and loading condition of thermal power plant.
- Identify the study year considering forecasted maximum solar and wind penetration levels and the period to focus considering load curve and unit generation commitment in each time period.
- Develop and modify the model of the transmission system of Sri Lanka for year 2030 by using PSS/E version 33.5.
- Validation of developed 2030 model of the transmission system of Sri Lanka by simulating it with actual data.
- Simulation of 2030 model with existing load shedding scheme
- Designing an algorithm for dynamic load shedding scheme
- Simulation of 2030 model with new load shedding scheme
- Performance evaluation using simulation studies

CHAPTER 2

LITERATURE REVIEW

2.1 Power System Stability

The stability of power system is categorized mainly into three categories as rotor angle stability, voltage stability and mid-term and long-term stability [6]. These studies could further categorized according to the physical nature or main system parameter, size of disturbance and time span. This thesis is focused on transient stability, where frequency response is evaluated. In Sri Lanka, the national grid is being operated at 50 Hz nominal frequency and at the steady state, it can vary between 49.50 Hz - 50.50 Hz according to the standards [5]. Under stable operation, at normal frequency, the total mechanical power input from prime movers to the generators is equal to the sum of all connected loads including real power losses in the power system. Due to a tripping of a main generator or tripping of a main transmission line, a significant unbalance occurs creating system frequency variations. At emergency conditions, the system frequency shall be between a high of 52.50 Hz and a low of 47.50 Hz as allowable frequency window given by the system utility provider [5]. The maximum allowable frequency variations are presented in Table 1.

Table 1: Allowable Maximum Frequency Variation [5]

Nominal System Frequency	Maximum Frequency Variation	
	Normal Operating Conditions	Emergency Operating Conditions
50 Hz	±1% (49.50 Hz - 50.50 Hz)	±5% (47.50 Hz - 52.50 Hz)

Swing Equation

The equation of motion or swing equation is used for system frequency analysis, which constitutes a general model of the movement of generator rotors.

$$\frac{2\mathrm{H}}{f_0}\frac{df}{dt} = \mathrm{P}_m - \mathrm{P}_e \quad (1)$$

Where,

P_m = Mechanical Power Input (per unit)

P_e = Maximum Electrical Power Output (per unit)

H = Inertia Constant (per unit)

f_0 = Nominal Frequency of the system

The system will experience reduction in power generation than load demand, when one main generator in the system trips. The power balance is obtained by kinetic energy of rotating masses converted into electrical energy and to supply the system, which causes a decrease the system frequency, which can be explained using the swing equation shown in equation (1) [6]. However, sudden loss of a larger generator unit will create a severe unbalance between generation and load, which may neither be catered by system inertia, nor through governor control of generators. When high capacity of inverter integrated power sources like solar PV are connected to the system, which are having low inertia, the frequency will drop fast according to equation (1). The impact of high solar and wind penetration into the power system on power system stability is discussed in many literatures. Therefore, this research evaluates the transient stability of the system with high penetration of solar and wind energy and to identify the limit of penetration levels of wind and solar energy. Load shedding is used to restore system frequency back to normal state as an effective solution for a contingency event in the system. Different load shedding techniques are proposed as effective solutions in many literatures for mainlining system stability. These are discussed in following sections.

2.2 Frequency Control Basics

In a power system, the efficient frequency regulation mechanism is significant as a proper control of system frequency assures the constant speed of synchronous and induction loads in the power system. The system frequency depends on a variation in active power demand at any point in power system, therefore it is necessary to keep power balance between the active power generation and load demand in a power system. The swing machine is the single unit, which is configured on lower droop setting (e.g. 0.016 to 0.02) with faster response for tracking the dynamic changes in load demand to

keep frequency stability of the power system. All the other connected machines provide free governor support (on droop control) for primary regulation on a higher droop setting (e.g.0.04 to 0.06).

The National System Control Center (SCC) of CEB monitors the system load demand variation in long term, based on system frequency and present active power generation of swing machine or frequency controlling power plant. The instructions are verbally given by SCC to the other relevant power plants to reduce or increase their active power generation set point to match the active power generation of the power system. Figure 3 shows a typical frequency control reserves based on activation times [7].

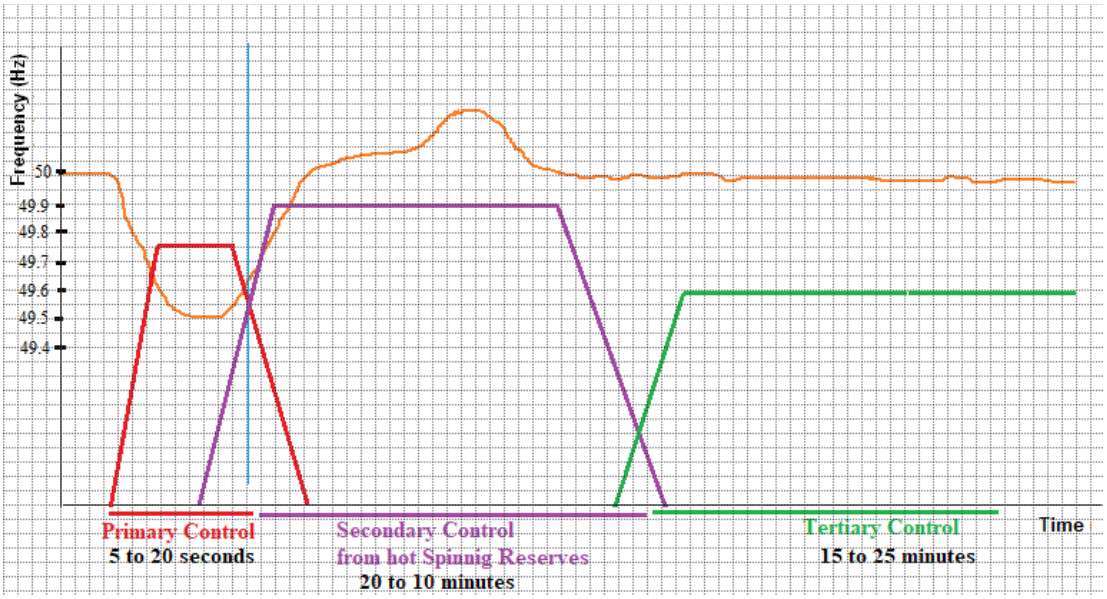

Figure 3: Typical Activation Time of Frequency Control Reserves [7]

After a disturbance, the initial power balance is obtained by absorbing kinetic energy of rotating machines, which causes the system frequency to decline. The equilibrium is restored from frequency load reduction of loads; hence power system stabilizes at new frequency called quasi-steady state frequency as mentioned in [7].

2.2.1 Primary Control

The power output of connected generators will be increased by primary governor action when the frequency change is not in the dead-band of connected generators governor. The equilibrium of the power system is obtained by combination of shedding loads and increasing power generation due to primary governor action. The action time is usually, 5 to 20 seconds and the support amount is determined by the speed droop setting of the governor [7].

2.2.2 Secondary Control

The steady state error of system frequency is corrected by the activation of secondary frequency control from manually varying a set point of a particular power plant. The secondary frequency control will minimize the steady state error of system frequency while resetting the primary control. The action time is usually, 20 to 10 minutes [7].

2.2.3 Tertiary Control

This control reserve is to adjust generating units towards economical operating points. Tertiary control reserve is based on impact of the disturbance. The action time is usually 15 to 25 minutes [7].

2.3 Load Shedding Schemes

System variations of a power grid during operation conditions are normal to every power system. Contingency situations may occur by sudden increase of electrical load demand, forced outage of a transmission line or generator. If the system performance deviates from the permissible range, it may lead to outage of other equipment of power system. As a result, overload of transmission lines and generators occur and protection relays start to operate and it may lead to blackout situation if required actions are not taken to match the system generation and demand. Automatic load shedding is used as a solution under such contingencies to avoid system blackout.

2.3.1 Methods of Load Shedding

Several methods of static load shedding schemes and dynamic load shedding schemes are reviewed in [8]. The comparisons are made between traditional load shedding schemes and adaptive load shedding schemes in [9]. According to both [8] and [9], three main methods of load shedding could be identified as bellow:

1. **Static Load Shedding Schemes**

Static LSS is a decentralized scheme, which sheds a fixed, pre-specified amount of load at each frequency stage after pre-determined time delay. In this method, it is better to increase the number of stages with small and equal load amounts in each stage. Static LSS are designed based on frequency or voltage or both frequency and rate of change of frequency (df/dt) as named below [8].

- Under Frequency load shedding (UFLS)
- Under Voltage load shedding (UVLS)
- Combination of Under Frequency and df/dt

2. **Dynamic Load Shedding Schemes**

Dynamic LSS is a centralized scheme, which shed the dynamic amount of load by considering the size of the disturbance and with the voltage and frequency characteristics. This method allows to shed loads according to the power imbalance occurred by the disturbance and amount of load to be curtailed is not defined for each stage. Dynamic LSS discussed in [9] are designed based on combination of under frequency and under voltage.

3. **Adaptive Load Shedding Schemes**

Adaptive schemes involve intelligence and combination of UFLS and UVLS with power imbalance, frequency, rate of change of frequency (df/dt) and rate of change of voltage (dV/dt). These measurements are used to determine disturbance location, area and severity of the disturbance. Adaptive methods depend on different indices, which are

used for decision making. The decision is based on the state of specific elements in the power system such as major transmission lines or generators.

Adaptive load shedding schemes discussed in [9] can be categorized as:

- Response based methods
- Combination of event-based and response-based methods

The traditional static LSS has several disadvantages when compared with other two methods. Adaptive methods are easy to simulate but implementation would be difficult. The algorithm is complex and need to train intelligent tools. Therefore, this research is focused on developing a dynamic load shedding scheme.

2.3.2 Present Load Shedding Scheme in CEB

As discussed in [2], the minimum standard applicable to the transmission network of Sri Lankan power system for stability is single contingency. In other words, the supply to any consumer should not be interrupted by the loss of a single element in the system, which can be loss of a generating unit or loss of a transmission line. Theoretically, a power system needs to maintain the spinning reserve, which is equal to the size of the single largest generator unit in the system [2]. As the worst case, tripping of the single largest generating unit could be recovered by spinning reserves. Ceylon Electricity Board (CEB), the utility of Sri Lanka, has limited the generation of any single generating unit to equal or less than 30% of the total load demand at any given instant. Therefore, a spinning reserve of about 30% is needed in Sri Lanka. However, maintaining of the spinning reserve is expensive. Due to this reason, the spinning reserve is kept at a lower value than the required value. Thus, the load shedding scheme is used to restore the power system stability during a contingency situation, when the capacity of largest generation unit is higher than the available spinning reserves [2].

The existing LSS of Sri Lankan network is shown in [2]. Currently, a Static UFLS Scheme is used, which is initiated through a rate of change of frequency (df/dt) value. The existing scheme consists of six load shedding stages. The load reconnection criterion is introduced in third and fourth stages.

Table 2: Under Frequency Load Shedding Scheme in CEB as of January 2020

Stage	Load Shedding Criteria	Loads per Stage	Reconnection Criteria	Reconnecting Load
I	48.75 Hz + 100 ms	7.50%		
II	48.50 Hz + 500 ms	7.50%		
III	48.25 Hz + 500 ms	11%	51 Hz + 500 ms AND df/dt < 0.2 Hz/s	2%
IV	48.00 Hz + 500 ms	11%	51 Hz + 500 ms AND df/dt < 0.2 Hz/s	2%
V	47.50 Hz instantaneous	5.50%		
	47.50 Hz instantaneous OR 49 Hz AND df/dt < -0.85 Hz/s + 100 ms	4.50%		
df/dt	49 Hz AND df/dt < -0.85 Hz/s + 100 ms	13.5% and 4.5% embedded in V		
Total	df/dt	18% (4.5% embedded in V)		
	Frequency only	42.50%		

According to Table 2, if the system frequency is lower than 48.75 Hz for 100 ms, 7.5% of the total load is rejected at the first stage. If the frequency is not restored to its nominal value, then the second load shedding stage is activated. In the second stage, an additional 7.5% of the total load is shed, when the system frequency decreases below 48.5 Hz and stays for 500 ms. In the third stage, 11% of the total load is shed, if the system frequency is lower than 48.25 Hz for 500 ms. If the system frequency is not built up and is lower than 48 Hz for 500 ms, an additional 11% of the total load is rejected in the fourth stage. An additional 10% of the total load would be shed at 47.5 Hz instantaneously in the fifth stage. The percentage of the total rejected load is 47% of the total load after the fifth stage. If a larger disturbance occurred in the system, the system frequency decline would be high and df/dt value would be high. During such situations, a considerable amount of the load shedding is required to stabilize the system. The fifth and sixth stages of the existing load shedding scheme are designed by considering the df/dt value. In fifth and sixth stages, 18% of the total load is rejected, if the df/dt of -0.85 Hz/s is detected and if the system frequency decreases to 49 Hz. According to Table 2,

the existing LSS will reject 60.5% of the total system load, if all six stages are operated. This LSS is designed for a 100% overloading [2].

2.2.3 Disadvantages of Traditional Load Shedding Schemes

The differences between the traditional static load shedding scheme and the dynamic load shedding scheme are compared and discussed in [8]. The paper defined the static load shedding scheme as a load shedding scheme, which sheds a fixed, predetermined amount of load at each frequency setting. It has defined that the dynamic load shedding scheme is a load shedding scheme, which sheds the load by considering the size of the disturbance and the characteristics of voltage and frequency. A power system which contains five buses is simulated to obtain the amount of load shed, minimum under-frequency, number of stages and the completion time [8]. The paper concluded that the simulation results of the dynamic load shedding scheme gives better performance in the system frequency recovery.

According to the principle of the UFLS, a load shedding action is realized by a trip signal issued by an under-frequency relay to the circuit breaker. In general, the tripping frequencies for each stage are distinct enough to influence the frequency in the particular stage before activating the next stage [8]. If the time difference between stages is not enough to improve the system frequency, an excessive amount of load will be rejected. It may lead to an overshoot in the system frequency [8].

In [8], it states that the load shedding should not consider frequency only, because the system might not be able to restore the system frequency fast enough, as the time delay between the stages of the scheme can lead to unnecessary tripping. It is a one major disadvantage of UFLS scheme. Because of this, over-tripping might occur in the system. It will cause a phenomenon, which is commonly known as the frequency overshoot. Therefore, it is important to consider the rate of change of frequency (df/dt) along with the frequency setting. According to [8], it is better to design with more number of stages with smaller load amount in each stage to minimize over shedding in static load shedding schemes. A dynamic or adaptive load shedding scheme provides the shedding of a larger load for a larger system imbalance, and a smaller load for a smaller system

imbalance [8]. Therefore, [8] concludes that one step dynamic load shedding scheme is favored over static load shedding scheme.

The major disadvantages of the UFLS and UVLS methods are stated in [9]. One disadvantage is, these two methods do not consider the combination of different forms of instability in their designs. The system blackouts could be occurred due to the frequency instability as well as the voltage instability and the combination of voltage and frequency instabilities involving a loss of various generators and transformers and an outage of different transmission lines [9]. In such events, frequency variation is usually accompanied with voltage variation. Thus, the frequency and voltage stability of the system are jeopardized simultaneously [9]. The UFLS and UVLS schemes have been designed to restore the system stability. However, these traditional algorithms cannot offer an adequate protection against the cascading events for securing the power system stability.

According to [10], the conventional UFLS scheme does not consider the area of the tripping event and the real or the reactive power imbalance for determining the locations of loads to be shed. In other words, in the conventional UFLS schemes, the locations of the loads shed amount are predetermined and not dependent of the location of the disturbance. Therefore, there is always a risk of increasing tie-line loadings and a risk of voltage instability [11]. This exact situation occurred in November 1987 in Italy, and resulted in the Italian blackout [11].

There are many literatures reviewing LSS of the power system of Sri Lanka. In [12], simulations are carried out by considering the transmission network of 220 kV and 132 kV voltages for the year 2011. It is proposed to increase the size of the single largest generating unit up to 25% of the load demand for the year 2011 Sri Lankan power system. The proposed LSS in [12] considers the selection of the df/dt ratings such that a large generation loss is detected swiftly. The study concludes that, a power system can restore the system stability by selecting df/dt ratings, during a larger generation loss without leading to a total system collapse. It shows the importance of researching new method for load shedding by considering the drastic system changes for each year based on system transient stability.

In [13], it presents a new static UFLS scheme for the Sri Lankan power system of the year 2013 and mentioned disadvantages of existing LSS in CEB used for the 2013 power system. The simulations are carried using PSS/E software and showed the comparison between two LSSs. Three UFLS schemes referring to the power system of Sri Lanka in 2016 are compared in [14]. It states the necessity of reviewing the performance of load shedding for the recent power system changes in Sri Lanka for maintaining frequency stability. The authors of the paper compared the existing LSS with two proposed LSS and explained the disadvantages of UFLS without df/dt and also stated the suggestions by simulating the power system in PSCAD/EMTDC. All the proposed LSS in [2], [13], [12], [14] are static under frequency load shedding schemes, where there are disadvantages as listed below. However, this research is focused on designing a dynamic LSS, which will be shedding loads according to the power mismatch.

By considering aforementioned literature, the major weaknesses of the traditional UFLS methods are:

1. Excessive amount of load shed
2. Inadequate amount of load shed, which may lead to power system blackout
3. Pre-determined load shedding amount is used which is independent of the time of the day
4. The location of the disturbance is not considered for the selection of load shedding feeders
5. The combination of voltage and frequency instability is not considered against the cascading events

2.3.4 Dynamic Load shedding Schemes

Reference [9] discusses the drawbacks of conventional UFLS and UVLS systems and proposes several combinational adaptive load shedding algorithms to improve the adaptability of load shedding relays, and to enhance the security of power system during large disturbances by improving the system voltage stability margin [9]. The validated model of the real power network has used to achieve accurate simulation results

accurately. The effectiveness of the proposed algorithms in [9] is demonstrated through simulations under different operating conditions.

Reference [15] presents a simple and efficient algorithm based on the variations in the generator outputs for a given variation in load demand, and droop characteristics of the generating units. This LSS is designed to find the sensitivities of generator outputs and load demand and to use them to distribute the load shedding amount among several feeders. In this method, the variations in the power generations due to the variations in the load demand are computed using a network equation created by using the generator and load bus voltage vectors, current vectors, and impedance sub matrices. The equation of the deviation in frequency along with the droop characteristics of the generator and the equation of the deviation in the frequency of the equivalent inertial center are used to find sensitivities [15]. The main contribution of the paper is for finding the sensitivity of the frequency of the inertial center of a power system with respect to the changes in load at the individual load buses [15]. This method was simulated in IEEE 39 bus system and the results are compared with the results obtained from two traditional methods. The simulation results show the usefulness of the selection of the most sensitive buses for load shedding.

New under-frequency load shedding technique based on the combination of random and based on the fixed priority of loads is discussed in paper [16]. It has observed that placing all the loads in the distribution system with the fixed priority loads would result in un-optimum load shedding [16]. The LSS proposed in [16] has provided some flexibility in achieving the optimal load shedding. Simulation results of the proposed scheme on different scenarios has proved that the proposed method is capable of achieving the optimal load shedding and recovering frequency to the nominal value without any overshoot.

Two centralized adaptive load shedding designs are proposed and evaluated in [17]. This paper considers major system disturbances or the cascaded events. This proposed adaptive scheme is designed to select the settings for the scheme adaptively. The load amount needs to be shed in this method are selected based on the magnitude of sub-transmission bus voltages and also the static voltage stability VQ margins of the buses

[17]. The proposed methods are applied to a simulation model of a real power system to obtain the results of the performance. The obtained results have indicated that the proposed methods are capable of restoring the system stability efficiently against the major disturbances. When compared with the conventional scheme, the amounts of load to be shed by these algorithms are lower. As concluded in [17], various power system blackouts may be prevented by using the proposed algorithms.

Reference [18] presents a two-unit wide-area adaptive load shedding scheme based on the synchro-phasors for the Khorasan HV network in Iran grid. In the first unit, an adaptive precise System Frequency Response (SFR) model is developed [18]. The amount of load shedding is determined to fulfill the dynamic and steady state frequency limitations. This algorithm considers both static and dynamic loads. Therefore, calculation errors are negligible. The main task of the second unit is to select the best location of the load to be shed, which is decided based on a voltage stability criterion. Two units are executed parallel and therefore, the computation of the proposed approach is not complex. Thus, the implementation is simple in the real world applications.

Reference [19] proposes a LSS based on the selection of the location of load to be shed, which allows the control to achieve a quick and exact response of the load shed location. This method is implemented on a two area power system. The algorithm contains three main stages. The first stage measures frequency and ROCOF by measuring elements of every plant and upload data to a decision center. The system frequency and ROCOF are calculated at the decision center. The second stage shows the occurrence of disturbance of system or the system instability and calculates power mismatch to determine the load amount to be shed. Then, it ranks the loads and forms a load shedding plan to be executed in the last stage. The simulation result shows that the performance of the new method is more efficient and accurate than the traditional LSS methods.

2.4 Selection of Study Year

CEB has already conducted and published frequency stability studies for 2018, 2019, 2021, 2023, 2025 and 2027. The year 2030 is the next available study year for analyzing the power system stability with the maximum renewable penetration in to the national

grid. The total solar energy penetration will be 25.6% and total wind energy penetration will be 20.5% by the year 2030 as proposed [3].

According to the least cost long term generation expansion plan proposed by CEB [3], the cumulative ORE capacities envisaged at the end of 20 years are 1,323 MW from wind, 2,210 MW from solar, 654 MW from mini-hydro and 144 MW from biomass [3]. Higher ORE share is expected to maximize the utilization of indigenous natural resources and 2,700 MW of ORE capacity will integrate to the system by 2030 [3]. A moderate growth is identified in mini-hydro and biomass technologies whereas the energy generation from the solar and wind are contributed a significant share for the increase of ORE capacity. In the long term plan [3], the total capacity of ORE is proposed to increase from 1,245 MW in 2020 to 4,330 MW by 2039. Beyond 2023, the power generation of solar energy is expected to be the major share of the ORE capacity followed by wind power. By 2022, ORE segment will exceed the major hydro capacity and become dominant.

Figure 4 illustrates the contribution of renewable energy sources and the percentage energy share variation for the next twenty years [3]. The generation capacity of major hydro resources is the largest contribution at present Sri Lanka. In the forthcoming years, major hydro capacity will have a slow growth due to the smaller amount of the capacity additions. During the period of next 20 years, the development of ORE resources will contribute to increase the decline of the renewable energy share by maintaining the total percentage above 35-40% [3].

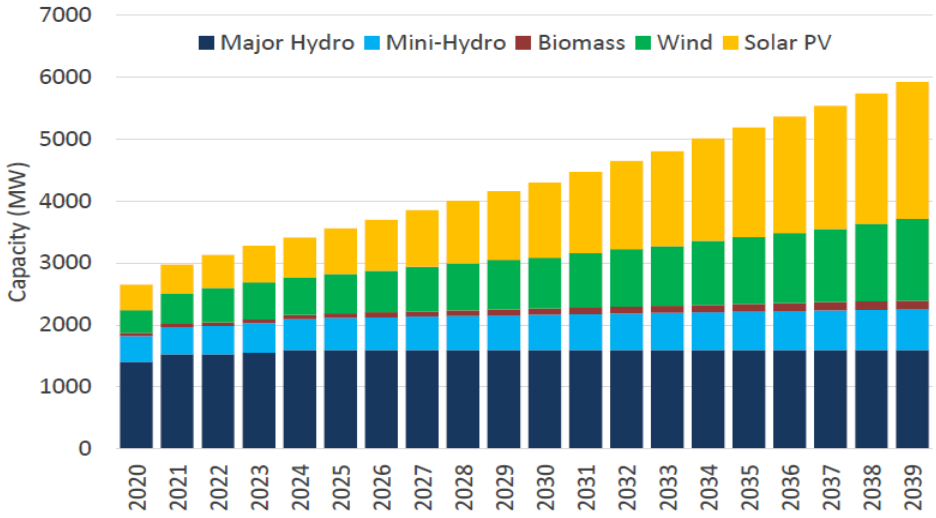

Figure 4: Total Renewable Energy Capacity Development [3]

In Sri Lanka hydro, wind, solar, biomass and waste energy are the renewable energy forms which show the significant growth with the rapid growth of electricity demand. Renewable energy sources are also known as Distributed Renewable Energy (DER) sources. They have become a viable option in Sri Lanka to meet the future energy demand because the renewable energy sources reduce the environmental issues when compared to the fuel based energy generation. The prospective power plant capacity developments in renewable energy sources, which are projected for the next 20 year planning period in [3] are given in Table 3.

Among the ORE capacity, the wind and solar power are considered as clean energy resources with a higher potential for the future development in Sri Lanka. Mannar, Pooneryn, Puttalam and North are the main resource areas, which presently focused for the large scale wind power development in the country. The 100 MW large scale wind power plant in Mannar was considered as a committed project, which is currently being developed by CEB. Pooneryn, Siyambalanduwa and Monaragala are the main areas initiated for the large scale solar power plant for the future developments. The rooftop solar PV capacity will be further expanding in the next 20 years as planned.

Table 3: Projected Future Development of ORE [3]

Year	Cumulative Mini hydro Capacity (MW)	Cumulative Wind capacity (MW)	Cumulative Biomass capacity (MW)	Cumulative Solar capacity (MW)	Cumulative Total ORE capacity (MW)	Annual total ORE generation (GWh)	Share of ORE from total %
2020	419	368	49	410	1,245	3,403	18.40%
2021	439	488	54	470	1,450	3,970	19.90%
2022	459	558	59	530	1,605	4,376	20.90%
2023	479	598	64	590	1,730	4,677	21.20%
2024	499	598	69	650	1,815	4,863	20.90%
2025	519	638	74	730	1,960	5,193	21.20%
2026	529	673	79	820	2,100	5,483	21.30%
2027	539	723	84	910	2,255	5,819	21.60%
2028	549	763	89	1,010	2,410	6,144	21.80%
2029	559	803	94	1,110	2,565	6,469	21.90%
2030	569	823	99	1,210	2,700	6,738	21.80%
2031	579	883	104	1,310	2,875	7,114	22.00%
2032	589	933	109	1,420	3,050	7,487	22.20%
2033	599	968	114	1,530	3,210	7,801	22.10%
2034	609	1,038	119	1,650	3,415	8,244	22.40%
2035	619	1,083	124	1,770	3,595	8,613	22.40%
2036	629	1,133	129	1,880	3,770	8,985	22.40%
2037	639	1,183	134	1,990	3,945	9,357	22.40%
2038	649	1,253	139	2,100	4,140	9,786	22.50%
2039	654	1,323	144	2,210	4,330	10,198	22.60%

According to [3], it is proposed to integrate 1,218 MW of solar capacity and 976.9 MW wind capacity into the Sri Lankan power network by the year 2030. Among this, 1,018 MW solar capacity will be connected as 1 MW – 10 MW solar plants or solar parks to the medium and high voltage networks. The remaining solar capacity will be connected to low voltage network as rooftop solar plants. All the transmission development projects already commissioned and planned to be commissioned by 31st December 2029 is taken into the analysis for the year 2030. The 2030 Sri Lanka system considered in the study includes large scale solar and wind power plants as shown in Table 4.

Table 4: Large Scale Solar and Wind Power Plants in 2030 model

	Year of Operation	**Capacity (MW)**
Solar Power Plants		
Siyambalanduwa	2022	100
Pooneryn	2024	150
Mannar	2026	170
Hambanthota	2027	170
Wind Power Plants		
Mannar Nadukuda 1	2020	100
Mannar Nadukuda 2	2021	80
Mannar 3	2021	65
Pooneryn 1	2021	100
Pooneryn 2	2025	150
Vadamarachchi	2030	50

Table 5 shows the base demand forecast for planning period starting from 2020 to 2044 as described in the least cost long term generation expansion plan 2020 – 2039 of CEB [3]. It has shown that the day peak would surpass the night peak from the year 2027 onwards. Therefore, the effect of solar and wind energy contribution in the day peak time would be considerably increase since 2027.

Based on the fuel price forecasts considered for the planning purposes and at the average weather conditions, the coal power generation is expected to have a share of 41% by 2030 [3]. The Energy contribution from liquefied natural gas in 2030 would be 22% [3] respectively and the contribution of renewable energy is going to be over 35% by 2030 [3]. Under favorable weather conditions, the latter is expected to go further up. The generating capacity mix is identified in this plan is operationally capable of raising the share of generation from cleaner sources, (Natural Gas and renewable energy) up to 70% of total generation [3].

Table 5: Base Demand Forecast for the years 2020 – 2044 [3]

Year	Demand		Loss (Net)	Generation (Net Value)		Peak Demand
	(GWh)	Rate of Growth (%)	(%)	(GWh)	Rate of Growth (%)	(MW)
2020	16914	7.40%	8.78	18542	7.20%	3050
2021	18194	7.60%	8.62	19910	7.40%	3254
2022	19187	5.50%	8.46	20959	5.30%	3403
2023	20233	5.50%	8.3	22065	5.30%	3561
2024	21337	5.50%	8.15	23230	5.30%	3728
2025	22501	5.50%	8	24458	5.30%	3903
2026	23667	5.20%	7.9	25696	5.10%	4079
2027	24819	4.90%	7.8	26918	4.80%	4241
2028	26025	4.90%	7.7	28195	4.70%	4444
2029	27279	4.80%	7.6	29522	4.70%	4655
2030	28573	4.70%	7.5	30890	4.60%	4872
2031	29917	4.70%	7.45	32325	4.60%	5101
2032	31279	4.60%	7.4	33778	4.50%	5332
2033	32675	4.50%	7.35	35267	4.40%	5569
2034	34119	4.40%	7.3	36806	4.40%	5814
2035	35607	4.40%	7.25	38390	4.30%	6067
2036	37126	4.30%	7.25	40028	4.30%	6328
2037	38692	4.20%	7.25	41716	4.20%	6597
2038	40298	4.20%	7.25	43448	4.20%	6873
2039	41937	4.10%	7.25	45215	4.10%	7155
2040	43623	4.00%	7.25	47033	4.00%	7445
2041	45368	4.00%	7.25	48914	4.00%	7745
2042	47170	4.00%	7.25	50857	4.00%	8054
2043	49037	4.00%	7.25	52870	4.00%	8376
2044	50978	4.00%	7.25	54963	4.00%	8709
5 year Average Growth	6.00%	N/A	N/A	5.80%	N/A	5.10%
10 year Average Growth	5.50%	N/A	N/A	5.30%	N/A	4.80%
20 year Average Growth	4.90%	N/A	N/A	4.80%	N/A	4.60%
25 year Average Growth	4.70%	N/A	N/A	4.60%	N/A	4.50%

2.5 Effects of Renewable Energy on Power System Stability

Sri Lanka being a country located within the equatorial belt has a larger potential of solar resource. The development of large scale solar PV power plants has both advantages in economies and also challenges in technical side. The increased penetration of solar power generation has intermittency nature, which introduces more power output variations into the power system starting from finer time scale [3]. The geographical distribution of solar PV installations is one of the strategies to minimize the effect of inherent power output variation of solar PV systems as there is a greater diversity in intermittent characteristics in smaller time scales.

In Sri Lanka the North-western coastal area, Northern area and central highland area are the areas where wind resources mainly available to generate quality wind energy. However, integration of wind resource needs to consider various technical constraints due to its intermittency nature and strong seasonality. The wind power capacities presented in this report are expected to experience daily and weekly curtailments to overcome the technical and operational restrictions [3]. The amount of wind power capacity is expected to increase gradually over the years with higher wind penetration. Therefore, the features to remotely curtail the wind generation (if so required) to meet the technical and operational requirements and methods to treat such curtailments need to be incorporated to future contracts, agreements and specifications [3].

Effects of Solar PV systems on power systems have been discussed in many research works including [20]. It states that, the replacement of conventional, fossil based generation with renewable generation resources is increasing in present power systems as a need of clean, environmentally friendly and renewable energy resources, which do not produce greenhouse gases. Also this paper described, that the exact effect of larger amounts of penetration of solar PV levels is still to be fully identified. It affects the steady state as well as the transient stability of the power systems due to their distinct characteristics, which are different from the conventional generation resources. A significant amount of conventional generation will be replaced with distributed PV resources comprised of utility scale PVs and rooftop solar PVs.

Power system collapses due to high penetration of solar and wind energy and failures of traditional UFLS methods are analyzed in [21]. According to [21], the grid connected solar PV and wind, which has no rotational inertia is effectively displacing the rotating systems of the conventional generators. This reduces environmental effects and the cost of generation. However, frequency dynamics become faster with low inertia and it affects the frequency stability of the power system. Frequency stability becomes a challenge due to this, and makes the frequency control complex and difficult. The importance of having smaller gaps in under frequency settings of UFLS is discussed and it concludes that for larger frequency gaps may lead to a total system black out in the worst case. According to [21], there has been increased penetration of wind and solar into the Kenyan power system. A total system black out was occurred in Kenya in June 2016 in day peak, which has last for almost three hours due to transformer tripping fault at Gitaru Hydroelectric Power Station [21]. It has led to a loss of more than 180 MW from the grid. This paper revisits frequency stability, UFLS and proposes new approach for mitigating frequency instability with grid connected solar PV and wind. It has mentioned that the consideration of frequency only is not sufficient to protect a power system with a high renewable penetration against severe disturbances.

In [22], it discusses the challenges introduced by intermittent sources to the utility operators in balancing the generation and demand at all times, and guaranteeing the system reliability [22]. When the power system is not capable to depend on renewable energy generation due to highly dependence on the environment, the utility operators are practiced to curtail an amount of loads. Most importantly, it is mentioned that load shedding has been designed to prevent the power system from blackouts while the system is allowed integrating more renewable energy resources. A LSS is proposed to maintain both voltage and frequency stability when high penetration of renewable energies into the grid. The scheme is designed to achieve stability with minimum amount of load shedding during a disturbance.

CHAPTER 3

MODELING APPROACH

3.1 Power System Modeling

Grid planning, designing, and operating decisions are based on the results of power system simulation studies. All these simulations are carried out through power system models to predict system performance during contingency events. Therefore, power system modeling is considered as the foundation for all power system studies. Power system performance assessments, calculation of operating limits, power system planning studies, and all the other power system studies depend on the models of the power system. A power system model is identified as an approximate mathematical representation of the generation, transmission, and loads along with a set of models detailing each part's characteristics of the power system.

There are a few model categories that required to be modeled for modeling a larger power system. Mainly they are Generating Units, Transmission system, and Loads. Generating units include supply resources of the entire power system which can be further categorized into Hydro, Thermal, liquefied Natural gas (LNG), Solar, Wind, and Biomass power plants. Transmission system represents Transmission lines, power transformers, phase-shifting transformers, flexible AC transmission systems (FACTS), mechanically switched shunt capacitors and reactors, static VAR compensators (SVC), and high voltage (HVDC) transmission systems. Load models include all electrical loads in the system.

Power System Simulator for Engineering (PSS/E), Power System Computer Aided Design (PSCAD), PSLF, DigSILENT, and ETAP are a few of the most commonly used power system software for computer simulations. In this research, Sri Lankan power system was modeled using PSS/E software, taking all actual/ typical system parameters into consideration for the determination of power system stability. The evaluation of the performance of existing LSS and implementation and evaluation of the new LSS were carried out using the developed simulation model of Sri Lankan power system.

Importance of Power System Modeling

- Prediction of system behavior by simulating power system model with accurate parameters
- System security enhancement
- Increase the effectiveness of generation dispatch and utilization of transmission asset
- Increase the reliability of integration of generation stations, grid substations, loads and reactive compensators

3.1.1 Overview of PSS/E

The PSS/E software is categorized as a high performance transmission planning and analysis software tool, which allows developing models, perform simulations and visualize the behavior of power system. A wide variety of analytics including power flow, dynamics, short circuit, contingency analysis, optimal power flow, voltage stability transient stability simulation, etc. [23] can be performed with PSS/E, which comes with a rich library of built-in models.

3.1.2 Steady State and Dynamic Analysis

It is necessary to examine both steady state behavior and dynamic behavior of the power system to study the impact of renewable energy penetration on frequency stability. Static and dynamic analyses are the most commonly used two methods in CEB for simulations of stability of power system in Sri Lanka. These studies ensure the power system frequency stability and secure operation under contingency situation.

The steady state analysis is conducted to determine the calculation of power flow on overloading of the transformers, transmission lines and voltage profile on the bus bars of the power system. Static or steady state analysis is the load flow studies performed when the power system is in steady state or equilibrium state. In this state, generation is always equal to the addition of total load and losses.

Dynamic stability analysis is performed in time-domain to involve investigation of the power system when faced with sudden disturbances, which affects the power system stability. The objective of the dynamic stability study is to observe the behavior of the power system when a critical generator unit or a multiple larger generator units of critical power plants tripped in the system under ***n-1***, and ***n-2*** contingency levels.

The steady state models are used for the steady state analysis and dynamic models are used for the dynamic analysis. All the components including transmission elements, generators and loads can be represented by a steady state model. Model development for transmission lines, and shunt capacitors/ reactors, transformers is accomplished by an accurate calculation of the ratings, impedances and other parameters in steady state model. The generator steady state models represent active and reactive power capability and voltage control. Loads are represented as constant current models, constant impedance models and constant active and reactive power models. The individual component models are combined and modeled the complete system model for representing Sri Lankan power system network.

The dynamic models are used to model dynamic behavior of power plants and their controls, power electronic transmission devices, certain load components, on load tap changes, PLC controls on shunt devices, protection action schemes, and other control devices. The parameters of steady state model components are required to be compatible with their corresponding dynamic model.

3.2 Modeling of 2019 Power System

Simulation of future power system models is based on the validation of the existing power system for a critical failure event occurred recently. Therefore, modeling of 2019 power system was carried out for a more precise representation of actual system events. The information on operation records of generation power plants in 2019 Sri Lankan power system was obtained from System Control Branch in CEB. These details were maintained by individual power generation stations and the Generation Planning Branch of CEB.

3.2.1 2019 Power System

When considering the generation mix of 2019 power system, it was observed that major part of generating stations is owned by CEB. The 84% of the total dispatchable capacity is owned by CEB including thermal and hydro generation capacity. A considerable percentage of power plants are owned by private sector in 2019 [3]. The total installed capacity of the system was approximately 4,217 MW in 2019, which includes non-dispatchable power plants owned by the private sector.

The existing and committed hydro and ORE power plants in 2019 Sri Lankan power system are shown in Table 6. There are three major Hydro complexes in 2019 power system. They are Mahaweli complex, Laxapana complex, and Samanala complex. Seven hydro power stations are installed in Mahaweli complex including Ukuwela, Bowatenna, Kotmale, Upper Kotmale, Victoria, Randenigala and Rantambe. Laxapana complex consists of five hydro power stations including Canyon, Wimalasurendra, Old Laxapana, New Laxapana, Polpitiya. Samanala complex consists of two hydro power stations including Samanalawewa and Kukule. The committed hydro plants in 2019 system are Moragolla, Uma Oya, and Broadlands. The seven hydro power stations in Mahaweli complex added a total installed capacity of 817 MW and five power generating stations of Laxapana complex added a total installed capacity of 369.8 MW to the national grid. The committed other renewable plant of Mannar wind park added a total installed capacity of 100 MW to the national grid [3].

The existing and committed thermal power plants both are shown in Table 7. Total of eight thermal Power stations are contributed to national grid in 2019. They are Lakvijaya coal plant, Kelanitissa plant (Sojitz plant), Sapugaskanda (Asia power), Uthuru Janani, CEB Barge Mounted plant, West Coast plant, Northern power, and ACE power Embilipitiya.

Table 6: Hydro and ORE Power Plants (Existing and Committed) [3]

Plant Name	No. of Units x Capacity (MW)	Total Capacity (MW)	Expected Annual Average Energy Generation (GWh)	Commissioning Year
Laxapana Complex				
New Laxapana	2 x 58	116	552	1974
Polpitiya	2 x 45	90	453	1969
Canyon	2 x 30	60	160	1983 – Unit 1 1989 – Unit 2
Old Laxapana	3 x 9.6 + 2 x 12.5	53.8	286	1950 1958
Wimalasurendra	2 x 25	50	112	1965
Total (Laxapana)		**369.8**	**1,563**	
Mahaweli Complex				
Victoria	3 x 70	210	865	1985 – Unit 1 1984 – Unit 2 1986 – Unit 3
Kotmale	3 x 67	201	498	1985 – Unit 1 1988 – Unit 2and3
Upper Kotmale	2 x 75	150	409	2012 – Unit 1 2012 – Unit 2
Randenigala	2 x 61.3	122.6	454	1986
Rantambe	2 x 25	50	239	1990
Ukuwela	2 x 20	40	154	1976
Bowatenna	1 x 40	40	48	1981
Nilambe	2 x 1.6	3.2	-	1988
Total (Mahaweli)		**816.8**	**2,667**	
Samanala Complex				
Samanalawewa	2 x 60	120	344	1992
Kukule	2 x 37.5	75	300	2003
Small Hydro		317.25		
Total (Samanala)		**212.25**	**644**	
Total (Existing)		**1,398.85**	**4,874**	
Committed				
Broadlands	2 x 17.5	35	126	2020
Moragolla	2 x 15.1	30.2	97.6	2023
Mannar Wind Park		103.5	337	2020
Uma Oya	2 x 61	122	290	2021
Total (Committed)		**290.7**	**850.6**	

Table 7: Thermal Power Plants (Existing and Committed) [3]

Plant Name	Units x Nameplate Capacity (MW)	Units x Capacity used for studies (MW)	Maximum Annual Energy Generation (GWh)	Commissioning Year
Lakvijaya Coal Power Plant				
Lakvijaya CPP	3 x 300	3 x 270	5355	2011 and 2014
Total (Lakvijaya Coal)	**900**	**810**	**5355**	
Kelanitissa Power Station				
Gas turbine (Small GTs)	4 x 20	4 x 17	382	1981 and 1982
Gas turbine (GT7)	1 x 115	1 x 115	703	1997
Combined Cycle (JBIC)	1 x 165	1 x 161	1196	2002
Total (Kelanitissa)	**360**	**344**	**2281**	
Sapugaskanda Power Station				
Diesel	4 x 20	4 x 17	493	1984
Diesel (Ext.)	8 x 10	8 x 9	481	4 Units 1997, 4 Units 1999
Total (Sapugaskanda)	160	140	974	
Other Thermal Power Plants				
Uthuru Janani	3 x 8.9	3 x 8.9	184	2013
Combined Cycle (JBIC)	4 x 16	4 x 15.6	515	2015
Total Thermal (Existing)	**1,510.7**	**1,383.1**	**9,309**	
Committed				
Kelanitissa Gas	3 x 45	130		2021
Total Thermal (Committed)	135			

The total capacity of ORE power plants Owned by IPP is approximately 610 MW by 31st December 2018. Mainly non-dispatchable ORE plants are connected to the national grid by 33 kV distribution lines. The capacity contribution from ORE is tabulated in Table 8 [3].

Table 8: Other Renewable Energy (ORE) Capacities (Existing) [3]

Power Plant Type	No. of Projects	Total Capacity (MW)
Mini Hydro power	197	393.5
Wind Power	15	128.45
Biomass	12	37.09
Solar Power	8	51.36

Additionally, 170 MW capacity of rooftop solar PV is integrated into the system by 31st December 2018. The existing wind power plants and solar power plants in the 2019

system are mentioned in Table 9 and Table 10 respectively. The map of the transmission network in Sri Lanka in the year 2019 is attached in Appendix - A.

Table 9: Existing Wind Power Plants

Plant Name	Capacity used for studies (MW)
Ambewela Aitken Spence Power Plant	3
Kilinochchi (Pollupalai, Vallimunai)	24
Chunnakam	20
Puttalam Wind (Seguwantivu, Vidatamunai)	20
Madurankuliya (Narakkaliya)	12
Mampuri Wind Farms	31
Nirmalapura Wind	10.5
Kalpitiya Wind Farm	10.2

Table 10: Existing Solar Power Plants

Plant Name	Capacity used for studies (MW)
Welikanda Solar	12.6
Vavniya Solar	10
Laughs Solar	20
Sagasolar	10

3.3 PSS/E Models used for 2019 Power System Model

3.3.1 Power Flow Data Entry

1. Case Identification data: consists of system MVA base, Units of transformer ratings, Units of ratings of non-transformer branches, System base frequency in Hertz
2. Bus data: In PSS/E, each network bus is represented with Bus number, Bus Name, base Voltage data, Bus type
3. Load data: In PSS/E, each load is represented with Bus number, Load Identifier, Load status, and the machine data. Load bus, generator bus swing bus are the types of buses used to model the power system. The load model is used in load

flow study is shown in Figure 5. The parameters of load modeling for load flow studies are shown in Appendix B-1.

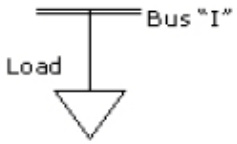

Figure 5: Load Model in PSS/E [24]

4. Fixed Bus Shunt data: Each fixed shunt bus in PSS/E is represented with Bus number, Identifier, Shunt status. The fixed bus shunt model is used in load flow study is shown in Figure 6.

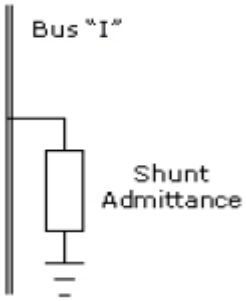

Figure 6: Fixed Bus Shunt Model in PSS/E [24]

5. Generator data: Each generator in PSS/E is represented as a generating unit or plant bus with Bus number, Identifier and the machine data. The generator model is used in load flow study is shown in Figure 7. The generator parameters for load flow studies are shown in Appendix B-2.

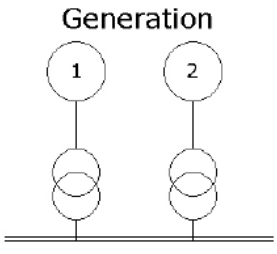

Figure 7: Generator Model in PSS/E [24]

The equivalent circuit of generator model is used in load flow study is shown in Figure 8, which consists of a voltage source behind a step up transformer. The step up transformer parameters for load flow studies are shown in Appendix B-3.

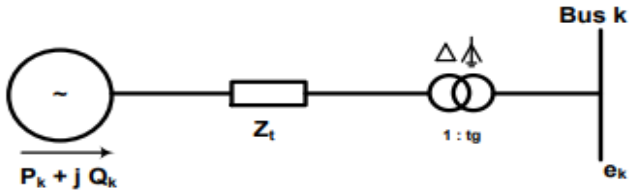

Figure 8: Generator model used in load flow studies [24]

6. Non-Transformer Branch data: Branches in the network which are modeled without transformers are specified in this data category. Branch from bus number, Branch to bus number, Branch resistance, Branch reactance, Rating data, complex admittance, branch status, line length are the details to be included for this category.
7. Transformer data: Each ac transformer is represented with bus number, winding data, impedance data, magnetizing admittance data, transformer status. The transformer model is used in load flow studies is shown in Figure 9. Five data records are required for three- winding transformers. A block of four data records is required for two winding transformers.

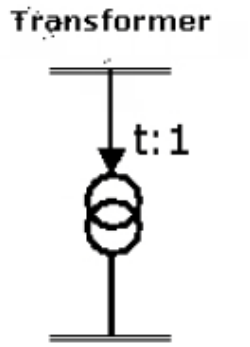

Figure 9: Transformer Model in PSS/E [24]

3.3.2 Power System Dynamic Modeling

A wide variety of equipment models is available in the PSS/E model library for satisfying various requirements in power system modeling. Most of these models contain generation power plant equipment. However, if there is no matching library model in the equipment library in PSS/E with the corresponding actual equipment model, there is a second option with modifying the data characteristics of the equipment to fit the block diagram of an actual existing model. Also PSS/E users are encouraged to develop models, which match the corresponding actual models as a "User Defined Model". Dynamic models in the PSS/E dynamic model library can be categorized as follows:

1. Device Models: These models are attached with corresponding equipment in power flow models such as generator models, excitation models, turbine governor models, load characteristic models, etc.
2. Protection Models: Load relay models which used to model LSS are categorized as protection models. Machine and wind machine protection models are also included in this model category.
3. Miscellaneous Other Models: Under voltage or over voltage generator bus disconnection or trip relays, under frequency or over frequency generator bus disconnection or trip relays, transformer saturation models, switched capacitor bank models are categorized into this type.
4. Data Models: CONS, VARS, ICONS, channels are categorized into this type.

The power system dynamic modeling in Sri Lanka for the year 2019 was carried out under four main categories; Hydro power plant modeling, thermal power plant modeling, wind power plant modeling, and solar power plant modeling.

3.3.2.1 Hydro Power Plant Modeling

All large hydro and mini hydro power plants in Table 6 modeled as discussed in this section. Mainly, a hydro power plant consists of Generator model, Turbine-Governor model and Excitation System model in PSS/E power system dynamic modeling.

1. Generator model - GENSAL

A generator consists of two main parts: namely stator and rotor. The stator has armature winding and the rotor has field winding. The stator converts the mechanical rotational energy of the rotor into electrical energy of the stator by applying an excitation system on rotor. Synchronous generators and asynchronous generators are the main classifications of generators. PSS/E model library includes a family of generator models, which allows to model different levels of generator rotor effects based on the requirement. In this research work, synchronous generators were used to model the hydro power stations. The synchronous generators are classified into two types, that is, round rotor and salient pole type which are having different properties. GENSAL model, which is a salient pole synchronous generator (Quadratic saturation on d-Axis) type in PSS/E was used for hydro power plant modeling.

The generator is to be converted to the Norton equivalent circuit for dynamic simulation as illustrated in Figure 10. The corresponding transfer block diagram of GENSAL generator model in PSS/E is shown in Figure 11. The Norton equivalent current is represented by the current source "I source" and the Norton equivalent admittance is represented by "Y" and the unsaturated sub-transient reactance is represented by the "Z". The Norton equivalent current phase angle is represented by "δ" and step up transformer impedance is "Z_t" and tap ratio is "t_g". The generator parameters for dynamic analysis in PSS/E are given in Table 11. The generator parameters, H, D, Xd, Xq and X'd are specified in per unit on machine MVA base and X"q must be equal to X"d. The equal value to the reactive part of the corresponding ZSOURCE in power flow is used for sub transient reactance specified in machine data.

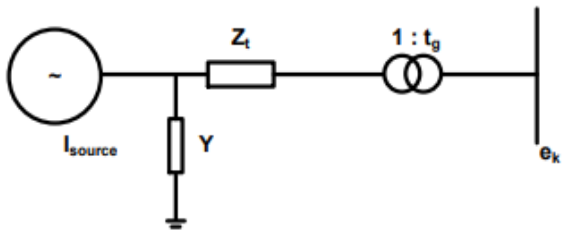

Figure 10: Generator model used for dynamic simulation [24]

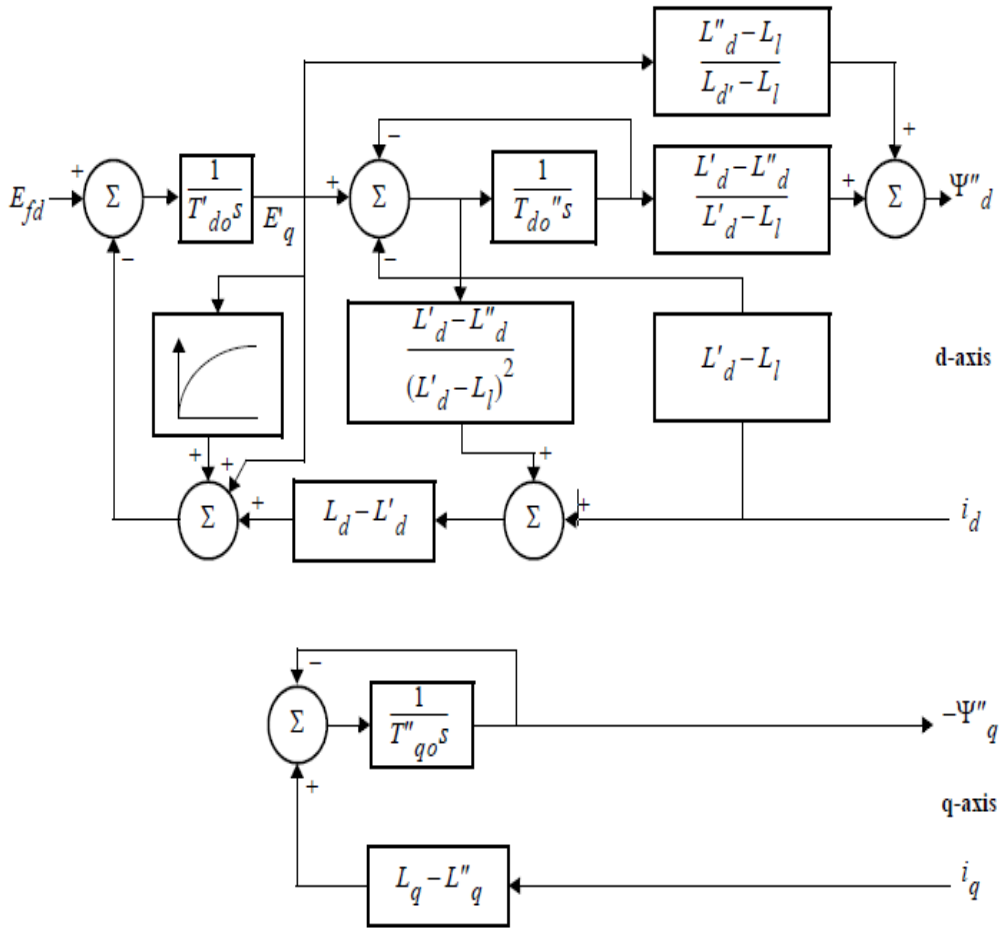

Figure 11: Salient Pole Synchronous Generator Model – GENSAL [24]

Table 11: Parameters of GENSAL Model [24]

Parameter	Description
T'd0 (>0)	d-axis Transient Time Constant (sec)
T''d0 (>0)	d-axis Sub transient Time Constant (sec)
T''q0 (>0)	q-axis Sub transient Time Constant (sec)
H	Inertia Constant (sec)
D	Speed damping factor (pu)
Xd	d-axis Synchronous Reactance (pu)
Xq	q-axis Synchronous Reactance (pu)
X'd	d-axis Transient Reactance (pu)
X''d = X''q	d-axis and q-axis Sub transient Reactance (pu)
Xl	Stator leakage reactance (pu)
S(1.0)	Saturation Factor at 1 pu flux
S(1.2)	Saturation Factor at 1.2 pu flux

2. Turbine-Governor model – HYGOV, PIDGOV

A turbine governor models are designed to perform the function of speed/load control to schedule real power output. This model gives representations of the effects of generating stations on power system stability. PSS/E turbine governor models represent the principle effects inherent in conventional hydro, steam turbine, nuclear, and gas turbine plants. Two types of hydro turbine governors were used in hydro plants modeling in Sri Lankan power system. They are HYGOV and PIDGOV models. All the larger hydro and mini hydro power plants were modeled using HYGOV, other than the Victoria, Samanala, New Laxapana, and Upper Kothmale hydro power plants which were used PIDGOV model for governor frequency control support.

Hydro-Turbine Governor – HYGOV

HYGOV model represents the most used hydro turbine governor which contains a model of the penstock with unrestricted head race and tailrace [24], although this model does not contain a surge tank. This represents a straightforward hydroelectric plant governor [24]. The speed/ load control function provides a feedback speed error to control the gate position. The parameters of the HYGOV model are provided in Table 12. Figure 12 shows the corresponding transfer block diagram of the HYGOV model.

Table 12: Parameters of HYGOV Model [24]

Parameter	Description
R	Permanent Droop
r	Temporary Droop
Tr (>0)	Governor Time Constant (sec)
Tf (>0)	Filter Time Constant (sec)
Tg (>0)	Servo Time Constant (sec)
+ VELM	Gate Velocity Limit
G_{MAX}	Maximum Gate Limit
G_{MIN}	Minimum Gate Limit
Tw (>0)	Water Time Constant (sec)
At	Turbine Gain
Dturb	Turbine Damping
qNL	No power flow

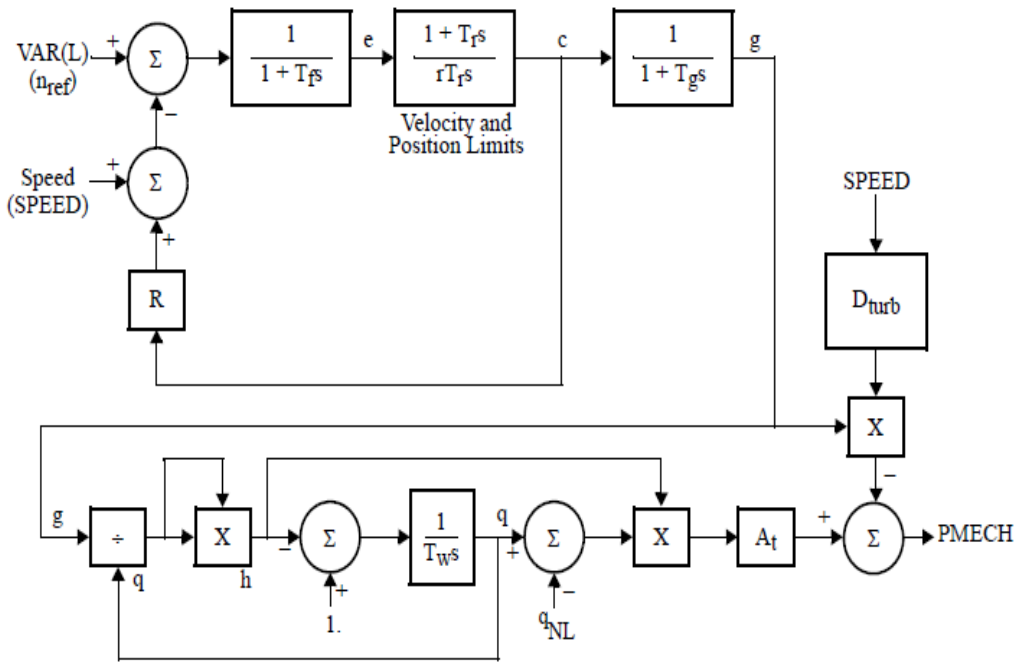

Figure 12: Hydraulic and Governor Model – HYGOV [24]

Hydro Turbine and Governor – PIDGOV

The modeling of plants with straight forward penstock configuration and three term electro-hydraulic governors was carried out with PIDGOV model in PSS/E model library. This model represents a simple turbine-penstock model that does not consider for variation of water inertia effect, which is caused by gate opening [24]. The feedback signal which is used by the governor has two types. They are the gate positon feedback signal and an electrical power feedback signal. The selection of one from these feedback signals is done by setting the feedback flag to one for gate position or zero for electrical power. The generator shaft speed deviation is the input of this model and turbine gate position and mechanical power are the outputs of this model. The parameters of the PIDGOV model are provided in Table 13. Figure 13 shows the complete block diagram of the model. The Modeling of Victoria, Samanala, and New Laxapana power plants were carried out using this PIDGOV type governor model.

Table 13: Parameters of PIDGOV Model [24]

Parameter	Description
R	Permanent Droop (pu)
Treg	Speed Detector Time Constant (sec)
Kp	Proportional Gain (pu/sec)
Ki	Reset Gain (pu/sec)
Kd	Derivative Gain (pu)
Ta (>0)	Controller Time Constant (sec)
Tb (>0)	Servo Time Constant (sec)
Dturb	Turbine Damping Factor, (pu)
G_0	Gate opening at Speed no load (pu)
G_1	Intermediate Gate opening (pu)
P_1	Power at Gate opening G1 (pu)
G_2	Intermediate Gate opening (pu)
P_2	Power at Gate opening G2 (pu)
P_3	Power at full opened gate (pu)
G_{MAX}	Maximum Gate opening
G_{MIN}	Minimum Gate opening
Atw (>0)	Factor multiplying Tw (pu)
Tw (>0)	Water Inertia Time Constant
Velmax	Minimum Gate Opening Velocity (pu/sec)
Velmin < 0	Minimum Gate Closing Velocity (pu/sec)

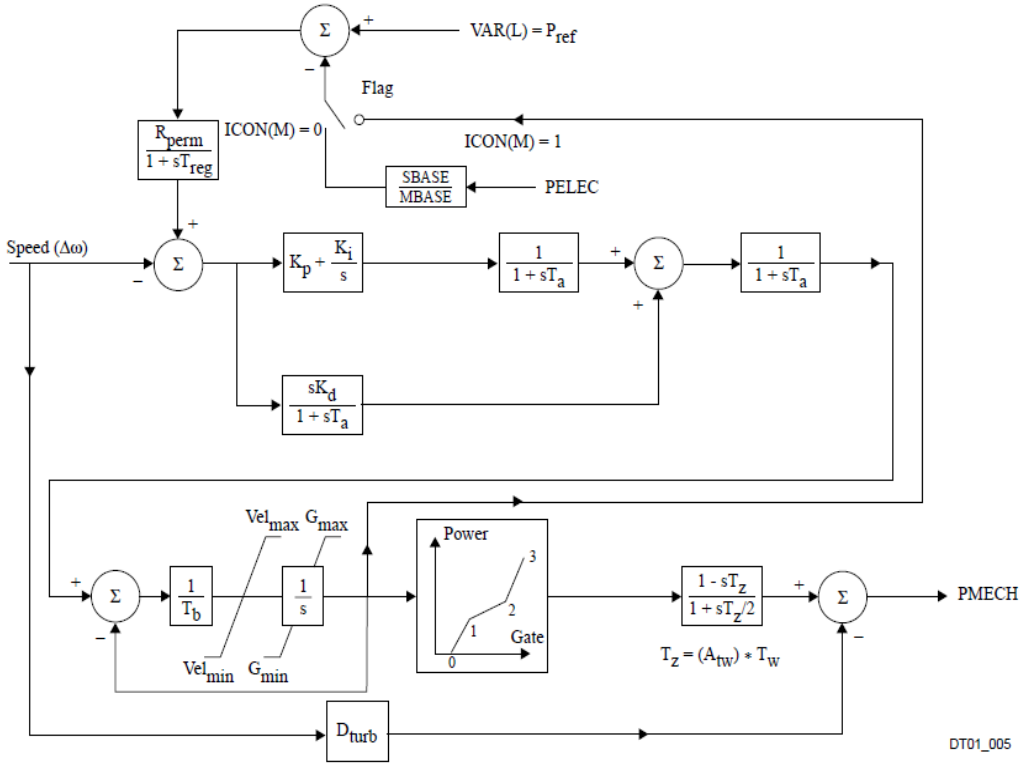

Figure 13: Hydro Turbine and Governor – PIDGOV [24]

3. Excitation System model – SEXS, SCRX, ESAC1A and ESST1A

Three basic approaches of the excitation power source of larger generators are found in Literature [6]. They are rotating direct current exciters, rotating alternating current exciters, and excitation power fed from generator terminals. In all of these cases, the excitation system consists of a high power source of direct current, an intermediate power level controlling circuit, and an instrument power level voltage regulator. The nonlinear characteristics of the excitation power source determine the dynamic behavior of the system influential than the voltage regulator. Therefore, the modeling of an excitation system requires proper consideration of the parameters assigned to the voltage regulators (Gains and time constants) and of the characteristics of excitation power component. PSS/E dynamic model library provides different excitation models to match the requirement of the user to model the power network dynamic characteristics.

Simplified Excitation System

The voltage regulator action of all hydro and mini hydro power plants which are modeled using GENSAl, GENROE, GENROU and GENSAE except Victoria, Samanala, and New Laxapana power plants should be represented by a simple excitation system model. Simplified Excitation System model in PSS/E dynamic model library provides to represent typical conservative response characteristics for this purpose. Figure 14 shows the complete block diagram of the model. The parameters of the Simplified Excitation System model are provided in Table 14. This model is particularly used in cases where the detailed design of the excitation system is not known.

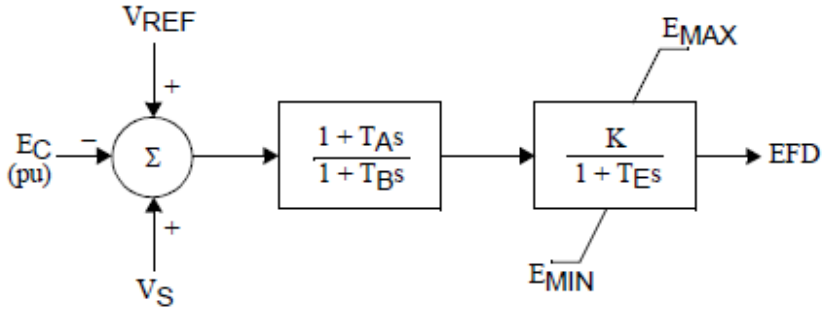

Figure 14: Simplified Excitation System [24]

Table 14: Parameters of Simplified Excitation System Model [24]

Parameter	Description
T_A/T_B	Transient gain reduction time constants
T_B (>0)	Time Constant Exciter (sec)
K	Proportional gain (pu/sec)
T_E	Time constant (sec)
E_{MIN}	Field Voltage Limits (pu)
E_{MAX}	Field Voltage Limits (pu)

Bus or Solid Fed Silicon-Controlled Rectifier Bridge Excitation System – SCRX

This model is also a simplified general model similar to Simplified Excitation System model and not represents any specific excitation system. It represents the general characteristics of excitation systems. This model is used for modeling of Kukuleganga hydro power plant. The first six parameters of Bus or Solid Fed Silicon-Controlled Rectifier Bridge Excitation System are similar to the first six parameters of Simplified Excitation System. Both systems are built with rectifier bridges, allowing field voltage to be represented as independent of field current. The rectifier bridge of this model is fed from a transformer connected directly to the generator terminal or from an independent plant auxiliary bus. The parameters of the model are provided in Table 15. Figure 15 shows the complete block diagram of the Bus or Solid Fed Silicon-Controlled Rectifier Bridge Excitation System model.

Table 15: Parameters of Bus or Solid Fed SCR Bridge Excitation System Model [24]

Parameter	Description
T_A / T_B	Transient gain reduction time constants
T_B (>0)	Time constant Exciter (sec)
K	Proportional gain (pu/sec)
T_E	Time constant (sec)
E_{MIN}	Field Voltage Limits (pu)
E_{MAX}	Field Voltage Limits (pu)
C_{SWITCH}	AC supply is proportional to generator terminal bus voltage or independent of generator terminal voltage
r_C / r_{fd}	Bidirectional and unidirectional excitation systems

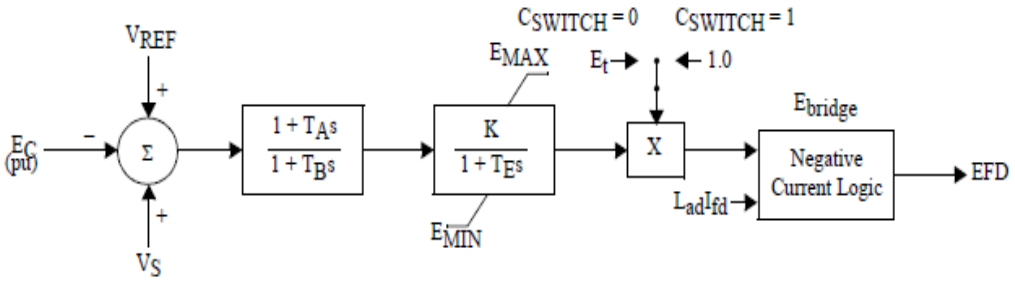

Figure 15: Bus or Solid fed SCR bridge excitation system [24]

IEEE Type AC1A Excitation System - ESAC1A

This model represents a field-controlled alternator rectifier excitation system and it includes an alternator, non-controlled rectifier main exciter. This is not used self-excitation and the power is supplied for voltage regulator through a source without affecting the external transients. This model is used with PIDGOV governors. New Laxapana hydro power station is modeled using this excitation model. Figure 16 shows the complete block diagram of the excitation model. The parameters of the model are provided in Table 16.

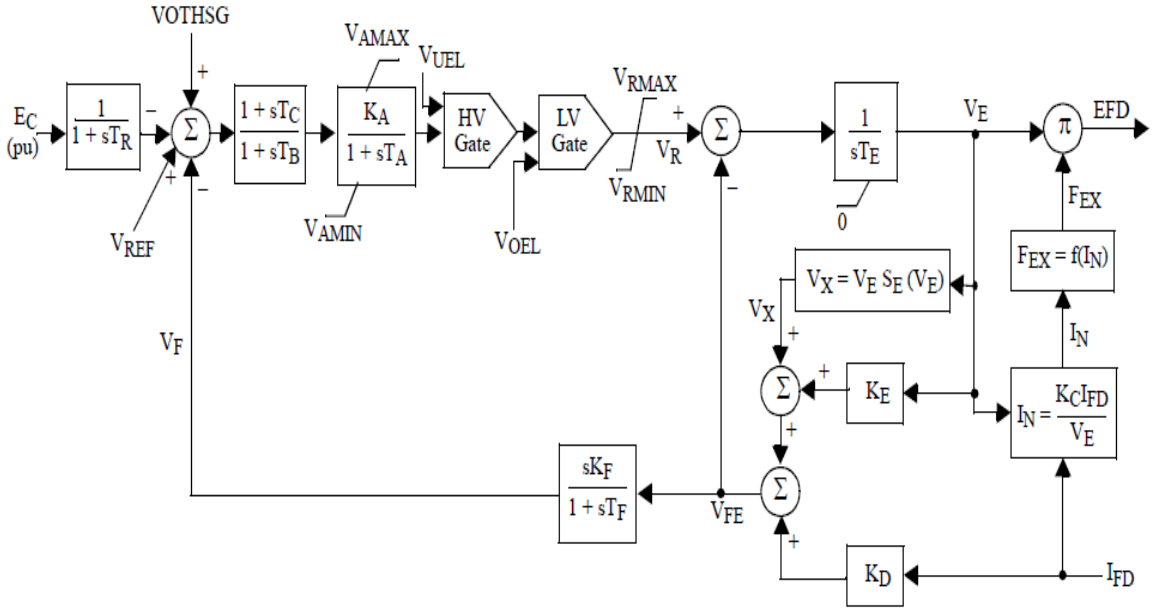

Figure 16: IEEE Type AC1A Excitation System [24]

Table 16: Parameters of IEEE Type AC1A Excitation System Model [24]

Parameter	Description
T_R	Transient gain reduction time constants
T_B	Time constant (sec)
T_c	Time constant (sec)
K_A	Voltage Regulator gain (pu/sec)
T_A	Time constant Voltage Regulator (sec)
V_{AMAX}	Voltage Limits (pu EFD base)
V_{AMIN}	Voltage Limits (pu EFD base)
T_E >0	Time Constant Exciter (sec)
K_F	Feedback Gain (pu/sec)
T_F >0	Time constant Feedback (sec)
K_C	Proportional Gain (pu/sec)
K_D	Proportional Gain (pu/sec)
K_E	Proportional Gain Exciter (pu/sec)
E_1	Field voltage (pu)
$S_E(E_1)$	Saturation Factor
E_2	Field voltage (pu)
$S_E(E_2)$	Saturation Factor
V_{RMAX}	Normalized control source maximum output (pu EFD base)
V_{RMIN}	Normalized control source minimum output (pu EFD base)

IEEE Type ST1A Excitation System - ESST1A

The PSS/E model of IEEE Type ST1A Excitation System is used to represent a potential source-controlled rectifier excitation system. The power supply is taken from a transformer through the auxiliary bus of the model and a controlled rectifier is regulated the output. The maximum voltage of the exciter is directly related to the terminal voltage of the generator. The modeling of the Victoria power station which is used for frequency control in the Sri Lankan power grid was done using this exciter model. Figure 17 shows the complete block diagram of the IEEE Type ST1A Excitation System model. The parameters of the model are provided in Table 17.

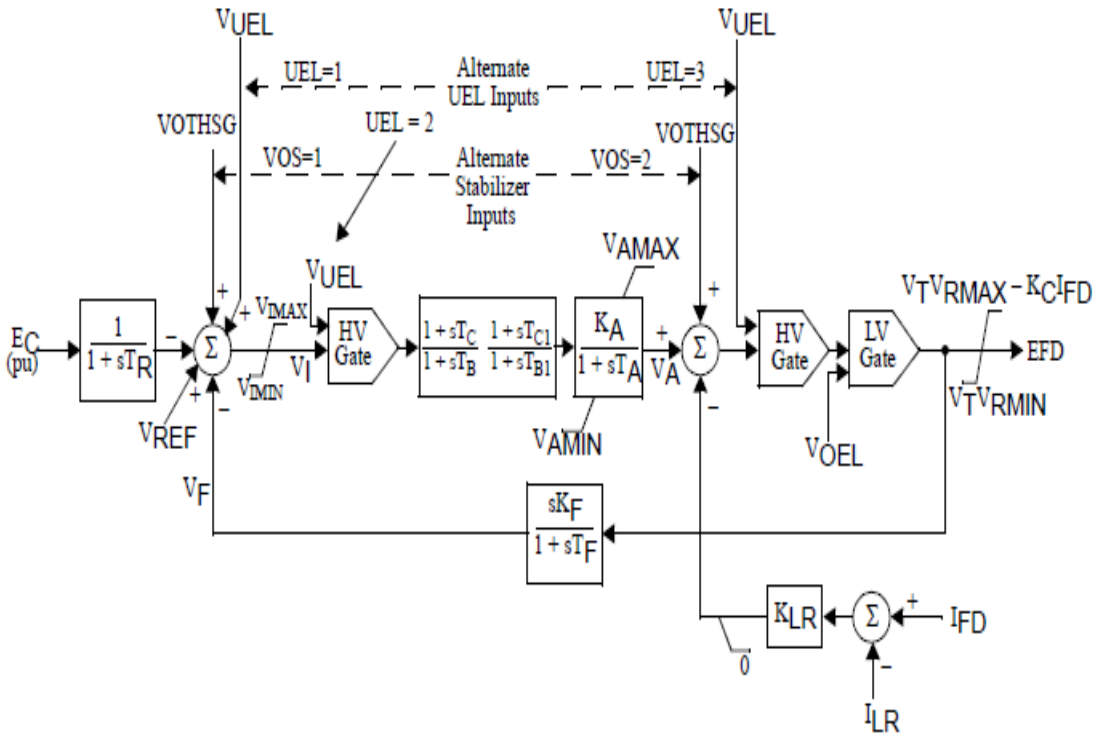

Figure 17: IEEE Type ST1A Excitation System [24]

Table 17: Parameters of the IEEE Type ST1A Excitation System Model [24]

Parameter	Description
T_R	Transient gain reduction time constants
V_{IMAX}	Voltage Limits (pu EFD base)
V_{IMIN}	Voltage Limits (pu EFD base)
T_C	Time constant forward (sec)
T_B	Time constant forward (sec)
T_{C1}	Time constant (sec)
T_{B1}	Time constant (sec)
K_A	Voltage Regulator gain (pu/sec)
T_A	Time constant Voltage Regulator (sec)
V_{AMAX}	Voltage Limits (pu EFD base)
V_{AMIN}	Voltage Limits (pu EFD base)
V_{RMAX}	Normalized control source maximum output (pu EFD base)
V_{RMIN}	Normalized control source minimum output (pu EFD base)
K_C	Proportional gain (pu/sec)
K_F	Feedback gain (pu/sec)
$T_F > 0$	Time constant Feedback (sec)
K_{LR}	Field Current Limiter Gain (pu/sec)
I_{LR}	Field Current Limiter start setting

3.3.2.2 Thermal Power Plant Modeling

All thermal power plants in Table 8 modeled as discussed in this section. Similar to hydro power plant, thermal power plant also consists of Generator model, Turbine-Governor model, and Excitation System model in PSS/E power system dynamic modeling.

1. Generator model - GENSROU

GENROU model which is a round rotor synchronous generator (Quadratic saturation) type in PSS/E is used for thermal power plant modeling other than Sapugaskanda Power Station which is used GENSAL model. The parameters of the GENROU model are provided in Table 18. Figure 18 shows the corresponding transfer block diagram of GENSAL generator model in PSS/E. Other than the additional q-axis data values, Tqo and Xq, GENROU model is used in exactly the same way as GENSAL model.

Table 18: Parameters of GENROU Model [24]

Parameter	Description
T'do (>0)	d-axis transient time constant (sec)
T''do (>0)	d-axis subtransient time constant (sec)
T'qo (>0)	q-axis transient time constant (sec)
T''qo (>0)	q-axis subtransient time constant (sec)
H	Inertia constant (sec)
D	Speed damping factor (pu)
Xd	d-axis synchronous reactance (pu)
Xq	q-axis synchronous reactance (pu)
X'd	d-axis transient reactance (pu)
X'q	q-axis transient reactance (pu)
X''d = X''q	d-axis and q-axis subtransient reactance (pu)
Xl	Stator leakage reactance (pu)
S(1.0)	Saturation factor at 1 pu flux
S(1.2)	Saturation factor at 1.2 pu flux

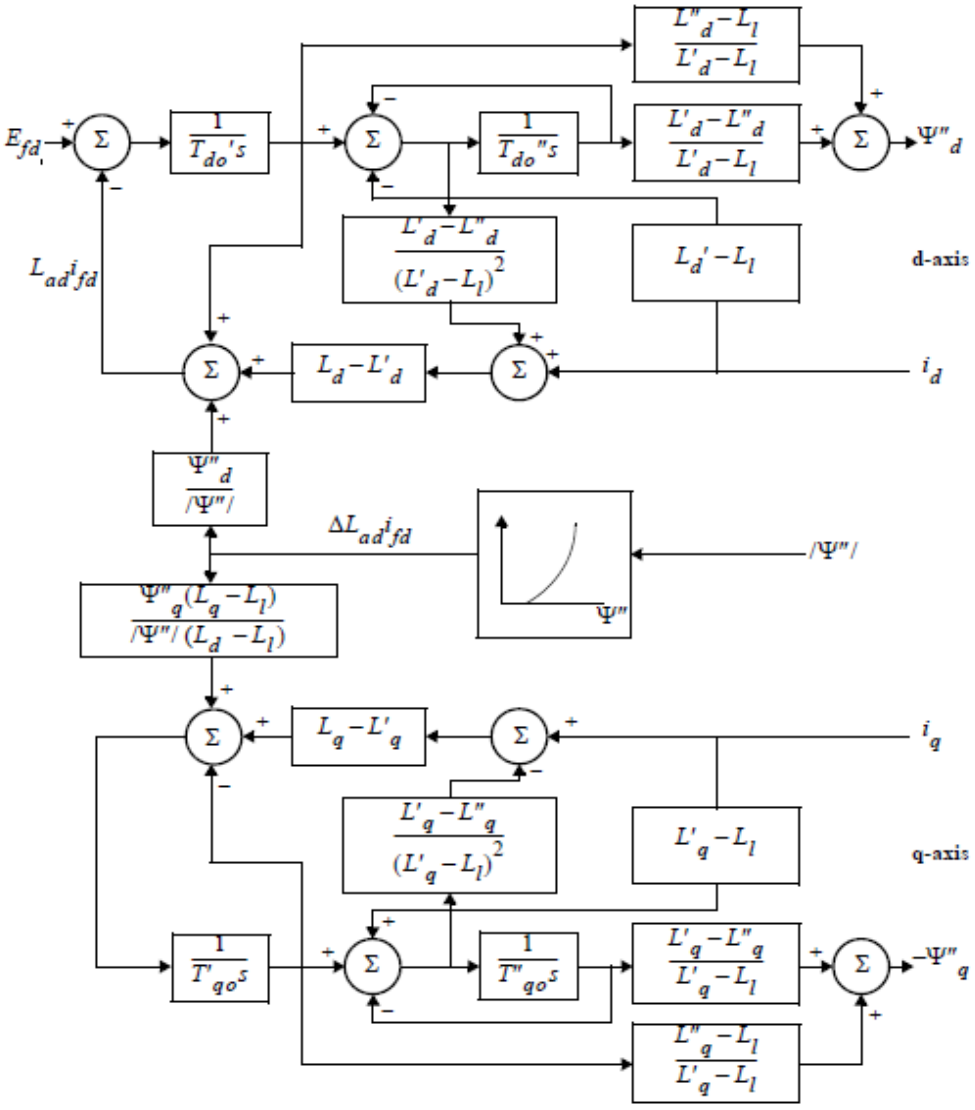

Figure 18: Round Rotor Synchronous Generator Model – GENROU [24]

2. Turbine-Governor model- TGOV1, GAST and DEGOV1

Two types of turbine governors used in modeling of thermal plants in Sri Lankan power system consisting coal fired power plant and oil fired power plants. The steam turbine of plant fired power plant in Norochcholei is modeled using TGOV1 steam turbine model in PSS/E. All the other thermal power plants are Oil fired power plants and the gas turbines of these power plants are modeled using GAST gas turbine governor model while steam turbines are modeled using TGOV1 model. Sapugaskanda Diesel power plant is modeled using DEGOV1 Woodward Diesel Governor.

Steam Turbine - Governor Model – TGOV1

This model represents the governor and the effect of time constant of reheater in a steam turbine. TGOV1 model in PSS/E dynamic model library is used for modeling of coal fired power plant in Norochcholei, which is known as Lakvijaya coal power plant. The modeling of the steam turbine governor in other Oil fired power plants also used TGOV1. Figure 19 shows the complete block diagram of the TGOV1 model. The parameters of the model are provided in Table 19.

Table 19: Parameters of Steam Turbine - Governor Model [24]

Parameter	Description
R	Permanent Droop (pu)
T_1 (>0)	Governor controller lag Time Constant (sec)
V_{MAX}	Maximum fuel valve opening (pu)
V_{MIN}	Minimum fuel valve opening (pu)
T_2	Governor controller lead Time Constant (sec)
T_3 (>0)	Reheater time constant (sec)
D_t	Turbine Speed damping coefficient of rotor (pu)

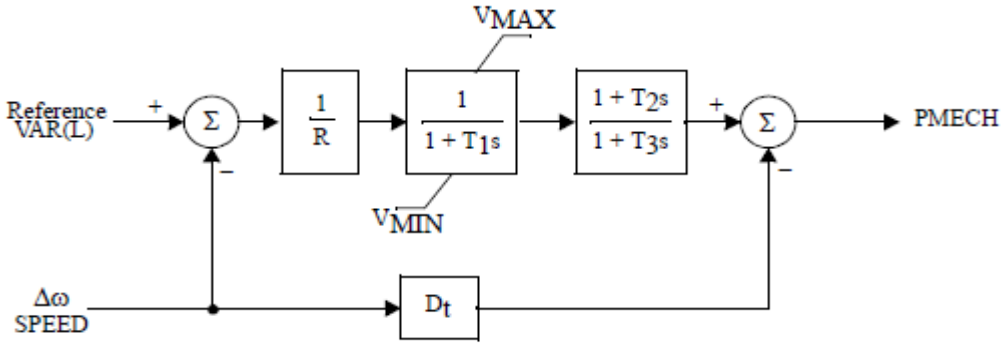

Figure 19: Steam Turbine - Governor Model [24]

Gas Turbine-Governor model – GAST

This model represents the basic dynamic characteristics of industrial gas turbines. The speed variations are expected to be small in this model. Kelanitissa, Sapugaskanda, Barge, Yugadanavi (Kerawalapitiya), Sojits Kelanitissa (AES Kelanitissa), Asia Power Sapugaskanda, and Chunnakam (Uthuru Janani) are the Oil fired power plants in Sri

Lankan power system in year 2019 model. All these thermal power plants are modeled by using GAST Gas Turbine-Governor model in PSS/E. The parameters of the model are provided in Table 20. Figure 20 shows the complete block diagram of the GAST model.

Table 20: Parameters of GAST Model [24]

Parameter	Description
R	Permanent Droop (pu)
T_1 (>0)	Forward path Governor Time Constant (sec)
T_2 (>0)	Combustion chamber Time Constant (sec)
T_3 (>0)	Exhaust gas measuring system Time Constant (sec)
A_t	Ambient Temperature Load Limit
K_T	Load limited feedback gain (pu)
V_{MAX}	Maximum fuel valve opening (pu)
V_{MIN}	Minimum fuel valve opening (pu)
D_{turb}	Turbine damping (pu)

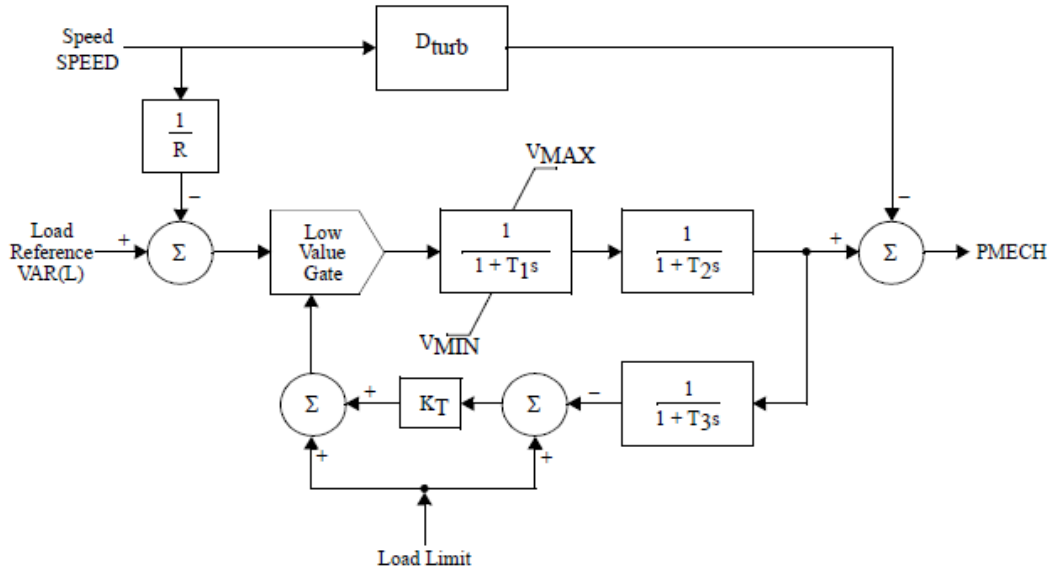

Figure 20: Gas Turbine-Governor Model – GAST [24]

Woodward Diesel Governor – DEGOV1

This model represents an isochronous governor for a diesel engine in a diesel power plant [24]. The turbine governor of Sapugaskanda diesel power plant is modeled using DEGOV1 in PSS/E where droop control is used with throttle or feedback of electric

power. Woodward Diesel Governor model consists of a diesel engine, a hydro-mechanical actuator, and an electric speed sensor. The output of the hydro-mechanical actuator is the position of the valve of the fuel supply. The use of this model is restricted to diesel generators operating isolated from other synchronous generators [24]. The parameters of the model are provided in Table 21. Figure 21 shows the complete block diagram of the Woodward Diesel Governor model.

Table 21: Parameters of Woodward Diesel Governor Model [24]

Parameter	Description
T_1	Governor controller lag time constant (sec)
T_2	Governor controller lead time constant (sec)
T_3	Valve servomotor time constant (sec)
K	The inverse of governor speed droop
T_4	Steam bowl time constant (sec)
T_5	Steam reheat time constant (sec)
T_6	Crossover time constant (sec)
T_D	Dead time (sec)
T_{MAX}	Time constant Maximum (sec)
T_{MIN}	Time constant Minimum (sec)
R	Permanent droop (pu)
T_E	Time constant (sec)

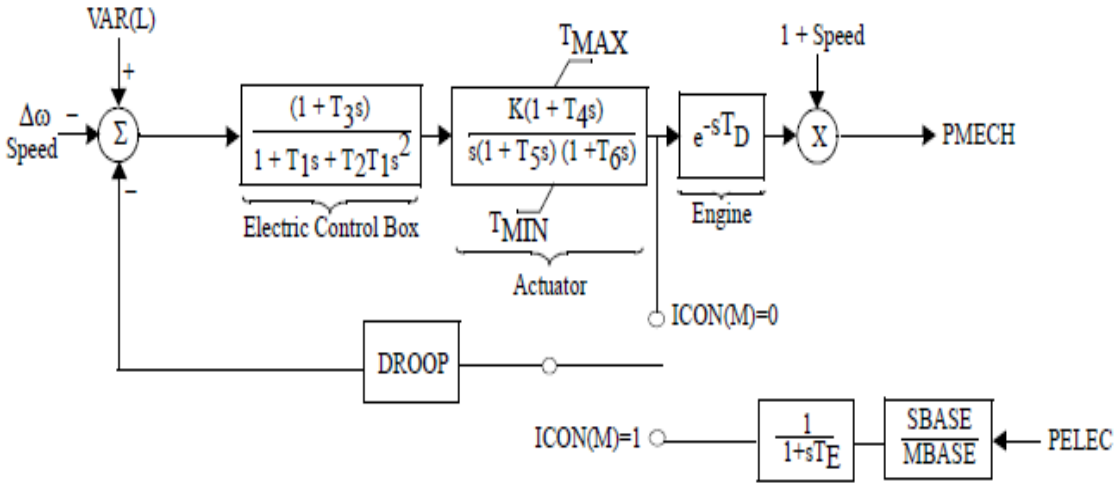

Figure 21: Woodward Diesel Governor [24]

3. Excitation System model – SEXS, EXST1 and ESAC1A

The Simplified Excitation System model is used for modeling of excitation systems all the thermal power plants in 2019 power system of Sri Lanka except Sapugaskanda diesel power plant, which is used IEEE Type AC1A Excitation System model and Lakvijaya coal fired power plant, which is used IEEE Type ST1 Excitation System model. The Simplified Excitation System model and IEEE Type AC1A Excitation System model were previously described in hydro power plant modeling section.

IEEE Type ST1 Excitation System – EXST1

The IEEE Type ST1 Excitation System model is a potential source-controlled rectifier excitation system. This model represents excitation systems in which power is supplied by a transformer from the generator terminal similar to the ESST1A model in PSS/E. Figure 22 shows the complete block diagram of the EXST1 model. The parameters of the model are provided in Table 22.

Table 22: Parameters of IEEE Type ST1 Excitation System Model [24]

Parameter	Description
T_R	Transient gain reduction Time Constants (sec)
V_{IMAX}	Voltage Limits (pu EFD base)
V_{IMIN}	Voltage Limits (pu EFD base)
T_C	Forward Time Constant (sec)
T_B	Forward Time Constant (sec)
K_A	Voltage Regulator gain (pu/sec)
T_A	Time Constant (sec)
V_{R_MAX}	Voltage Limits (pu EFD base)
V_{R_MIN}	Voltage Limits (pu EFD base)
K_C	Voltage Regulator Gain (pu/sec)
K_F	Voltage Regulator Gain (pu/sec)
T_F (>0)	Forward Time constant (sec)

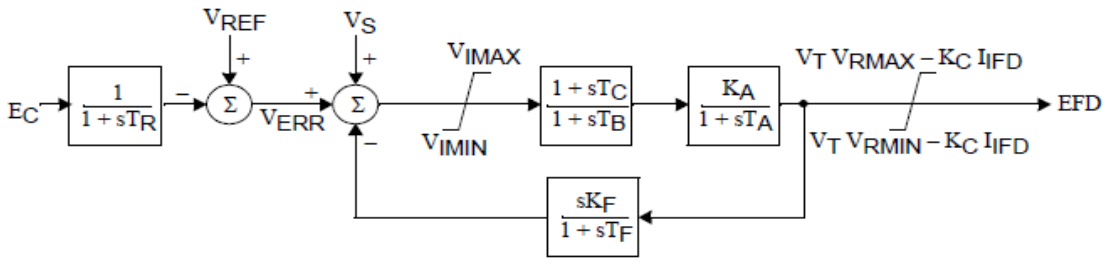

Figure 22: IEEE Type ST1 Excitation System [24]

3.3.2.3 Wind Power Plant Modeling

All wind power plants in Table 9 were modeled as discussed in this section. Similar to hydro power plants and thermal power plants, wind power plants also consist of a Generator-Turbine model in PSS/E power system dynamic modeling. The wind turbines are categorized into four types. According to the type, generic wind models in PSS/E are also categorized into four wind turbine generator models like WT1, WT2 WT3, and WT4.

1. Wind Turbine Generator Model – WT4 (Type 4)

WT4 wind turbine dynamic stability model is used to model all wind power plants in the year 2019. This model represents the wind turbine with a grid connected generating unit from the power converter. Figure 23 shows the representation of WT4 wind turbine dynamic stability model. In this model a grid connected power converter is used to decouple the generator from power grid as shown in Figure 23.

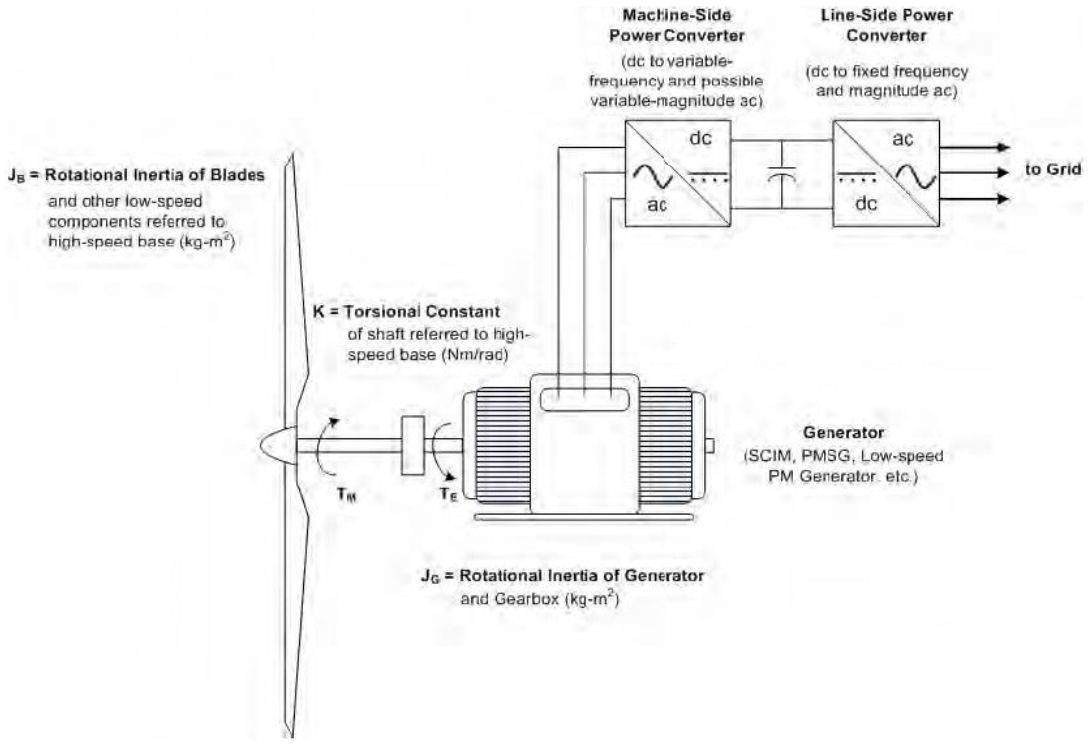

Figure 23: Representation of WT4 Generator connected to the grid through the power converter [24]

In the power flow setup of this model, this power converter is treated as a wind machine category of the existing generator record of the raw data file of power flow. In other words, it is similar to a wind machine that controls a remote bus voltage with a specific range of reactive power.

The dynamic setup of this model consists of two models. They are, WT4G1 which is a wind generator model (type 4) with power converter, and WT4E1 which is an electrical control model for type 4 wind generator. Figure 24 illustrates the connectivity diagram of WT4 module in PSS/E.

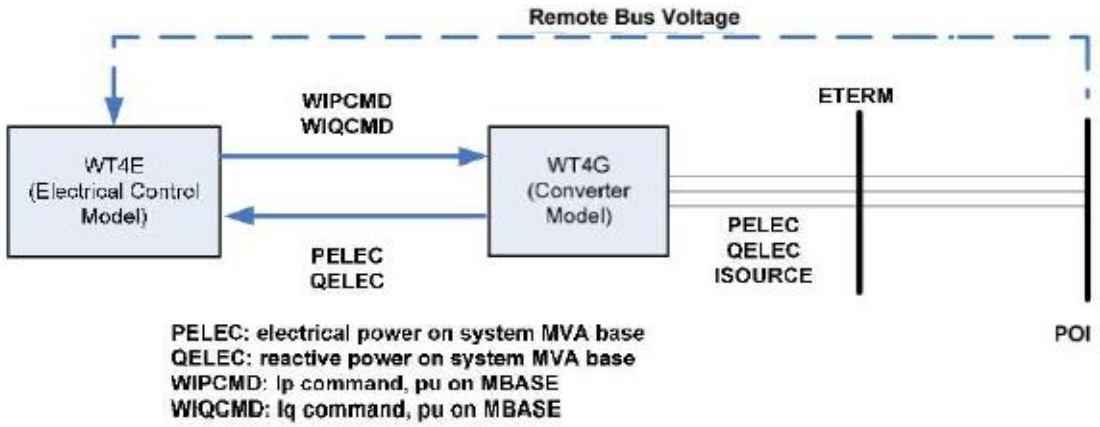

Figure 24: WT4 Connectivity Diagram [24]

The WT4G1 wind generator model calculates the current injection into the grid by considering the active and reactive power commands from the electrical control model. The parameters of the WT4G1 wind generator model are provided in Table 23. Figure 25 shows the WT4G1 wind generator model block diagram.

Table 23: Parameters of WT4G1 Wind Generator/Converter Model [24]

Parameter	Description
T_{Eqcmd}	Converter Time Constant for Iqcmd (sec)
T_{Ipcmd}	Converter Time Constant for Ipcmd (sec)
V_{LVPL1}	Low Voltage Power Logic Voltage 1 (pu)
V_{LVPL2}	Low Voltage Power Logic Voltage 2 (pu)
G_{LVPL}	Low Voltage Power Logic Gain (pu)
V_{HVRCR}	High Voltage Reactive Current Limiter Voltage (pu)
CUR_{HVRCR}	High Voltage Reactive Current Limiter Current (pu)
R_{Ip_LVPL}	Rate of Active Current Change in Low Voltage Power Logic
$T_{\_LVPL}$	Time Constant of Voltage sensor for Low Voltage Power Logic (sec)

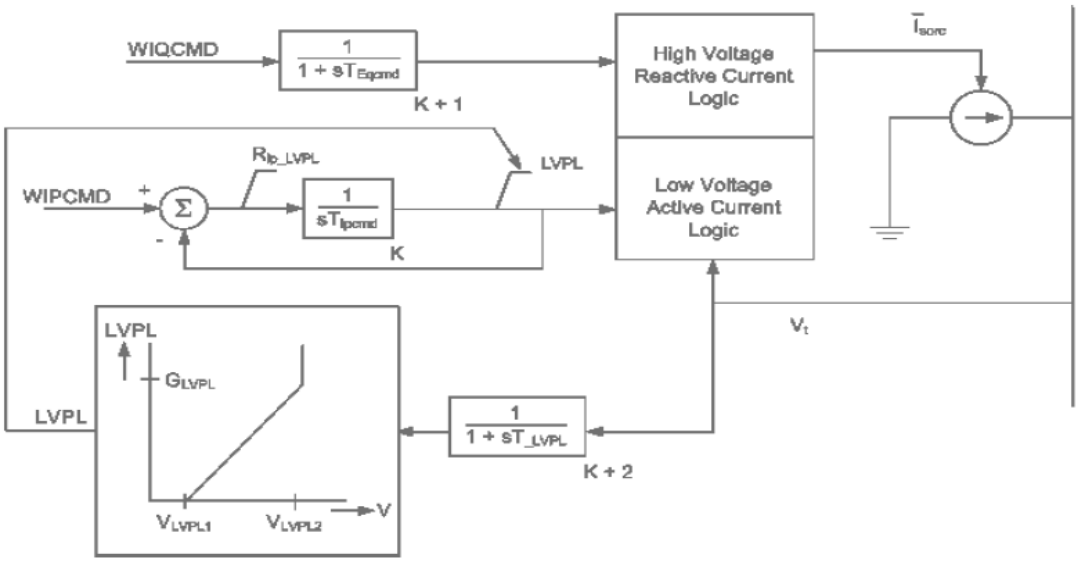

Figure 25: WT4G1 Wind Generator/Converter Model [24]

The WT4E1 electrical control model includes the reactive and active power controls. The reactive current commands for remote bus voltage control, power factor control and reactive power control are calculated by reactive control model, which is shown in Figure 26.

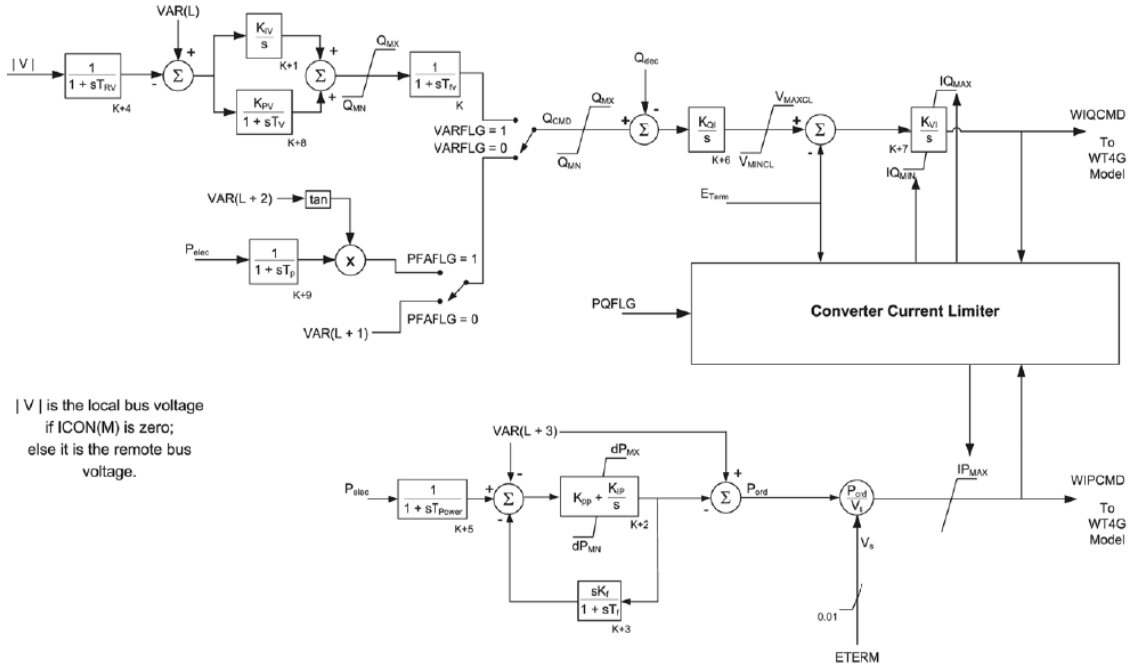

Figure 26: WT4E1 Electrical Control Model [24]

Table 24: Parameters of WT4E1 Electrical Control Model [24]

Parameter	Description
T_W	Filter Time Constant of Voltage Regulator (sec)
K_{pv}	Proportional Gain of Voltage Regulator (pu)
K_{iv}	Integrator Gain of Voltage Regulator (pu)
K_{pp}	Proportional Gain of Torque Regulator (pu)
K_{ip}	Integrator Gain of Torque Regulator (pu)
K_f	Rate Feedback Gain (pu)
T_f	Rate Feedback Time Constant (sec)
Q_{mx}	Maximum Limit in Voltage Regulator (pu)
Q_{mn}	Minimum Limit in Voltage Regulator (pu)
IPmax	Maximum Active Current Limit (pu)
Trv	Voltage Sensor Time Constant (sec)
dPMX	Maximum Power Order Rate (pu)
dPMN	Minimum Power Order Rate (pu)
Tpower	Power Reference Filter Time Constant (sec)
KQi	Volt/Mvar gain
Vmincl	Minimum Voltage Limit (pu)
Vmaxcl	Maximum Voltage Limit (pu)
KVi	Int. volt/Term. Voltage gain
Tv	Lag in Wind var Controller (sec)
Tp	Electrical Power Filter in Fast PF Controller (sec)
ImaxTD	Converter Current Limit (pu)
Iphl	Hard Active Current Limit (pu)
Iqhl	Hard Reactive Current Limit (pu)

3.3.2.4 Solar Power Plant Modeling

All solar power plants in Table 10 were modeled as discussed in this section. In the load flow setup of this model, a power converter connected to the grid is decoupled the PV panels from the grid similar to the WT4 wind machine model. This model represents a wind machine that controls a remote bus voltage with a specific range of reactive power. The source reactance of this model set to infinity as most power electronic devices for load flow models.

The dynamic setup of this model consists of four modules. Similar to wind power plants, solar power plants also consist of a power converter or a generator model (PVGU) and an electrical control model (PVEU). Other two different models are introduced specifically for solar power plants. They are a linearized model of a panel's output curve module (PANEL) and a linearized solar irradiance profile (IRRAD). These

modules are under Photovoltaic (PV) Generic Model category in PSS/E power system dynamic modeling for solar power plants. The PV model connectivity diagram is illustrated in Figure 27.

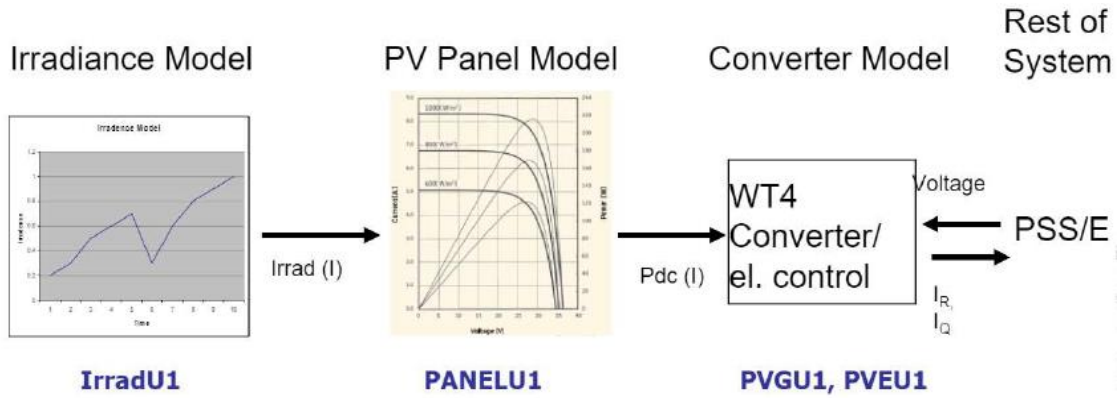

Figure 27: PV Connectivity Diagram [24]

1. Power Converter or Generator Model – PVGU1 (PV Converter)

Figure 28 shows the PVGU1 power converter or a generator model block diagram. The parameters of PVGU1 model are similar to the parameters of WT4G1 wind generator model, which are provided in Table 23.

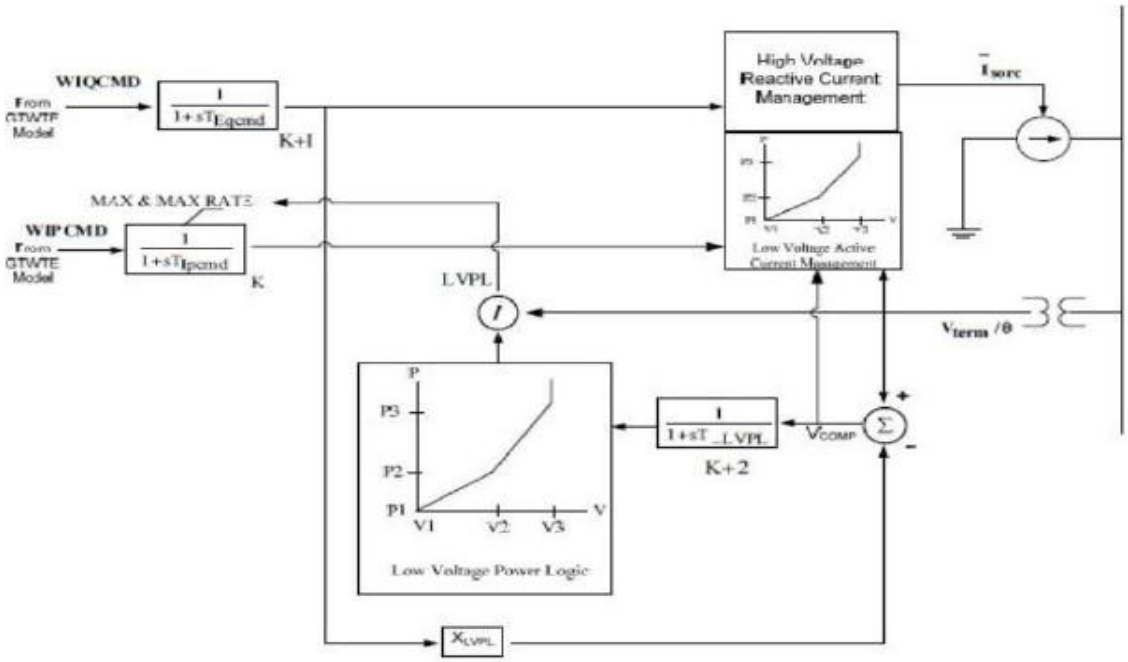

Figure 28: PVGU1 Power Converter/Generator Model [24]

2. **Electrical Control Model – PVEU1 (Electrical Control model for converter)**

The parameters of the PVEU1 electrical control model are similar to the parameters of WT4E1 wind generator model, which are provided in Table 24. Additionally, Maximum Power from Solar Plant (MW) parameter is provided in this model. Figure 29 shows the PVEU1 electrical control model block diagram.

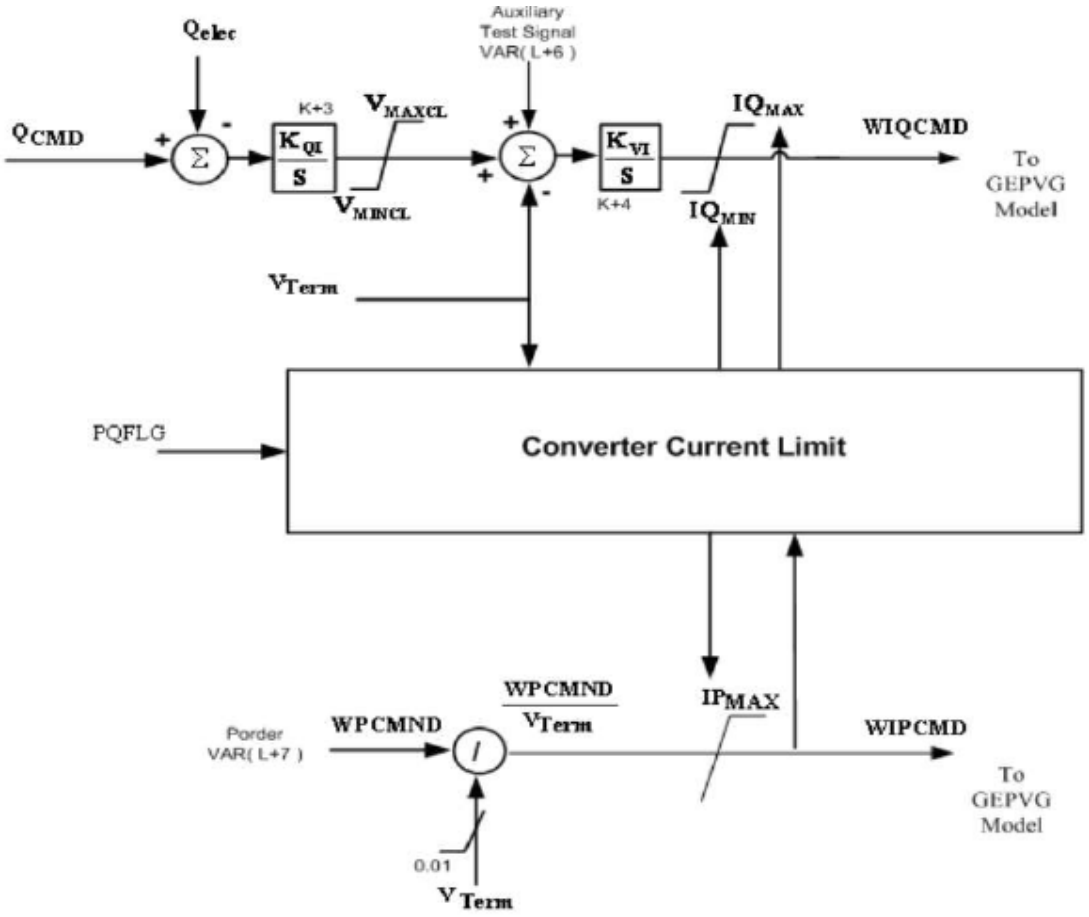

Figure 29: Block Diagram of PVEU1 Electrical Control Model [24]

3. **Linearized Model of a Panel's Output Curve Model – PANELU1 (I-P characteristics)**

The parameters of the Linearized Model of a Panel's Output Curve Model are provided in Table 25.

Table 25: Parameters of PANELU1 (I-P characteristics) [24]

Parameter	Description
PDCMAX200	Maximum Power of Solar Panel at an Irradiance Level of 200 W/m^2 (pu on PDCMAX1000 base)
PDCMAX400	Maximum Power of Solar Panel at an Irradiance Level of 400 W/m^2 (pu on PDCMAX1000 base)
PDCMAX600	Maximum Power of Solar Panel at an Irradiance Level of 600 W/m^2 (pu on PDCMAX1000 base)
PDCMAX800	Maximum Power of Solar Panel at an Irradiance Level of 800 W/m^2 (pu on PDCMAX1000 base)
PDCMAX1000	Maximum Power of Solar Panel at an Irradiance Level of 1000 W/m^2 (pu on PDCMAX1000 base)

4. Linearized Solar Irradiance Profile – IRRADU1 (PV Irradiance profile)

The parameters of the Linearized Solar Irradiance Profile or PV Irradiance profile are provided in Table 26.

Table 26: Parameters of IRRADU1 (PV Irradiance profile) [24]

Parameter	Description
TIME1	Time of Data Point 1 (sec)
IRRADIANCE1	Irradiance Level at Data Point 1 (W/m^2)
TIME2	Time of Data Point 2 (sec)
IRRADIANCE2	Irradiance Level at Data Point 2 (W/m^2)
TIME3	Time of Data Point 3 (sec)
IRRADIANCE3	Irradiance Level at Data Point 3 (W/m^2)
TIME4	Time of Data Point 4 (sec)
IRRADIANCE4	Irradiance Level at Data Point 4 (W/m^2)
TIME5	Time of Data Point 5 (sec)
IRRADIANCE5	Irradiance Level at Data Point 5 (W/m^2)
TIME6	Time of Data Point 6 (sec)
IRRADIANCE6	Irradiance Level at Data Point 6 (W/m^2)
TIME7	Time of Data Point 7 (sec)
IRRADIANCE7	Irradiance Level at Data Point 7 (W/m^2)
TIME8	Time of Data Point 8 (sec)
IRRADIANCE8	Irradiance Level at Data Point 8 (W/m^2)
TIME9	Time of Data Point 9 (sec)
IRRADIANCE9	Irradiance Level at Data Point 9 (W/m^2)
TIME10	Time of Data Point 10 (sec)
IRRADIANCE10	Irradiance Level at Data Point 10 (W/m^2)

3.3.2.5 Load Modeling - CLODAL

The loads were modeled as Complex Load Models (CLODAL model) along with ZIP load model (Constant Power/Current/Admittance) as shown in Table 27. This complex type load models will replace all constant MVA, Current, and admittance load with a composite load including induction motors, lighting and other types of equipment. This model used the situations where it is necessary to represent loads at the dynamic level. Figure 30 shows the representation of block diagram of CLODAL load model.

Table 27: Details of CLODAL model (Complex Load Model)

Load Type	Load category (%)		
	Industrial Loads	Commercial Loads	Domestic Loads
Large Motors	5	1	0
Small Motors	25	30	10
Discharge Lighting	1	1	1
Transformer Saturation	10	10	20
Constant MVA	30	30	30
Constant Current and Impedance loads	29	28	39
Total	100	100	100

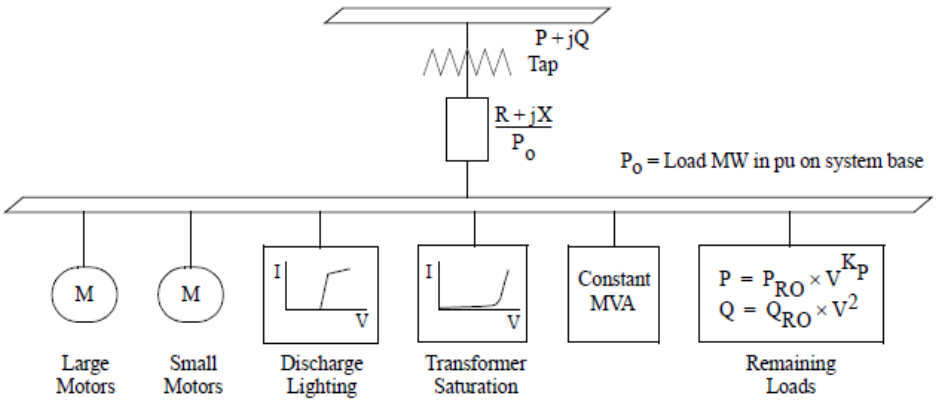

Figure 30: Representation of Block Diagram of CLODAL Load Model [24]

3.3.2.6 Load Shedding Scheme Modeling – LDSHBL, DLSHBL

The modeling of the present LSS for this study, which is in Table 2, is discussed in this section. The load relay models in PSS/E model library include mainly two types: under frequency and under voltage load shedding relays. These models provide multiple

stages. Each stage consists of a defined specific frequency or a voltage threshold, a pickup time and a fraction of load to shed. LDSHBL model of DLSHBL load relay model type is used for this study to model present UFLS scheme. It represents solid state type load shedding relays. This model disconnects fraction of the load at each load bus according to the defined stages of LSS. The parameters of LDSHBL are provided in Table 28 and the parameters of DLSHBL are provided in Table 29.

Table 28: Parameters of LDSHBL [24]

Parameter	Description
f1	Load Shedding Frequency Point 1 (Hz)
t1	Pickup Time Point 1 of Load Shedding Relay (sec)
frac1	Fraction of load to be shed at Frequency Point 1
f2	Load Shedding Frequency Point 2 (Hz)
t2	Pickup Time Point 2 of Load Shedding Relay (sec)
frac2	Fraction of load to be shed at Frequency Point 2
f3	Load Shedding Frequency Point 3 (Hz)
t3	Pickup Time Point 3 of Load Shedding Relay (sec)
frac3	Fraction of load to be shed at Frequency Point 3
Tb	Breaker Time (sec)

Table 29: Parameters of DLSHBL [24]

Parameter	Description
f1	Load Shedding Frequency Point 1 (Hz)
t1	Pickup Time Point 1 of Load Shedding Relay (sec)
frac1	Fraction of load to be shed at Frequency Point 1
f2	Load Shedding Frequency Point 2 (Hz)
t2	Pickup Time Point 2 of Load Shedding Relay (sec)
frac2	Fraction of load to be shed at Frequency Point 2
f3	Load Shedding Frequency Point 3 (Hz)
t3	Pickup Time Point 3 of Load Shedding Relay (sec)
frac3	Fraction of load to be shed at Frequency Point 3
Tb	Breaker Time (sec)
df1	Rate of Change of Frequency at Load Shedding Point 1 (Hz/sec)
df2	Rate of Change of Frequency at Load Shedding Point 2 (Hz/sec)
df3	Rate of Change of Frequency at Load Shedding (Hz/sec)

The DLSH type model is an extension to the LDSH type with the defined frequency decay or ROCOF. The timers of Load shedding relay is activated when the frequency decay is below the shedding frequency point and magnitude of ROCOF is above threshold in the scheme. The timers will reset in any case of violation of defined setting values.

CHAPTER 4

MODEL VALIDATION

The model validation is an important procedure of the power system simulation studies for maintaining the reliability and accuracy of power system. It is necessary to ensure the power system models are up-to-date and accurate by validating the developed system model, which provides the foundation for all power system analysis. Therefore, model validation is an essential task to update with additions and ongoing power system changes. Recreation of the failure event, verification of the model, and correlation with actual data are the three main approaches of model validation to indicate the quality and accuracy of the developed system model. It is possible to analyze the performance of the real grid, once the power system model has been designed and validated using power system software. The models are used for both operating studies including setting real-time power transfer limits and for planning studies including analyzing conditions in the future.

The power system models used for future planning studies cannot be validated directly. However, future power system models are validated indirectly by using the present power system models, which represent the existing measurements and facilities. Planning system models are developed by modeling future forecasted measurements in the validated model with existing measurements, which are not expected to change in the future. The modeling of power systems with all of the performance is required for the prediction of power system performance. The power system planning engineers must understand the power system performances and assumptions for model development to model power system behavior. The simulations of past failure events are the best way to understand the system behavior by observing, measuring, and analyzing the power system's actual performance, which provides the best opportunity for system model validation.

Importance of Model Validation

The simulation results of power system studies are used for making decisions on grid planning and operating. The power system models are used for simulation studies to predict the system performance during contingency events. It is important to ensure, the power system is modeled including all dynamic simulation models with accurate and up-to-date data. As mentioned in [25], optimistic models can create unsafe operating conditions, which lead to system widespread power failures, such as the blackout that occurred in the summer of 1996 in the Western Interconnection. The planning engineers reproduced the event in simulations, but the actual disturbance and simulated response of the disturbance were failed to correlate. Successful validation studies are one of the important requirements for power system planning. On the other hand, pessimistic models and assumptions create the network capacity underutilization and unnecessary capital investment, which increases the power generation cost. Therefore, validated realistic models are required for ensuring the reliability and economic feasibility of power system operation.

4.1 Validation of 2019 Power System Model

Steady state models or power flow models are considered as the foundation of system studies. They are required for power system validation with actual system values and operational practices. In this research, the 2019 Sri Lankan power system was used for model validation, which was created in PSS/E software. The validation process was conducted by recreating and simulating the recent failure event on the existing power system model. It is required to compare actual system measured values and modeled values in a computer simulation software model. Transmission lines, transformers, shunt devices, generators, and loads data are required for modeling the load flow case as the first step of system validation. According to the selected failure event, actual measured data, generation dispatch, load demand profiles, power plant dynamic data, reactive power compensators, network configuration, and power plant operational characteristics were adjusted to match the conditions of the event. The comparison of the simulated

results and actual data were done after solving the power flow case using Newton Raphson, which is an iterative method.

Analysis of the Frequency Failure Event of 25th July 2019 at 11.09 am

A failure has occurred on 25th July 2019 at 11.09 am involving fully loaded GT 07 of Kelanitissa Power Station (KPS) tripped at 50.08 Hz. The recorded system demand and the recorded system generation before the fault occurred were as stated in Appendix C. System generation was 1,910.7 MW and load demand was 1,879.3 MW at the time before the fault occurred. For the model validation, system frequency variation during Kelanitissa GT 07 generator failure on 25th July 2019 was simulated in the year 2019 PSS/E model. System generation capacities and load data were changed according to the pre fault data of fully loaded GT 07 of Kelanitissa Power Station (KPS) tripping event in the developed 2019 PSS/E model. The frequency control machine was GEN-2 of Kothmale power plant on the time of the fault occurred. The hydro machines in Table 30 were used in free governor mode for primary frequency control. That implies, each machine unit in Table 30 is being able to provide support for the frequency error correction during disturbances. The speed droop setting of the hydro governor determine the amount of support and the typical action time from 5 to 20 seconds. These generators vary their output according to the frequency changes based on availability of generation technology. In 2019 PSS/E model, all of these data was changed according to the pre fault power generation data and load demand data.

Disturbance : Tripping of GT 07 of Kelanitissa Power Station (KPS)
Total Power Loss : 115.0 MW
Pre Fault System Demand : 1,879.3 MW
Pre Fault System Generation : 1,910.7 MW

Table 30: Machine Governors used in Free Governor Mode

Generator Name	PGen (MW)	PMax (MW)	Turbine Governor Model in PSS/E	Permanent Droop (R)
KOTHMALE GEN-2	52.2295	67	HYGOV	0.05
NEW LAXAPANA 1	39.9994	50	PIDGOV	0.059
UPPER KOTHMALE GEN-1	49.9999	75	HYGOV	0.05

The actual system data records of the failure event were collected from National System Control Center, CEB. Figure 31 and Figure 32 are illustrating the frequency response of the actual system data record of the event, which was recorded in Fault Event Recorder (Ben recorder) installed in Biyagama grid substation. This data includes not only the system frequency, but also currents and voltages of at the outgoing 220 kV Kelanitissa transmission line. Kelanitissa GT 07 generator was tripped at 11.09 hours on 25th July 2019 as recorded in the Ben recorder. After tripping of Kelanitissa GT 07 generator, system was recovered with UFLS by activating Stage I.

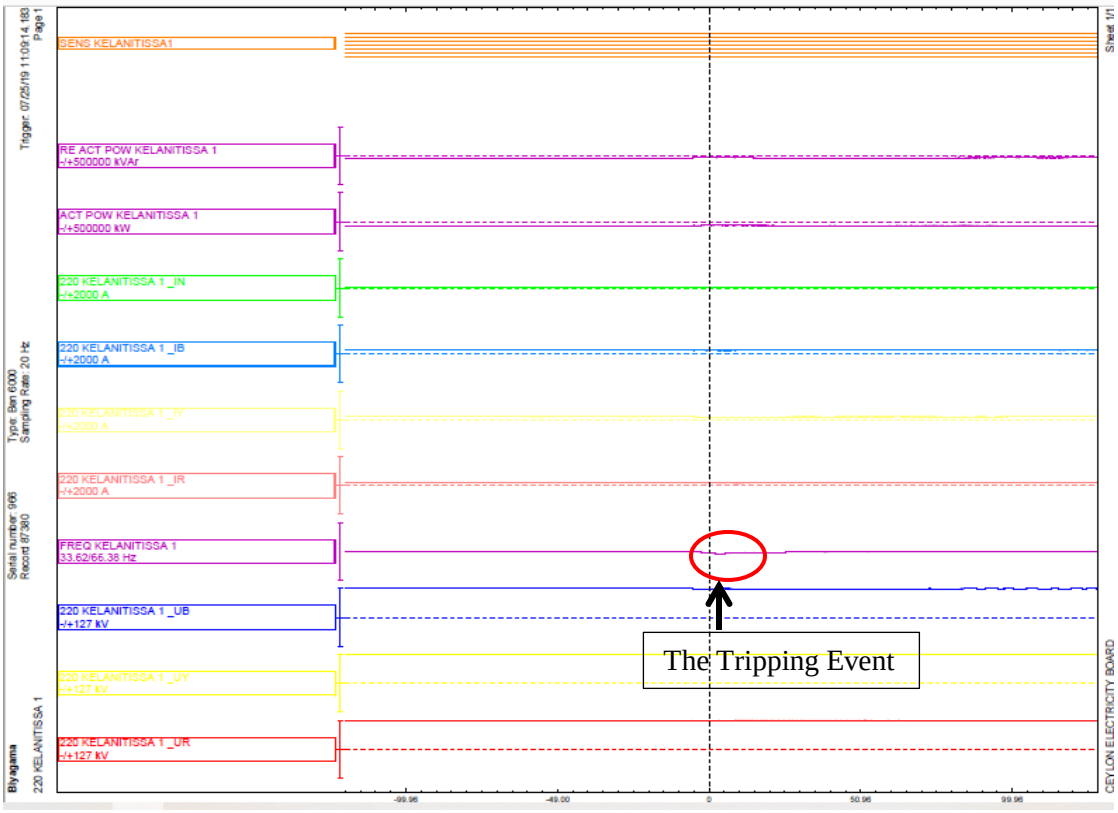

Figure 31: BEN Recording of the tripping of Kelanitissa GT 07 generator

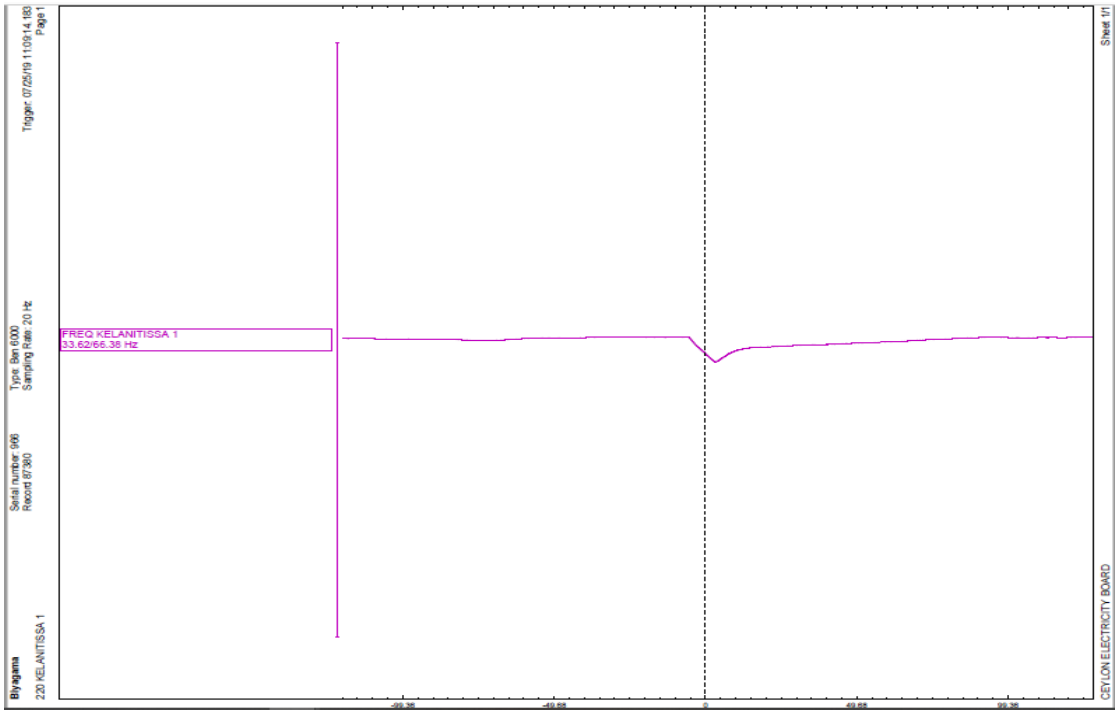

Figure 32: Frequency Response of 220kV Kelanitissa transmission line 1 as recorded in BEN Recorder

The system frequency variation during GT 07 generator failure including all pre fault load and generation data as recorded in the Ben recorder was simulated in the year 2019 PSS/E model of power system of Sri Lanka by tripping GT 07 at 5 s. The system frequency response of the actual System vs. PSS/E Model during GT 07 generator failure on 25th July 2019 is shown in Figure 33. The Actual variation of system frequency as recorded in the Biyagama Ben recorder of Kelanitissa transmission line 1 is shown in Blue color curve. The system frequency response in PSS/E is shown in Red color curve. Each important point in Figure 33 is labeled as described below:

Point A: represents the system frequency before the disturbance.

Point B: represents the system frequency at its maximum deviation due to the loss of GT 07 from the network

Point C: represents the system frequency at its maximum after the frequency stabilizes due to governor action and Load Shedding

Point D: represents the system settling frequency at 86.96 seconds after the Point A.

Point E: represents the system settling frequency at the end of simulation.

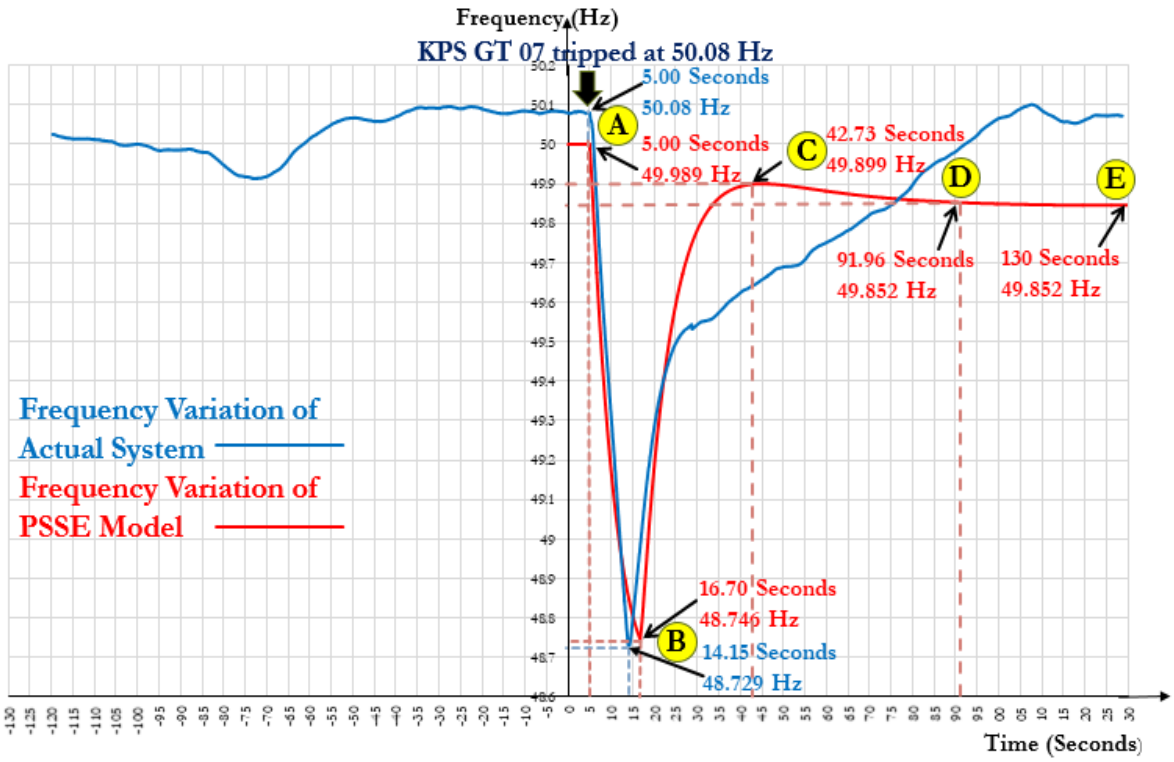

Figure 33: System frequency Variation of tripping of Kelanitissa GT 07 generator

The system is operating in normal conditions, with a frequency of 50.08 Hz in actual system and 50 Hz in PSS/E model, up to 5 s. At 11.09 am actual time or 5 seconds in PSS/E, 115 MW GT 07 generating unit was suddenly lost. The load exceeds the generation; therefore the system frequency decreases quickly. When system has more generating units or system has more inertia, and it delays the system frequency drops. The frequency minimum is reached at around 9 s in the actual response behavior and 11.7 s in the PSS/E model. The frequency minimum is a measure of the frequency stability of a system. 48.729 Hz in the current system and 48.746 Hz in the PSS/E model are the minimum frequency values of the event. It must be above the highest level of under-frequency load shedding.

In this case, UFLS stage I operated at 48.75 Hz at about 13.75 s in actual system and at about 16.58 s in PSS/E model. At that point in time, the loads were shed to match the generation and generating units with governor controls have started increasing the power generation, and thus the frequency is starting to recover. Frequency is increasing

with load shedding and at 25.20 s it has increased to 49.5 Hz in actual variation. In frequency variation of PSS/E model, frequency is increasing with load shedding and at 42.73 s it has increased to 49.9 Hz.

After about 60 s, the frequency has settled to a below value than the normal operating frequency of 50 Hz in the actual response behavior. After that, the National System Control center, CEB has informed about the fault and starts to connect generators manually to system manually to recover the frequency. In frequency variation of PSS/E model, the system frequency has settled at 49.5 Hz around 86 s. Frequency declines to a new lower equilibrium and remains flat for 30 to 40 seconds and then reduces further due to withdraw of primary frequency response from generation in PSS/E model. System frequency is at its maximum after the frequency stabilizes due to governor action and load shedding. In the actual system, frequency is stabilized at 50.06 Hz while the frequency is stabilizing at 49.852 Hz in PSS/E model. These results are summarized in Table 31.

Table 31: Tabulated results of system frequency response of the event, Actual System vs. PSS/E Model

Time Interval	**Time Period (Seconds)**	**Frequency Variation of Actual System**	**Frequency Variation of PSS/E Model**
0 to A	0 to 5	The system is operating normally at 50.08 Hz	The system is operating normally at 50 Hz
A to B	5 to 14.15 (Actual) 5 to 16.70 (PSS/E)	Frequency decaying to 48.729 Hz and at 13.75 s Stage I of UFLS Scheme operated.	Frequency decaying to 48.746 Hz and at 16.58 s Stage I of UFLS Scheme operated.
B to C	14.15 to 25.20 (Actual) 16.70 to 42.73 (PSS/E)	Frequency increasing with Load shedding and at 25.20 s it increased to 49.5 Hz (within range)	Frequency increasing with Load shedding and at 42.73 s it increased to 49.899 Hz (within range)
C to D	25.20 to 91.96 (Actual) 42.73 to 91.96 (PSS/E)	System Control center starts to connect generators manually.	At about 86 seconds, the frequency was stabled out 49.527 Hz.
D to E	91.96 to 130	At 130 s frequency is 50.06 Hz	Frequency is stabilized at 130 s is 49.852 Hz

The Figure 33 verifies that the PSS/E simulation results and actual scenario are almost similar within a small margin of tolerance. The reason for slight deviations can be; Fault Event Recorder (BEN) recorded data are not the exact moment of the event as the records are collected for every 30 minutes and as the normal procedure, after informing the event, National System Control center connect generators manually to get the frequency to 50 Hz. This will be done after LSS activated and stabilizes the frequency to the nominal range.

Therefore, by considering all the reasons of small margin of tolerances, it can be concluded that the 2019 transmission system of Sri Lanka which was modeled in PSS/E software is validated and could be used to perform future system studies by modeling forecasted system data on the validated model.

4.2 Modeling of 2030 Power System

The comparison of year 2019 and 2030 Transmission Network of Sri Lanka is shown in Figure 32.

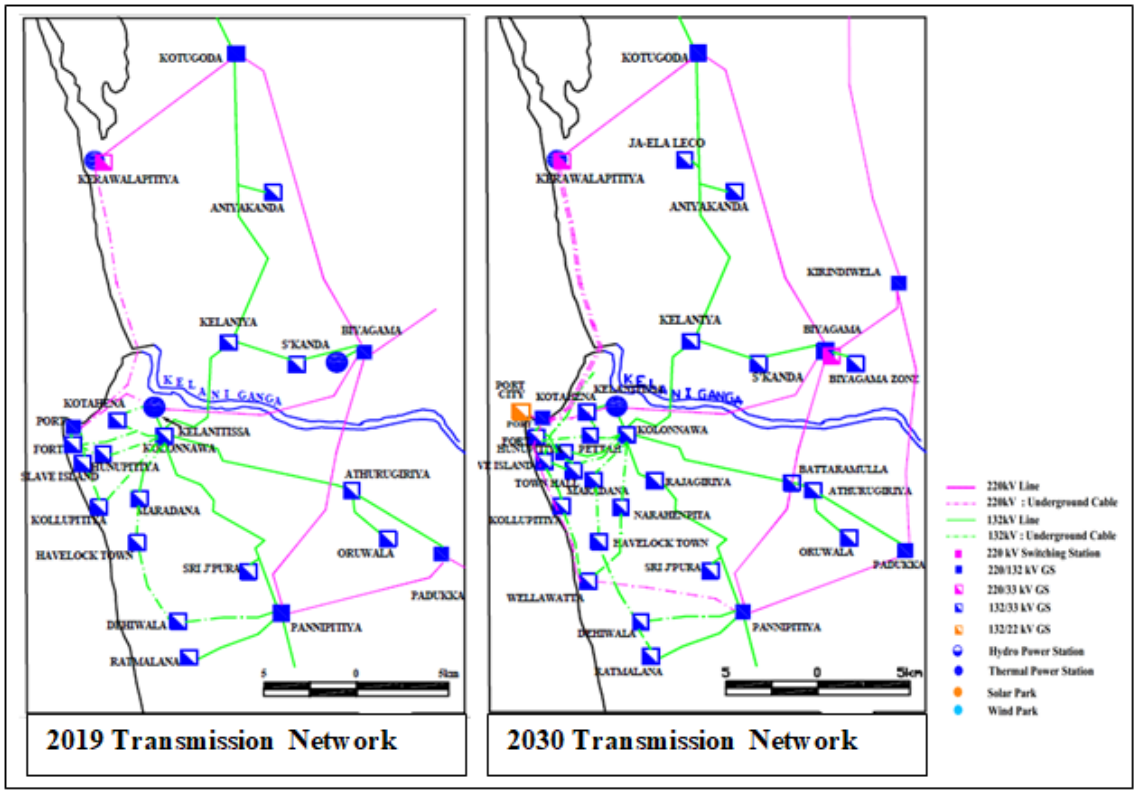

Figure 34: Comparison of year 2019 and 2030 Transmission Networks of Sri Lanka

The PSS/E simulation results of the frequency failure event of tripping of Kelanitissa GT 07 generator in 2019 PSS/E Model show similar behavior with certain deviations in comparison to actual behavior of frequency with log data. The 2030 system was developed by augmenting the validated 2019 power system model by adding forecasted elements according to the Long Term Generation and Transmission Plan published by CEB and the future forecasted data collected from Generation and Transmission Planning Branch of CEB. The schematic diagram of 2030 year transmission system of Sri Lanka which was modeled and simulated in PSS/E is attached in Appendix D.

4.2.1 Droop Settings, Active Power and Reactive Power Limits

The frequency control machine (swing machine) parameters are shown in Table 32. All the other connected generators are configured on free governor mode with droop setting of 4% to 6%. In Sri Lankan power system, mainly Victoria power plant, Upper Kothmale power plant, Samanala power plant and New Laxapana power plant are the turbine governor controllers that are in operation in all the simulation scenarios that were analyzed in this study and are given in Table 32, along with their inertia, damping and droop settings.

Table 32: Machine Governors used for Frequency Control

Generator Name	PGen (MW)	PMax (MW)	Inertia (H)	Damping (D)	Permanent Droop (R)
VICTORIA -1	30.4629	70	3.45	0.05	0.016
VICTORIA -2	0	70	3.45	0.05	0.016
VICTORIA -3	0	70	3.45	0.05	0.016
UPPER KOTHMALE -1	75.0001	75	4.3	0.5	0.05
UPPER KOTHMALE -2	75.0001	75	4.3	0.5	0.05
SAMANALA -1	60	60	3.75	0.05	0.043
SAMANALA -2	60	60	3.75	0.05	0.043
NEW LAXAPANA -1	39.9994	50	3.9	0.05	0.0590
NEW LAXAPANA -2	39.9994	50	3.9	0.05	0.0590

The active power and reactive power limits of the generators are illustrated in Appendix E. That is the Generated active power (Pgen), Maximum active power (Pmax), Minimum active power (Pmin) and the Generated reactive power (Qgen), Maximum reactive power (Qgen), Minimum reactive power (Qmin).

4.2.2 Pumped Storage Power Plant Development

CEB has identified the requirement of major storage technologies such as pumped hydro energy storage as a long term solution to increase the flexibility of power system. There are three 200 MW pumped storage power plants with speed pumping method modeled in the 2030 power plant model to improve the planned ORE absorption and give operational flexibility. Not only is it useful as an energy storage system, but it also facilitates the maximum ORE absorption and reduces ORE generation restrictions. Additionally, this facility operates as a peak power plant by reducing thermal generation, which is considered expensive. The pumped storage power plants will need to offer operational flexibility in the future, including the ability to rapidly ramp up and down and frequency control. The parameter of pumped storage power plant which is model in 2030 year power system is mentioned in the Table 27.

Table 33: Details of Pumped Storage Power Plant used in Free Governor Mode

Generator Name	PGen (MW)	PMax (MW)	Inertia (H)	Damping (D)	Permanent Droop (R)
PUMPED STORAGE UNIT-1	45	206	3.67	0.05	0.045
PUMPED STORAGE UNIT-2	45	206	3.67	0.05	0.045
PUMPED STORAGE UNIT-3	45	206	3.67	0.05	0.045

4.2.3 Frequency Limitation Settings

Following trip settings of over frequency and under frequency as mentioned in Table 34 have been installed in following machines for the generator protection using FRQTPAT under/over frequency generator trip model in PSS/E model library.

Table 34: Trip settings of over frequency and under frequency used for FRQTPAT Model

Generator Name	Lower Frequency Threshold (Hz)	Upper Frequency Threshold (Hz)	Relay pickup Time (s)	Breaker Time (s)
WIMAL GEN1 11.000	45	53	1	0.12
WIMAL GEN2 11.000	45	53	1	0.12
CAN GEN1 12.500	45	53	1	0.12
CAN GEN2 12.500	45	53	1	0.12
LAX GEN123 11.000	48	52	8	0.12
LAX GEN4 11.000	47.5	52	5	0.12
LAX GEN5 11.000	47.5	52	5	0.12
NLAX-1 12.500	45	53	1	0.12
NLAX-2 12.500	45	53	1	0.12
POL GEN1 12.500	47.5	52	5	0.12
POL GEN2 12.500	47.5	52	5	0.12
KOTM GEN-1 13.800	45	53.5	0.1	0.12
KOTH GEN-2 13.800	45	53.5	0.1	0.12
KOTH GEN-3 13.800	45	53.5	0.1	0.12
VIC GEN-1 12.500	45	53.5	0.1	0.12
VIC GEN-2 12.500	45	53.5	0.1	0.12
VIC GEN-3 12.500	45	53.5	0.1	0.12
RAND GEN1 12.500	45	53.5	0.1	0.12
RAND GEN2 12.500	45	53.5	0.1	0.12
RANTE-G1 12.500	45	53.5	0.1	0.12
RANTE-G2 12.500	45	53.5	0.1	0.12
UKUWELA GEN112.500	45	53.5	0.1	0.12
UKUWELA GEN112.500	45	53.5	0.1	0.12
UKUWELA GEN212.500	45	53.5	0.1	0.12
SAMAN GEN1 10.500	47	53.5	0.1	0.12
SAMAN GEN2 10.500	47	53.5	0.1	0.12
KUKU GEN1 13.800	47	53	3	0.12
KUKU GEN2 13.800	47	53	3	0.12
UPPER KOTH113.800	45	53.5	0.1	0.12
UPPER KOTH213.800	45	53.5	0.1	0.12
KELAN-1 132.00	47.5	53	3	0.12
KCCP GT 15.000	47.5	52	3	0.12
KCCP ST 11.500	48	51.5	3	0.12
AES GT 10.500	47	52.5	3	0.12
AES ST 10.500	47	52.5	3	0.12
KERAWALA-G 14.500	47	53.5	3	0.12
KERAWALA-G 14.500	47	53.5	3	0.12
KERAWALA-S 14.500	47	53.5	3	0.12

PUTTA_G1	20.000	47	51.5	0.1	0.12
PUTTA_G2	20.000	47	51.5	0.1	0.12
PUTTA_G3	20.000	47	51.5	0.1	0.12
PUTTA_G4	20.000	47	51.5	0.1	0.12
PUTTA_G5	20.000	47	51.5	0.1	0.12

4.3 Simulation Scenarios of 2030 Power System

4.3.1 Generation Dispatch Scenarios

Three generation dispatch scenarios were used to perform simulations by considering the various generation dispatch patterns in Sri Lankan power system. These generation scenarios are mainly categorized according to the seasonal changes and weather at a certain periods. The System Control Center of CEB defines these generation scenarios for every week of the year. There are mainly two generation dispatch scenarios identified as Hydro maximum (HM), and thermal maximum (TM). System Control Center of CEB has identified a new dispatch scenario, Maximum Wind and Solar scenario, which is considered as the worst case hydro maximum scenario with high solar and wind penetrations.

The main three generation dispatch scenarios used to perform detailed system studies in this research are as follows:

1. **Hydro Maximum (HM) Scenario -**

   This scenario is identified for rainy seasons or very wet conditions when the most of hydro reservoirs water levels are high. Therefore, high inflows to run of river plants generate maximum power output. A larger number of hydro power plants are used to contribute to the system generation to match the system demand. The frequency control swing machine is a hydro generator.

2. **Thermal Maximum (TM) Scenario -**

   This scenario is identified for dry seasons when the most of hydro reservoirs water levels are low due to lack of rain. Therefore, with low inflows run of river are not generating their maximum power output. A larger number of thermal

power generators are used to contribute to the system generation to match the system demand. However, hydro generator is used as the frequency control swing machine.

3. **Renewable Maximum (RM) Scenario -**

   This scenario is identified for the rainy seasons or very wet conditions when the most of hydro reservoirs water levels are high. Therefore, high inflows to run of river machines generate their maximum power output. A larger number of hydro power generators are used to contribute to the system generation to match the system demand. The frequency control swing machine is a hydro generator.

4.3.2 Demand Scenarios

The demand scenarios are mainly considered according to the peak values in daily load curve as a maximum or a minimum of the consumer demand considering a single typical day. There are four demand scenarios per day, which are known as morning peak, day peak, night peak and off peak. The morning peak is not significant compared to day peak, night peak and off peak; therefore, morning peak is omitted for simulation studies. Hence, clearly three different scenarios can be identified among all four basic demand scenarios for simulation studies, such as: day peak demand period, night peak demand period, and off peak demand period.

1. **Day Peak Demand Period** –

   The maximum demand during the day time occurs around 11:00 hours.

   Typical average day peak demand would be around MW in 2030

2. **Night Peak Demand Period –**

   The maximum demand during the night time occurs around 19:30 hours.

   Typical average night peak demand would be around MW in 2030

3. **Off Peak Demand Period -**

   The miniimum demand during the day time occurs around 03:00 hours.

Typical average day peak demand would be around MW in 2030

With combination of Generation scenarios and loading conditions, altogether nine simulation scenarios were used to simulate the system behavior. These nine scenarios, which are used to carry out the system studies in PSS/E are as follows:

All Simulations Scenarios

1. Hydro Maximum Day Peak (HMDP)

2. Hydro Maximum Night Peak (HMNP)

3. Hydro Maximum Off Peak (HMOP)

4. Thermal Maximum Day Peak (TMDP)

5. Thermal Maximum Night Peak (TMNP)

6. Thermal Maximum Off Peak (TMOP)

7. Renewable Minimum Day Peak (RE Min DP)

8. Renewable Minimum Night Peak (RE Min NP)

9. Renewable Maximum Day Peak (RE Max DP)

Table 35 shows the generation mix of above mentioned nine simulation scenarios. The demand in each scenario in year 2030 is mentioned in Table 36. According to Table it is clearly identify the most important three scenarios which are mainly focused on this research topic to show the effect of both solar and wind high penetrations in the system. They are all three day peak scenarios which have high solar and wind generation as during day time the availability of solar and wind resources are high. The main three scenarios are Thermal Maximum Day Peak scenario, Hydro Maximum Day Peak scenario and Renewable Maximum Day Peak scenario.

Table 35: Generation and Loading Scenarios considered for the studies

Scenario	Load	Generation Mix					
		Wind	Min-Hydro	Bio-Mass	Solar	Major Hydro	Thermal
Thermal Maximum Night Peak	Night Peak	50%	20%	100 %	0%	Balance	Max
Thermal Maximum Day Peak	Day Peak	50%	20%	100 %	100%	Balance	Max
Hydro Maximum Night Peak	Night Peak	100%	100%	60%	0%	Max	Balance
Hydro Maximum Day Peak	Day Peak	100%	100%	60%	50%	Max	Balance
Thermal Maximum Off Peak	Off Peak	50%	20%	0%	0%	Partial	Partial
Hydro Maximum Off Peak	Off Peak	100%	100%	0%	0%	Partial	Partial
Renewable Minimum Night Peak	Night Peak	0%	10%	20%	0%	Min	Max
Renewable Minimum Day Peak	Day Peak	0%	10%	20%	10%	Min	Max
Renewable Maximum Day Peak	Day Peak	100%	100%	100 %	100%	Max	Balance

Table 36: Demand used in each scenario

Scenario	Demand	
	Active Power (MW)	Reactive Power
TMNP/HMNP/RE Min NP	4266	1598
TMDP	4481	1107
HMDP	4622	1015
RE Min DP	3432	973
TMOP/HMOP	3166	1016
RE Max DP	4581	1113

Non-dispatchable power sources such as solar PV and wind due to the intermittency, have significant differences in performance compared to other dispatchable power sources such as Hydro power, and Biomass. This uncertainty and variability of solar PV and wind power generation affects power system stability and reliability. Solar PV and wind energy resources are not contributing to the strength of power system in terms of inertia, which creates stability issues in power system. Therefore, power system stability studies and analysis in this research is focused to determine stability and operational

constraints to determine necessary solutions for the problems. The total solar PV production of about 200 days in 2030 year overlaid on top of each other is shown in Figure 35. Black line is the average of the total solar PV production. This Figure verifies that the maximum solar generation occurs during the day peak time period and the maximum of the average curve occurs around 11.00 hours.

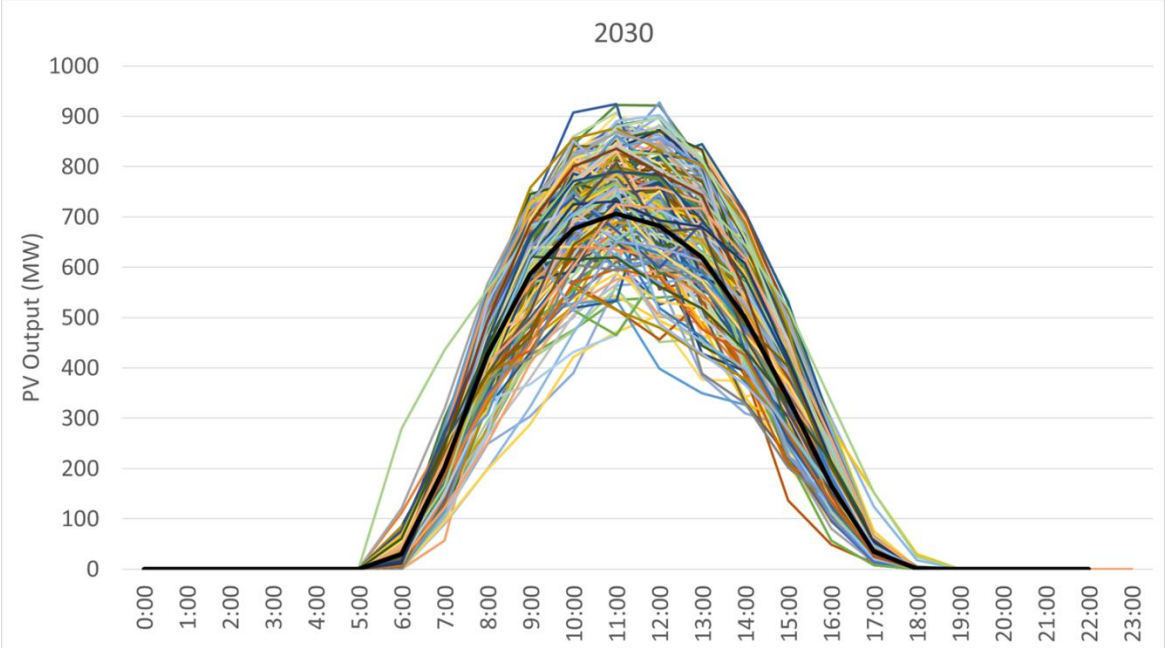

Figure 35: The total solar PV production of about 200 days in 2030

Table 37 shows the maximum generation from available thermal, hydro, wind, dendro, solar and mini hydro power resources in year 2030 for the main three selected scenarios. Table 38 shows the system demand, system inertia, spinning reserve, free governor action capability and reactive power absorption features of for the main three selected scenarios in year 2030. The typical average demand values for the main three selected scenarios are shown in Table 39.

Table 37: Total Maximum Generation for each of the selected study scenarios

	Thermal Maximum Day Peak (TMDP) - Year 2030	Hydro Maximum Day Peak (HMDP) - Year 2030	Renewable Maximum Day Peak (RE Max DP) - Year 2030
Source of Energy	**Total Maximum Generation (MW)**	**Total Maximum Generation (MW)**	**Total Maximum Generation (MW)**
Thermal	2539	1095	1119
Major hydro	919	2069.5	2110.5
Wind	488.5	976.9	976.9
Biomass/ Dendro	94	56.4	98.5
Solar	1018	509	1018
Mini hydro	115.8	559	559
Total	**5174.3**	**5265.8**	**5881.9**

Table 38: Features of Selected Simulation Scenarios

Condition	System Demand	System Inertia	Spinning Reserve percentage	Free governor action capability	Reactive power absorption capability
Thermal Maximum	Low	Low	High	High	High
Hydro Maximum	High	High	Low	Low	Low
Renewable Maximum	Low	Very Low	High	High	High

Table 39: Typical average demand values Selected Simulation Scenarios in 2030

Scenario	Thermal Maximum (Average System Demand in MW)	Hydro Maximum (Average System Demand in MW)	Renewable Maximum (Average System Demand in MW
Day Peak	4350	4450	4450
Night Peak	4000	4200	4200
Off Peak	3000	3000	NA

The following assumptions are made when carrying out stability studies.

- Approximately 5% spinning reserve is maintained for night peak loading conditions.
- An automatic load shedding scheme is incorporated in the study to sustain the stability of the system.

- Exact and typical exciter and governor models are included for all generators.

4.3.3 Proposed Simulation Scenarios

The 2030 Transmission network of Sri Lankan power system with future forecasted data was analyzed in PSS/E Software to observe the performance of existing LSS and proposed new LSS to maintain system stability with increased penetration of renewable energy sources.

1. Load Flow Analysis

Initially, the network model of year 2030 was studied under steady state condition to see the performance of existing transmission network under normal operating conditions to identify voltage criteria violation, transformer overloading and transmission line overloading. The simulation model of 2030 was initialized, and load flow analysis was performed using Newton-Raphson method for steady state analysis.

2. Dynamic Analysis

Contingency studies were carried to determine the capability of the system to deliver power from generating stations to load centers within the operating limits of equipment during loss of continuity of supply or widespread disturbance. The dynamic stability studies were performed to check the transient stability of the proposed transmission system against failures of major generators. The performance of the transmission system under contingency situation was taken into consideration. The following ***n-1*** and ***n-2*** contingency levels were investigated.

2.1 *n-1* with a Single Largest Generator Outage

Outage of any one element of the transmission system at a time is observed.
E.g.: One generator units of Lakvijaya coal power plant tripped at 50 s.
Maximum generation loss of 275 MW

2.2 *n-1* with a Single Large Power Plant Outage

Outage of any one element of the transmission system at a time is observed under ***n-1*** contingency.

E.g.: All generator units (all five generator units) of Lakvijaya coal power plant tripped at 50 s. Maximum generation loss of 5 × 275 MW.

2.3 *n-2* with two Large Power Plant Outage

Outage of any two elements of the transmission system at a time is observed under ***n-2*** contingency.

E.g.: All generator units (all five generator units) of Lakvijaya coal power plant tripped at 50 s. Maximum generation loss of 5 × 275 MW.

Two generator units of Sampoor coal power plant tripped at 53 s. Maximum generation loss of 2×270 MW.

CHAPTER 5

ANALYSIS OF PRESENT LOAD SHEDDING SCHEME

The simulations with existing static UFLS scheme are carried out to observe the weaknesses of the present load shedding scheme. Basically simulations were performed under three main simulation scenarios out of all nine simulation scenarios as described in chapter 4.

5.1 Scenario 1 - Hydro Maximum Day Peak (HMDP)

In the Hydro Maximum Day Peak (HMDP) scenario, total wind generation is 976.9 MW and solar generation is 509 MW as shown in Table 40. It is considered that 100% wind and 50% of solar power plants are committed in 2030. The forecasted total system demand was not changed and it is 4,622.99 MW and forecasted generation is 4,679.19 MW as mentioned in Table 40.

Table 40: Generation mix in HMDP Scenario

Total Load	**Total Generation = 4679.19 MW**					
	Generation Mix					
	Wind	**Solar**	Mini-Hydro	Bio-Mass	Major Hydro	Thermal
4622.99 MW	**100%**	**50%**	100%	60%	Max	Balance
	976.9 MW	**509 MW**	559 MW	56.4 MW	1655 MW	965 MW

Table 41 shows the hydro machines, which were partially loaded to cater any power imbalance. The swing bus, Victoria hydro power plant was giving 55 MW to the national grid. It has the lowest droop 0.016 and PIDGOV PSS/E model was used. Each unit of the pumped storage power plant (having three units) was generating 150 MW during the day peak time at hydro maximum season. It has the droop of 0.05. The two unites out of three units in Kothmale power station generate 40 MW each, having a droop setting of 0.05. All the other hydro power plants are operated in full load except

the generators mentioned in Table 41, which are considered to be operated in the free governor mode.

Table 41: Machine Governors used in Free Governor Mode in HMDP Scenario

Generator Name	PGen (MW)	PMax (MW)	Turbine Governor Model in PSS/E	Permanent Droop (R)
VICTORIA GEN-1	55	70	PIDGOV	0.016
VICTORIA GEN-2, 3	20	70	PIDGOV	0.016
PUMP STORAGE 1, 2, 3	150	206	HYGOV	0.050
KOTHMALE GEN-2	40	67	HYGOV	0.050
KOTHMALE GEN-3	0	67	HYGOV	0.050

As presented in Table 42, major hydro and thermal power plants were operated in HMDP scenario. Three units out of five units of Lakvijaya coal power plant were in operation and fully loaded at 275 MW. The unit 1 of Sampoor power plant is generating at 140 MW out of 270 MW maximum generation capacity. Umaoya power plant, power plants in Laxapana complex, power plants in Mahaweli complex and power plants in Samanala complex were supply power in HMDP scenario while a few machines mentioned in Table 41 were used in free governor mode to keep spinning reserve.

Table 42: Major Hydro and Thermal Power Plants in operation in HMDP Scenario

Power Plant Name	Power Generation (MW)
Umaoya Hydro Power Plant	120
Laxapana Hydro Power Complex	339.5
Mahaweli Hydro Power Complex	593
Samanala Hydro Power Complex	120
Sampoor Coal Power Plant	140
Lakvijaya Power Plant (G1, G2, G3)	3×275

Figure 36 illustrates the active power generation of selected solar power plants in HMDP scenario including Pooneryn, Mannar, Siyambalanduwa, Hambantota and Vavniya solar power plants. The simulation was performed to observe the solar power plants active power Generation without tripping a plant or without a disturbance within 150 s time frame. Fastest solar ramp rate was observed in Pooneryn solar power plant. The minimum power generated at 50 s is the time at which a contingency could be given to observe the behavior of the power system at its worst case. The tripping was done at 50 s. This simulation was carried out to determine the most vulnerable point to trip the single largest generator to get the worst case simulation.

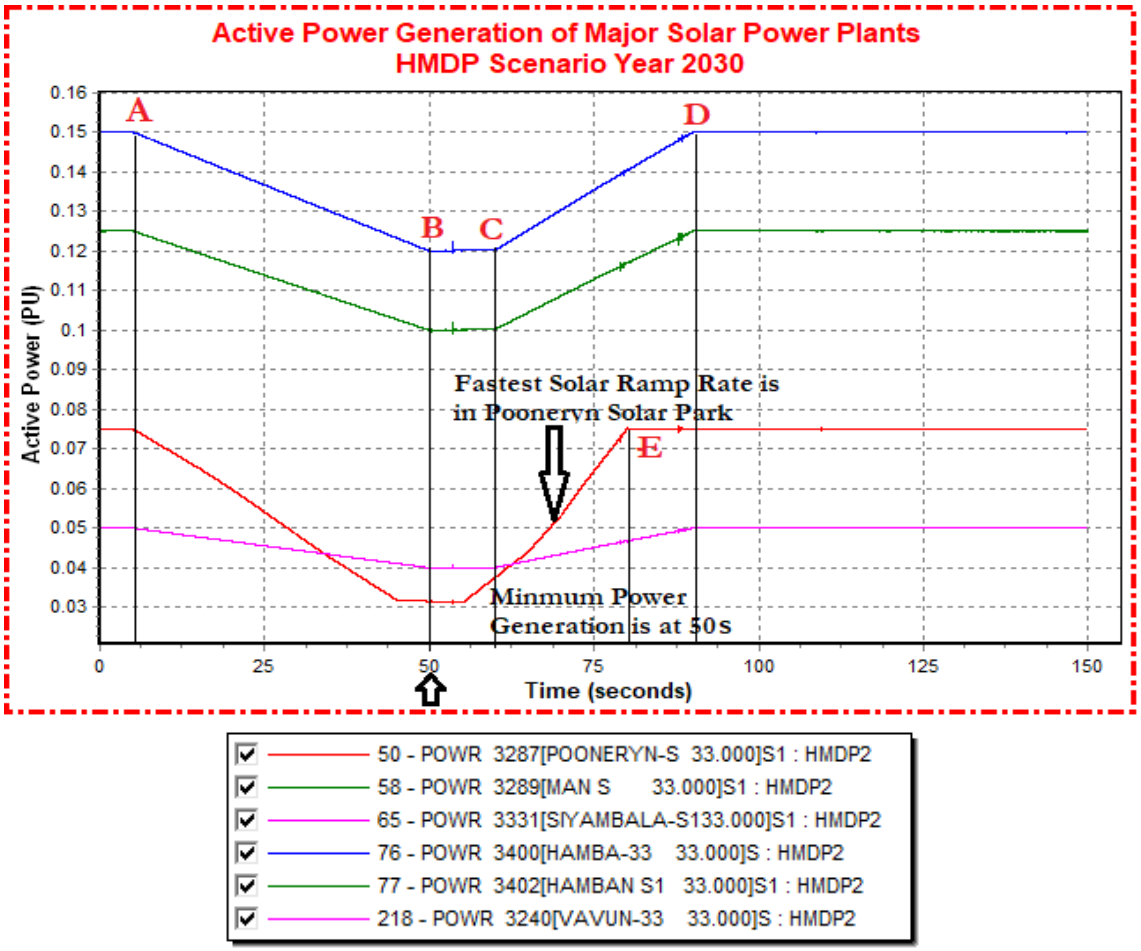

Figure 36: Active power generation of selected solar power plants in HMDP scenario rio

According to Figure 36, the solar generation starts to ramp-down at 6 s (at point A). Solar power generation decreases from point A to B. At point B (i.e. at 50 s) the minimum power is generated. The minimum power generation in Pooneryn solar park, is from 44 s to 56 s. Solar power generation is ramping up from point C to D. At point E (at 80 s), solar power generation in Pooneryn solar park is constant.

Dynamic analysis is done to determine the capability of the Sri Lankan transmission network for year 2030, to deliver power from generating stations to load centers within the operating limits of equipment during a contingency situation of a larger disturbance. The transient stability of the proposed transmission system was analyzed against failures of major generators by dynamic stability studies. The performance of the transmission system under contingency situation, ***n-1*** and ***n-2*** contingency levels were taken into consideration. The following simulations were carried out to analyze the existing LSS.

Case 1.1: Tripping 275 MW Loaded Lakvijaya 1 Unit (Loosing 6% Generation – Tripping Single Unit)

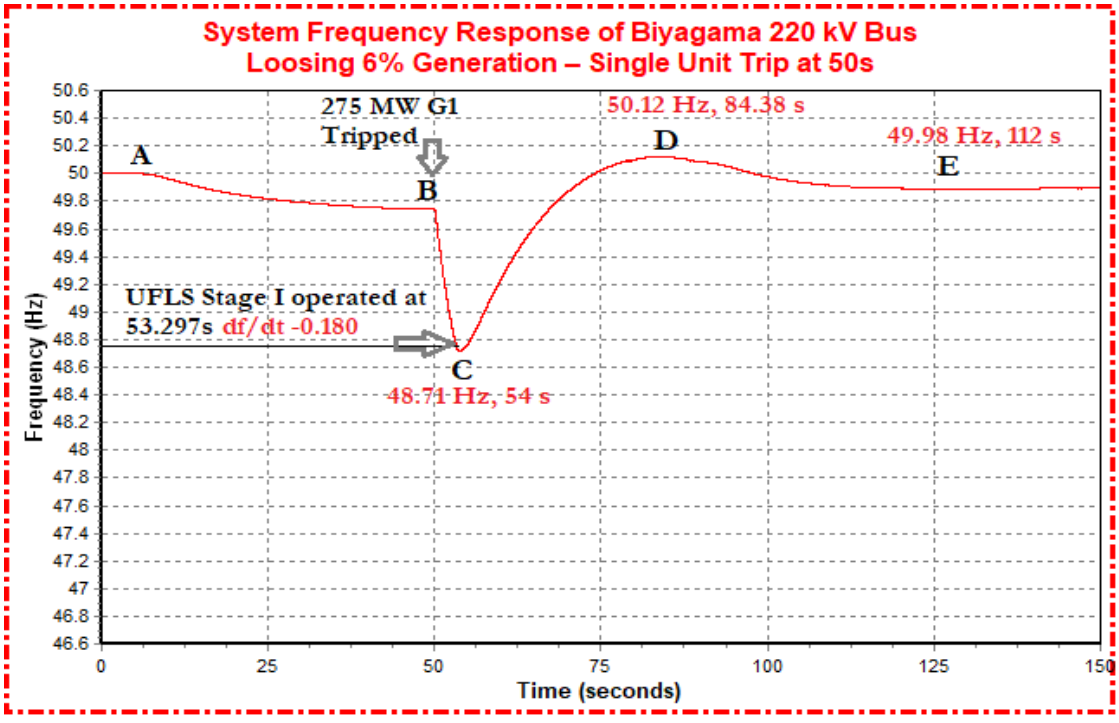

Figure 37: Frequency Response of Tripping 275 MW Loaded Lakvijaya 1 Unit in HMDP scenario

Figure 37 illustrates the system frequency response of tripping of 275 MW loaded generator unit 1 in Lakvijaya coal power plant at 50 s. The system frequency decreases gradually with ramping down of solar generation (see Figure 36) from point A to B. The frequency at point B is 49.76 Hz, and the minimum power is generated at point B (at 50 s). From point B to C, the system frequency decreases rapidly due to loss of generation. Frequency increases due to load shedding and governor action from point C to D. The maximum frequency or the stabilizing frequency is at point D (50.12 Hz). Frequency decreases and settles at 112.5 s (point E). The details of load shedding are mentioned in Table 43.

Case 1.2: Tripping 275 MW Loaded Lakvijaya 2 Units (Loosing 12% Generation – Tripping Two Units)

Figure 38 illustrates the system frequency response of tripping of 275 MW loaded generator unit 1 at 50 s and tripping of 275 MW loaded generator unit 2 at 54 s in Lakvijaya coal power plant. The frequency variation is almost similar to the case 1.1 as described in above. The details of load shedding are mentioned in Table 43.

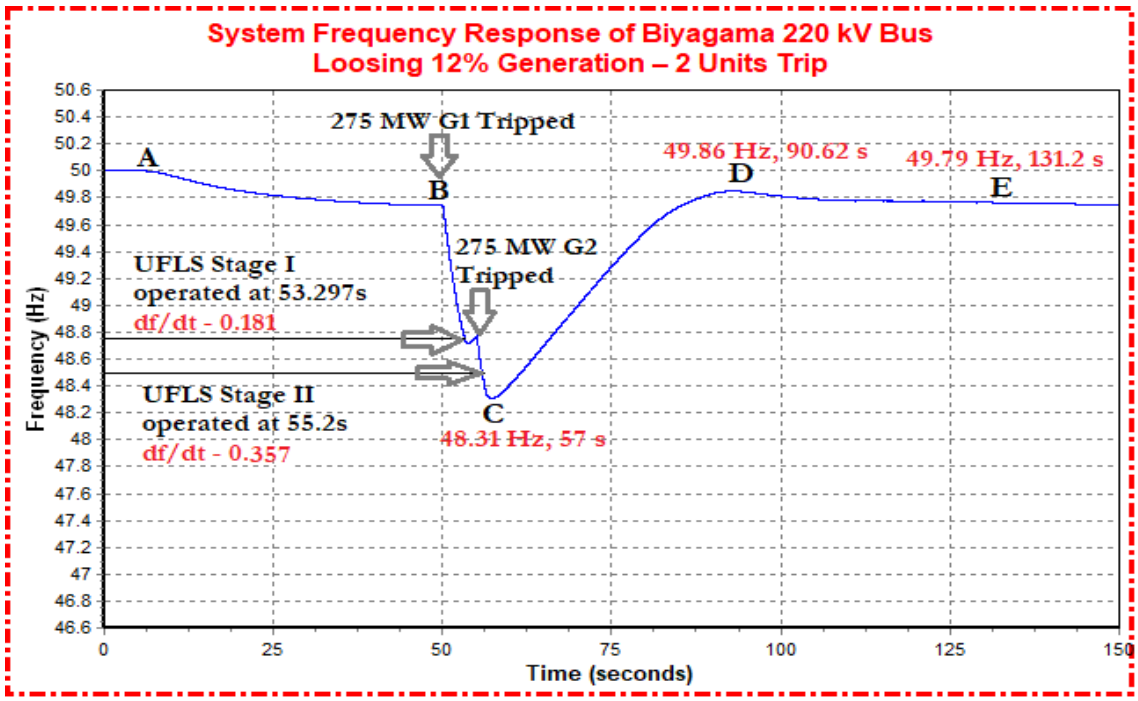

Figure 38: Frequency Response of Tripping 275 MW Loaded Lakvijaya 2 Units in HMDP scenario

Case 1.3: Tripping 275 MW Lakvijaya 3 Units and 140 MW Sampoor 1 Unit (1,115 MW) (Loosing 24% Generation – Tripping Two Plants)

Figure 39 illustrates the system frequency response of losing 1,235 MW power in system by tripping two power plants as mentioned below.

- Tripping of 275 MW loaded generator unit 1, 2 and 3 in Lakvijaya coal power plant at 50 s.
- Tripping of 140 MW loaded generator unit 1 of Sampoor coal power plant at 50.5 s.

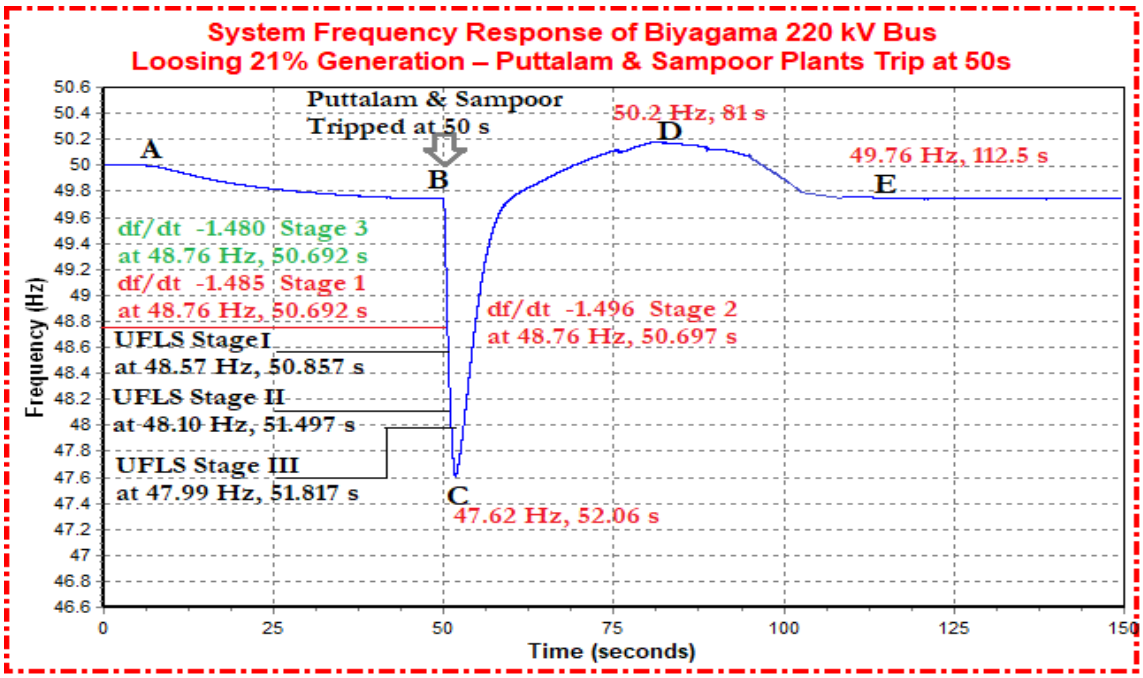

Figure 39: Frequency Response of Tripping 275 MW Lakvijaya 3 Units and 140 MW Sampoor 1 Unit (1115 MW) in HMDP scenario

Three stages of the UFLS were operated with df/dt and totally 956 MW loads were shed. The highest overshoot in frequency of 50.2 Hz compared to previous cases was observed. Due to fast governor action in Pumped storage and due to more loads being shed the frequency settles back to 49.76 Hz, the lowest compared to previous cases. The frequency has settled within the specified standard limits of 49.5 to 50.5 Hz. The frequency variation is almost similar to the case 1.1 and case 1.2 as described above.

The details of load shedding are mentioned in Table 43. All three units of Pump Storage Power plant has been over loaded to 208 MW.

Table 43 shows the tabulated results of case studies mainly focused on HMDP scenario. The main frequency points and load shedding details of each case study also mentioned in Table 43.

Table 43: Tabulates results of HMDP Scenario with existing LSS

Case	Frequency before disturbance	Decaying Frequency	Load Shedding Scheme	Stabilizing Frequency	Settling Frequency
1.1	49.76 Hz at 50 s	48.71 Hz at 54 s	Stage I at 53.297 s 152 MW df/dt -0.180	50.12 Hz at 84.38 s	49.98 Hz at 112 s
1.2	49.76 Hz at 50 s	48.31 Hz at 57 s	Stage I at 53.297 s 152 MW df/dt -0.180 Stage II at 55.2 s 320 MW df/dt -0.357 Total Load shed 472 MW	49.86 Hz at 90.62 s	49.79 Hz at 131.2 s
1.3	49.76 Hz at 50 s	47.2 Hz at 51.8 s	Stage I at 50.692 s 385.5 MW df/dt -2.345 Stage II at 51.257 s 299.72 MW df/dt -3.196 Stage III at 51.417 s 270.45 MW df/dt -2.637 Total Load shed 956 MW	49.79 Hz at 87.5 s	49.61 Hz at 114.5 s

5.2 Scenario 2 - Thermal Maximum Day Peak (TMDP)

In the Thermal Maximum Day Peak (TMDP) scenario, total solar generation is 1,018 MW and total wind generation is 488.45 MW as shown in Table 44. It was considered that 100% solar and 50% of wind power plants are committed in 2030. The forecasted total system demand was not changed and it is at 4,530.6 MW and forecasted Generation is 4,481.97 MW as mentioned in Table 44.

Table 45 shows the hydro machines, which were partially loaded to cater any power imbalance. The swing bus, Victoria hydro power plant was giving 11.5 MW to the national grid. It has the lowest droop 0.016 and PIDGOV PSS/E model was used. Each unit of all three units of Pumped storage was generating 150 MW, which has the maximum generating capacity of 206 MW during day peak time at thermal maximum season. The two unites of Colombo LNG power station generate 145 MW each, having a droop setting of 0.05. The maximum generation capacity of one unit in Colombo LNG power station is 300 MW. All the other hydro power plants were operated in full load except generators mentioned in Table 45 which were considered to be operated in the free governor mode.

Table 44: Generation mix in TMDP Scenario

Total Load	**Total Generation = 4530.6 MW**					
	Generation Mix					
	Wind	**Solar**	Mini-Hydro	Bio-Mass	Major Hydro	Thermal
4481.97 MW	**50%**	**100%**	20%	100%	Balance	Max
	488.45 MW	**1018 MW**	115.8 MW	94 MW	531.5 MW	2289 MW

Table 45: Machine Governors used in Free Governor Mode in TMDP Scenario

Generator Name	**PGen (MW)**	**PMax (MW)**	**Turbine Governor Model in PSS/E**	**Permanent Droop (R)**
VICTORIA GEN-1	11.5	70	PIDGOV	0.045
PUMP STORAGE 1, 2, 3	150	206	HYGOV	0.0160
COLOMBO LNG-2 G1, G2	50	100	GAST	0.05
COLOMBO LNG-2 ST	45	100	TGOV1	0.05

As presented in Table 46, major hydro and thermal power plants were operated in TMDP scenario. All five units of Lakvijaya coal power plant were in operation and fully loaded at 275 MW. All two units of Sampoor power plant were generating at 540 MW maximum generation capacity. Broadlands hydro power plant and Kukuleganga hydro

power plant were generating power in TMDP scenario as mentioned in Table 46. The two unites of Colombo LNG power station generate 425 MW while used in free governor mode to keep spinning reserve as mentioned in Table 45.

Table 46: Major Hydro and Thermal Power Plants in operation in TMDP Scenario

Power Plant Name	Power Generation (MW)
Broadlands Hydro Power Plant	10
Kukuleganga Hydro Power Plant	30
Sampoor Coal Power Plant	540
Lakvijaya Power Plant	5×275
Colombo LNG Power Plant	425

Figure 40 illustrates the active power generation of selected solar power plants in TMDP scenario including Pooneryn, Mannar, Siyambalanduwa, Hambantota, Mahiyanganaya, Valachchenei and Vaunativ solar power plants. Similar to the HMDP scenario, the simulation was performed to observe the solar power plants active power generation without tripping a plant or without a disturbance within 150 s time frame. Fastest solar ramp rate was observed in Pooneryn solar power plant. The minimum power generated at 50 s was the time at which a contingency could be given to observe the behavior of the power system at its worst case in TMDP Scenario. Similar to the HMDP scenario, the tripping for dynamics is done at 50s. This simulation was carried out to determine the most vulnerable point to trip the single largest generator to get the worst case simulation.

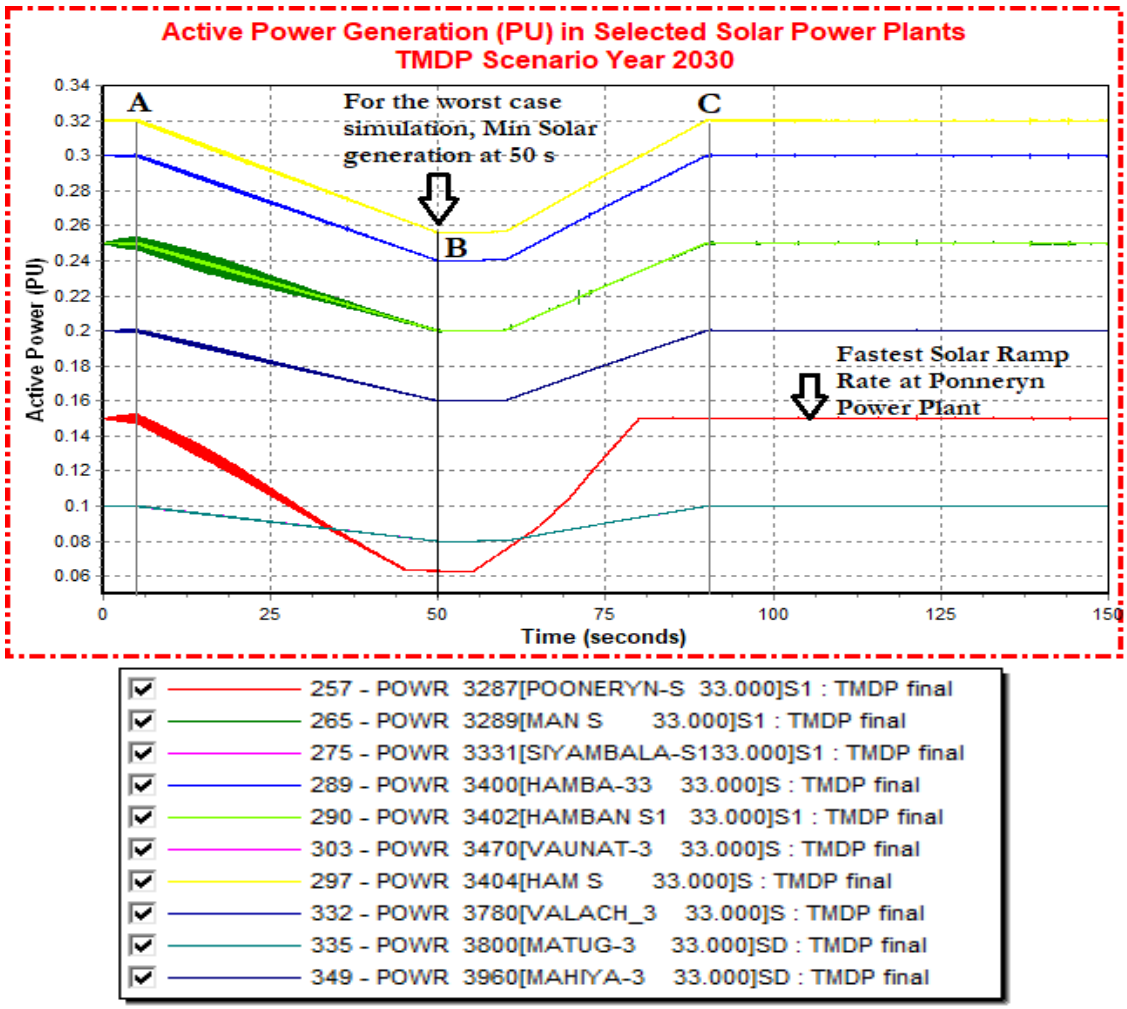

Figure 40: Active power generation of selected solar power plants in TMDP scenario

Case 2.1: Tripping 275 MW Loaded Lakvijaya 1 Unit (Loosing 6% Generation – Tripping Single Unit)

Figure 41 illustrates frequency variation for a single coal unit tripped at Lakvijaya coal power plant. At point A (50 Hz, 6 s), there is a decrease in frequency gradually until 50s (point B) due to solar ramp rate. The point B (49.6 Hz, 50 s) which is lower than HMDP cases, frequency goes rapidly down due to loss of 6% generation. No loads were shed during the simulation. . Power mismatch was handled of with the inertia of the system and spinning reserve. Minimum frequency was observed at point C (48.85 Hz, 52.08 s). Between point C and D, frequency increases due to governor action. There was no

frequency overshoot observed in this case. All three units of Pumped storage power plant fully loaded to 195 MW at 60 s. The frequency is within limits of 49.5 to 50.5 Hz.

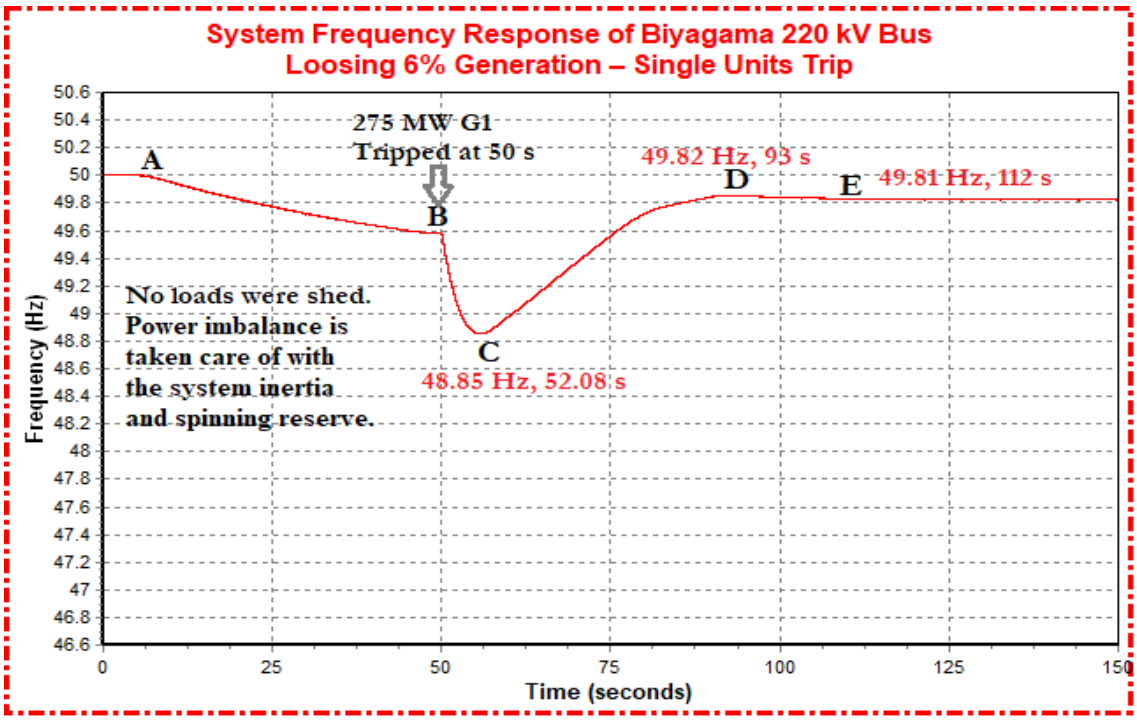

Figure 41: Frequency Response of Tripping 275 MW Loaded Lakvijaya 1 Unit in TMDP scenario

Case 2.2: Tripping 275 MW Loaded Lakvijaya 2 Units (Loosing 12% Generation – Tripping Two Units)

Figure 42 illustrates the system frequency response of tripping of 275 MW loaded generator unit 1 at 50 s and tripping of 275 MW loaded generator unit 2 at 54 s in Lakvijaya coal power plant. This graph shows how the system frequency behaves when loosing 550 MW power in system. The frequency variation is almost similar to the case 2.1 as described in above. Similar to previous case, frequency decreases gradually with solar ramp rate decreases. Two load shedding stages were operated and totally 556 MW loads were shed. Load shed amount is equal to the loss, but the frequency does not reach close to 50Hz like in the previous case. The frequency settles to 49.6 Hz and settling time also higher than the previous case. All three units of pumped storage power plant were over loaded to 210 MW at 59 s. The frequency was however has settled within the

standard limits of 49.5 to 50.5 Hz. The details of load shedding are mentioned in Table 47.

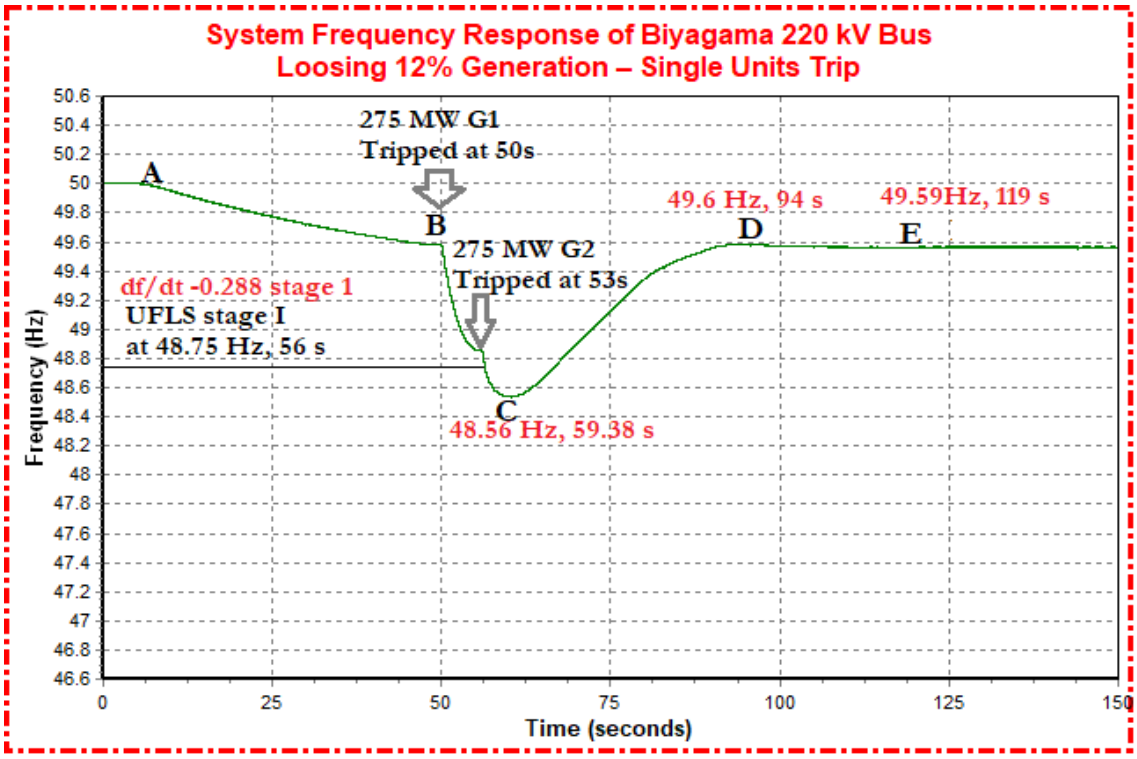

Figure 42: Frequency Response of Tripping 275 MW Loaded Lakvijaya 2 Units in TMDP scenario

Case 2.3: Tripping 275 MW Loaded Lakvijaya 3 Units and 270 MW Loaded Sampoor 2 Units (1,365 MW) (Loosing 30% Generation – Tripping Two Plants)

The system frequency response of losing 1,365 MW power in the system is illustrated in Figure 43. Three generators in Lakvijaya power plant and two units in Sampoor power plant were tripped at 50 s and 52 s respectively. UFLS three stages were operated with df/dt and totally 1,156.6 MW loads were shed. Minimum frequency was very low than previous cases. There was no frequency overshoot observed. The frequency settles back to 49.5 Hz, which is the lowest compared to the case 2.1 and case 2.2 as described above. All three units of Pumped storage power plant had been over loaded to 214 MW. Unit 2 of Colombo LNG power plant was fully loaded to 75 MW. The frequency has not restored within the standard limits and is in the lower limit of 49.5 Hz. The details of load shedding are mentioned in Table 47.

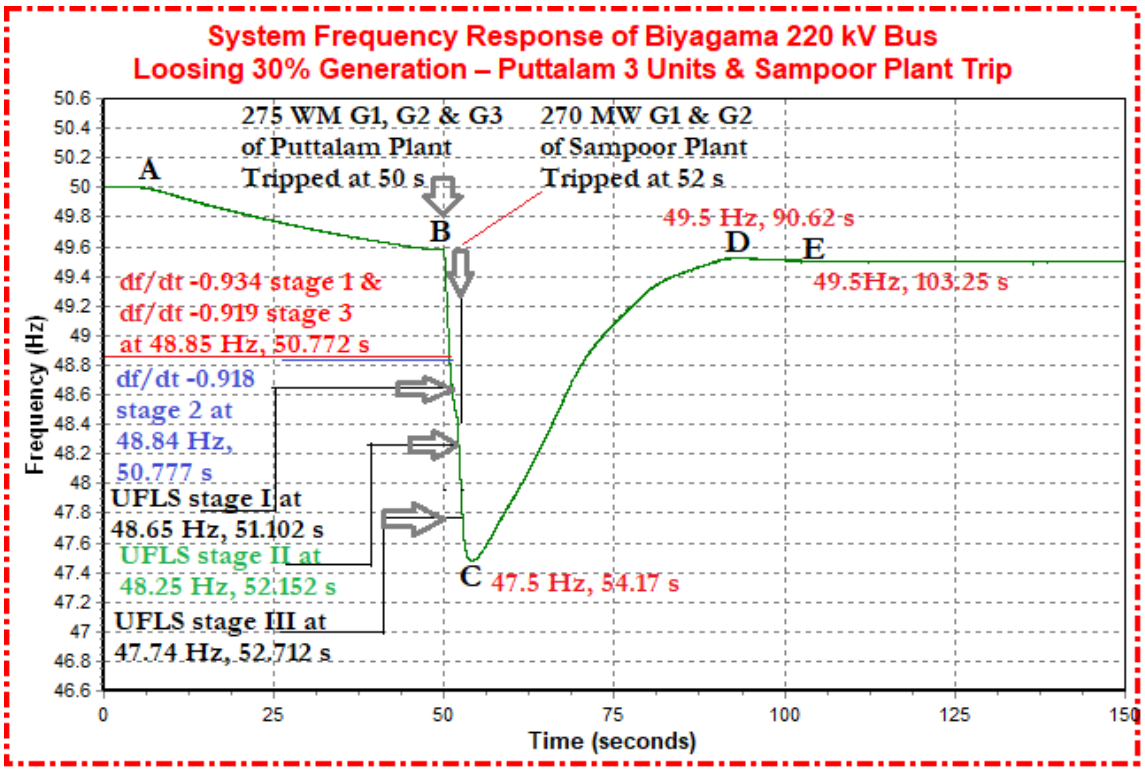

Figure 43: Frequency Response of Tripping 275 MW Loaded Lakvijaya 3 Units and 270 MW Loaded Sampoor 2 Units in TMDP scenario

Case 2.4: Tripping 275 MW Loaded Lakvijaya 5 Units (Loosing 31% Generation – Tripping Single Plant) (1375 MW)

Figure 44 illustrates the system frequency response of tripping of 275 MW loaded five generator units in Lakvijaya coal power plant. Three stages of UFLS were operated with df/dt and totally 1,075.89 MW loads had been shed. Minimum frequency was 47.56 Hz, which is the lowest of previous cases in this scenario. No overshoot in frequency was observed. The frequency settles back to 49.4 Hz and it's the lowest compared to the case 2.1, case 2.2 and case 2.3 as described above. All three units of Pumped storage power plant were over loaded to 214 MW. Unit 2 generator of Colombo LNG power plant was fully loaded to 90 MW. The frequency has not restored within limits and it has stabilized at 49.4 Hz.

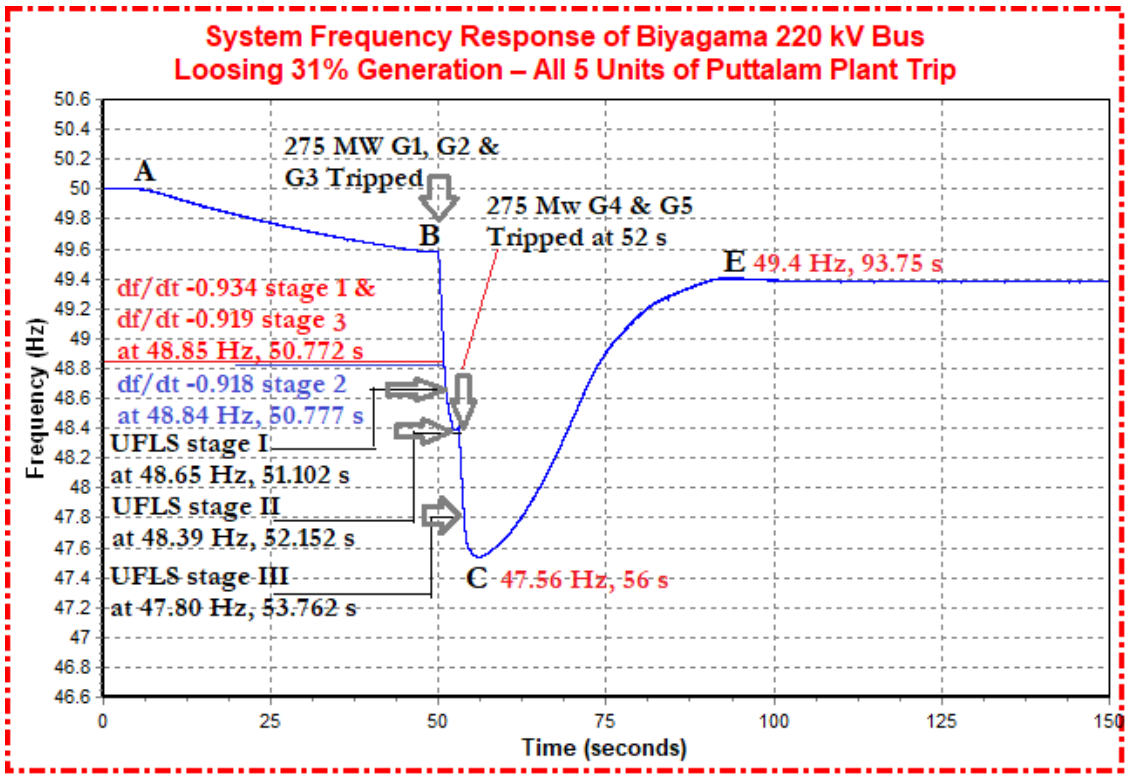

Figure 44: Frequency Response Tripping 275 MW Loaded Lakvijaya 5 Units in TMDP scenario

Only four case studies were explained in this chapter and other case studies was performed in this scenario are described in the Chapter 7. Table 47 shows the tabulated results of case studies mainly focused on HMDP scenario. The main frequency points and load shedding details of each case study also mentioned in Table 47.

Table 47: Tabulated results of TMDP Scenario with existing LSS

Case	Frequency before disturbance	Decaying Frequency	Load Shedding Scheme	Stabilizing Frequency	Settling Frequency
2.1	49.6 Hz at 50 s	48.85 Hz at 52.08 s	No loads were shed	49.82 Hz at 93s	49.81 Hz at 112 s
2.2	49.6 Hz at 50 s	48.56 Hz at 59.38 s	Stage I at 56 s 452 MW df/dt -0.288 104 MW Total Load shed 556 MW	49.6 Hz at 94 s	49.59 Hz at 119 s
2.3	49.6 Hz at 50 s	47.5 Hz at 54.17 s	Stage I at 51.102 s 364.25 MW df/dt -0.934 Stage II at 52.152 s 146.62 MW Stage III at 51.817 s 161.28 MW df/dt -0.919 484.45 MW Total Load shed 1156 MW	49.5 Hz at 90.62 s	49.5 Hz at 103.25 s
2.4	49.6 Hz at 50 s	47.56 Hz at 56 s	Stage I at 51.102 s 364.25 MW df/dt -0.934 Stage II at 52.152 s 176.62 MW Stage III at 53.762 s 261.28 MW df/dt -0.919 484.45 MW Total Load shed 1286 MW	49.4 Hz at 933.75 s	49.4 Hz at 100 s

5.3 Scenario 3 - Renewable Maximum Day Peak (RMDP)

In the Renewable Maximum Day Peak (RMDP) scenario, total solar generation is 1,018 MW and total wind generation is 976.9 MW as shown in Table 48. It is considered that 100% wind and 50% of solar power plants are committed in 2030. Wind and solar power plants are generating 100% of their full capacity from all available wind power plants in 2030. This 100% is equal to the Maximum wind generation during very wet season. This scenario is similar to the HMDP scenario with Maximum generation from

wind, solar, mini hydro, and biomass, which are non-conventional renewable power sources. The forecasted total system demand was not changed and it was at 4,581.99 MW and forecasted generation is 4,766.06 MW as mentioned in Table 48.

Table 48: Generation mix in RMDP Scenario

Total Load	**Total Generation = 4766.06 MW**					
	Generation Mix					
	Wind	**Solar**	Mini-Hydro	Bio-Mass	Major Hydro	Thermal
4581.99 MW	**100%**	**100%**	100%	100%	Balance	Max
	976.9 MW	**1018 MW**	558.7 MW	98.5 MW	1389.9 MW	724 MW

Table 49 shows the hydro machines, which were operated in low load without generating maximum load to cater any power imbalance similar to HMDP scenario. The swing bus Victoria power station was giving 30 MW to the national grid. It has the lowest droop 0.016 and PIDGOV PSS/E model was used in the simulation. Each unit of all three units of Pumped storage was generating 45 MW, which has the maximum generating capacity of 206 MW during day peak time at thermal maximum season. It has the droop 0.05. Two units of Kothmale power station can vary power between 0 to 67 MW, which has the droop setting of 0.05. The maximum generation capacity of one unit in Colombo LNG power station is 67 MW. All the other hydro power plants were operated in full load except generators mentioned in Table 49, which were considered in free governor mode.

Table 49: Machine Governors used in Free Governor Mode in RMDP Scenario

Generator Name	**PGen (MW)**	**PMax (MW)**	**Turbine Governor Model in PSS/E**	**Permanent Droop (R)**
VICTORIA GEN-1	30	70	PIDGOV	0.016
VICTORIA GEN-2, 3	0	70	PIDGOV	0.016
PUMP STORAGE 1, 2, 3	45	206	HYGOV	0.045
KOTHMALE GEN-2, 3	0	67	HYGOV	0.05

As mentioned in Table 50, major hydro and thermal power plants were operated in RMDP scenario. Only three units out of five units of Lakvijaya coal power plant were in operation and two units were loaded at 200 MW. Other unit of Lakvijaya coal power plant was partially loaded to 150 MW, due to high generation of wind, solar, mini hydro and bio mass power plants. One unit of Sampoor power plant was generating at 140 MW while its maximum generation capacity is 270 MW. Umaoya power plant, power plants in Laxapana complex, power plants in Mahaweli complex and power plants in Samanala complex were committed in RMDP scenario while a few machines mentioned in Table 49 were used in free governor mode to keep the spinning reserve.

Table 50: Major Hydro and Thermal Power Plants in operation in RMDP Scenario

Power Plant Name	**Power Generation (MW)**
Umaoya Hydro Power Plant	120
Laxapana Hydro Power Complex	339.5
Mahaweli Hydro Power Complex	593
Samanala Hydro Power Complex	120
Sampoor Coal Power Plant	140
Lakvijaya Power Plant (G1, G2, G3)	2×200+150

Figure 45 illustrates the active power generation of all solar power plants available in 2030-year power system model in RMDP scenario including mainly Pooneryn, Mannar, Siyambalanduwa, Hambantota and Vavniya solar power plants. This is almost equal to the active power generation of selected solar power plants in HMDP scenario. The similar solar power ramp rates and irradiance level values used for both RMDP and HMDP scenarios because this RMDP scenario is considered as the worst case of HMDP scenario by increasing wind and solar power generation. The simulation was performed to observe the solar power plants active power generation without tripping a plant or without a disturbance within 150 s time frame. The fastest solar ramp rate was observed in Pooneryn solar power plant. The highest variations of solar can be observed within 75 s to 100 s. The minimum power generated at 50 s is the time at which a contingency could be given to observe the behavior of the power system at its worst case. This

simulation was carried out to determine the most vulnerable point to trip the single largest generator to get the worst case simulation.

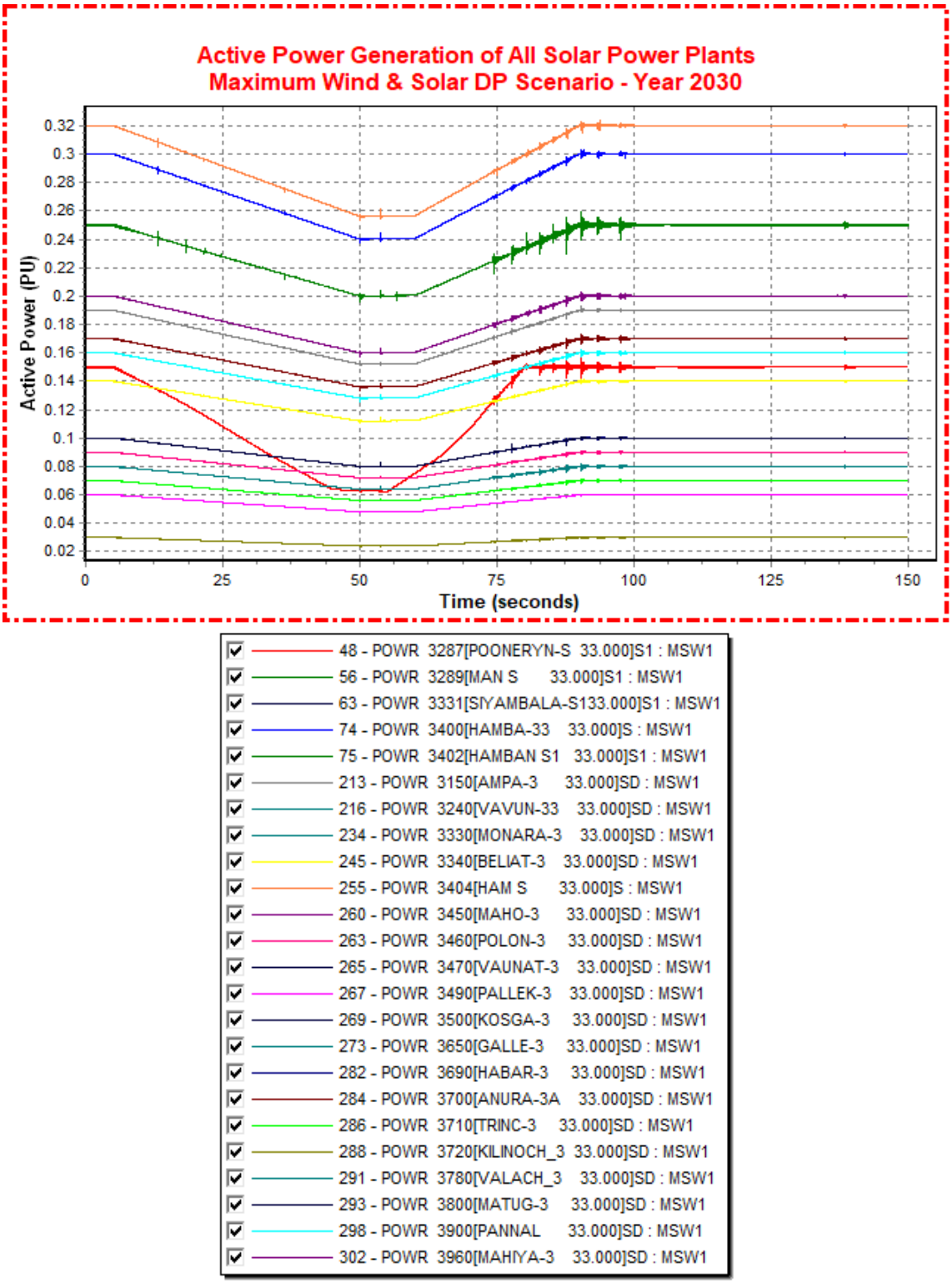

Figure 45: Active power generation of all solar power plants in RMDP scenario

Figure 45 illustrates the active power generation of selected wind power plants available in 2030-year power system model in RMDP scenario including mainly Chunnakam, Puttalam, Kalpitiya and Mannar. The wind variations were high within 75 s to 100 s during 150 s time frame of simulation. The active power generation of wind power plants for all three simulation scenarios HMDP, TMDP and RMDP were almost similar.

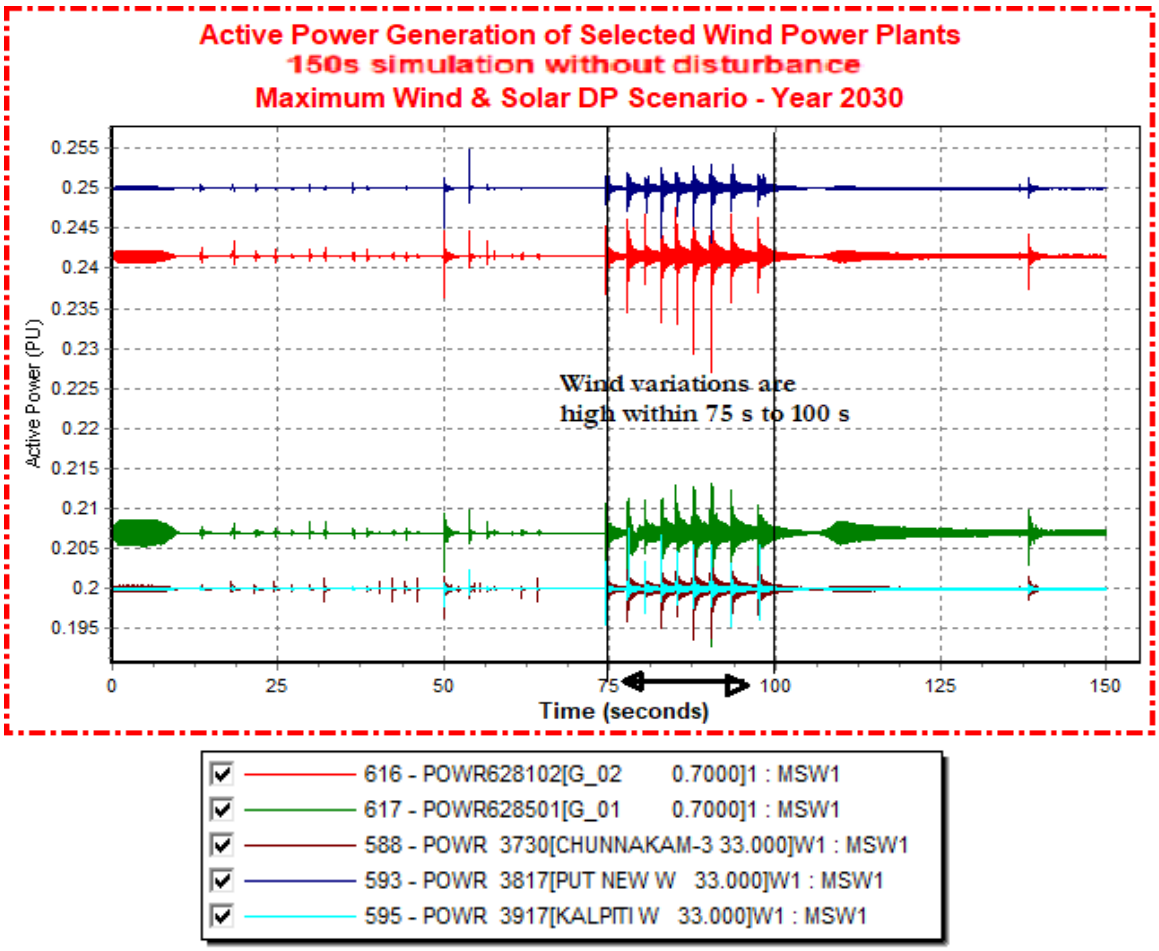

Figure 46: Active power generation of selected wind power plants in RMDP scenario

Case 3.1: Tripping 200 MW Loaded 2 Units and 150 MW Loaded 1 Unit in Lakvijaya (Loosing 11.5% Generation – Tripping Three Units)

Figure 47 illustrates the system frequency response of tripping of 200 MW loaded generator units 1, 2 and 150 MW loaded generator unit 3 at 50 s in Lakvijaya coal power plant. This graph shows how the system frequency behaves when loosing 550 MW power in system. The frequency variation is almost similar to the case 1.1 and 2.1 as

described in above. Similar to previous cases frequency decreased gradually with solar ramp rate decreases. The 1st gen tripped at 50 s, 2nd one tripped at 51 s and 2nd one tripped at 51.5 s, which is the minimum point of frequency curve. Two stages of UFLS were operated and totally 548 MW loads were shed. Load shed amount was equal to the loss and settling frequency reaches 50 Hz. Highest overshoot in frequency was 50.2 Hz. The frequency has settled to 50 Hz (within the standard limits of 49.5 to 50.5 Hz) and settling time was higher than the previous case. All three units of Pumped storage power plant were over loaded to 206 MW. The details of load shedding are mentioned in Table 51.

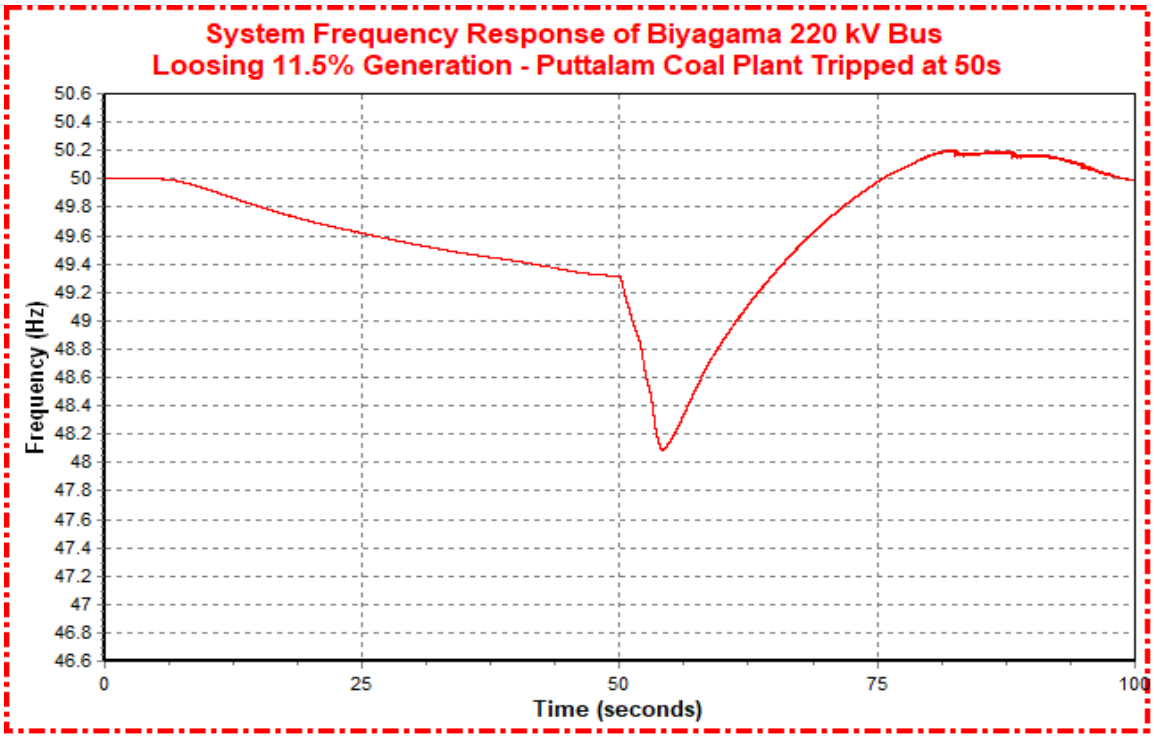

Figure 47: Frequency Response of Tripping 200 MW Loaded 2 Units and 150 MW Loaded 1 Unit in Lakvijaya at 50 s in RMDP scenario

Figure 48 illustrates the system frequency response of tripping of 200 MW loaded generator units 1, 2 and 150 MW loaded generator unit 3 at 3 s in Lakvijaya coal power plant. The tripping time was changed to 3 s to observe the high solar energy generation effect because the solar generation was at its maximum until 6 s within simulation time frame.

The frequency variation was almost similar to the case 1.1, 2.1 and 3.1 as described in above with a few differences. Similar to previous cases, frequency decreased gradually with solar ramp rate decreases. Three generator units of Lakvijaya coal power plant were tripped respectively at 3 s, 3.5 s and 4 s, which was in the maximum solar generation duration of frequency curve. Then LSS activated and started shedding loads at 7.5 s, free governor mode generators and spinning reserve supported to restore frequency but solar was ramping down gradually until 50 s. Therefore, the curve shows a frequency valley at 50 s which is not less than the minimum frequency observed at 10 s.

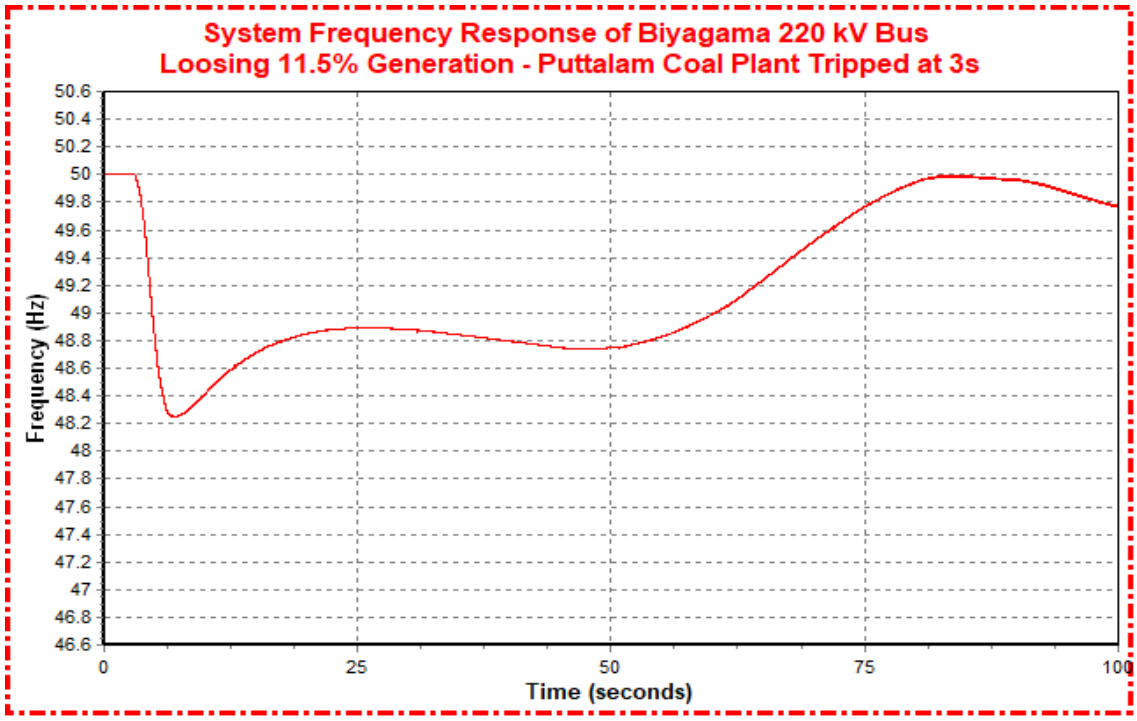

Figure 48: Frequency Response of Tripping 200 MW Loaded 2 Units and 150 MW Loaded 1 Unit in Lakvijaya at 3 s in RMDP scenario

Two stages of UFLS were operated and totally 556 MW of loads were shed. Load shed amount is equal to the loss, but frequency has not reached close to 50 Hz like in the previous case. There was no overshoot in frequency and frequency has reached 50 Hz at 63 s however, due to solar ramping, frequency has decreased again. The frequency has settled around 49.8 Hz and the settling time also higher than the previous case. All three

units of Pumped storage power plant full loaded to 206 MW at 19 s. Compared to other simulations, in this case study, the effect of high solar generation was clearly observed.

Case 3.2: Tripping 200 MW, 150 MW Loaded Lakvijaya 3 Units and 150 MW Loaded Sampoor 1 Unit (700 MW) (Loosing 15% Generation – Tripping Two Plants)

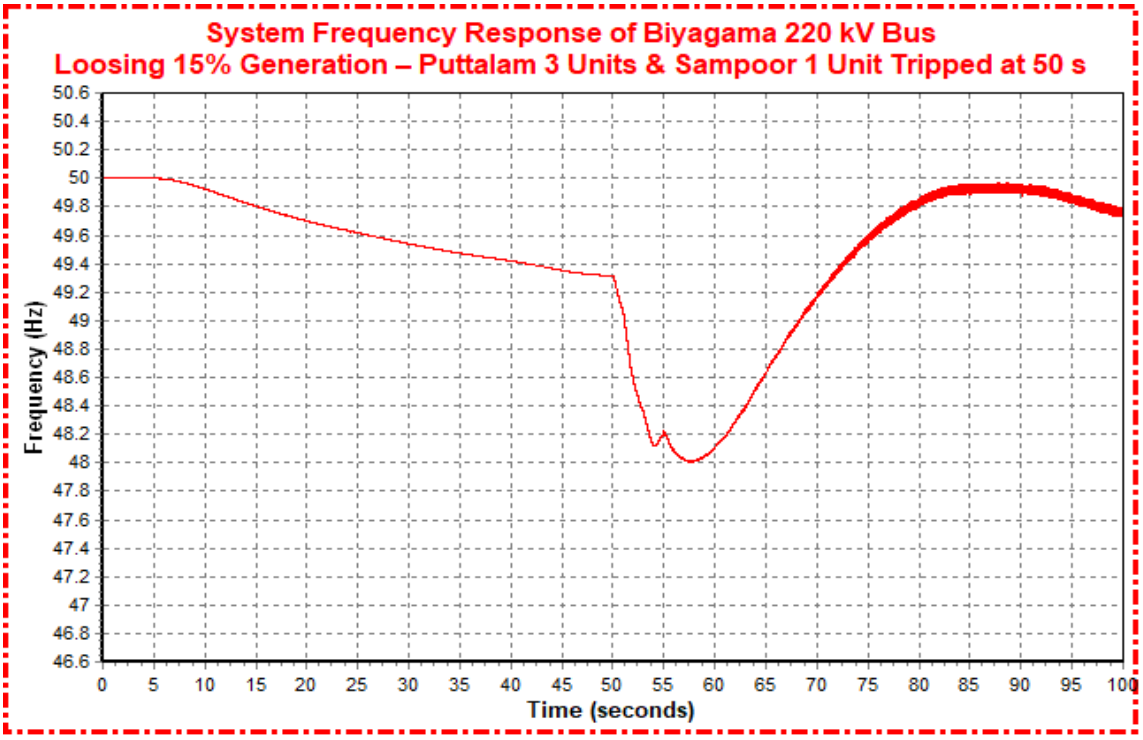

Figure 49: Frequency Response of Tripping 200 MW, 150 MW Loaded Lakvijaya 3 Units and 150 MW Loaded Sampoor 1 Unit at 50 s in RMDP scenario

Figure 49 illustrates the system frequency response of tripping of 200 MW loaded generator units 1, 2 and 150 MW loaded generator unit 3 at 50 s in Lakvijaya coal power plant and tripping of 150 MW loaded unit 1 in Sampoor coal power plant. The total generation loss was 700 MW. The frequency variation is almost similar to the case 1.2, 2.2 and 3.1 as described in above. Similar to previous cases, frequency decreased gradually with solar ramp rate decreases. Three generator units of Lakvijaya coal power plant were tripped at 50s, 51 s and 52 s respectively. The power imbalance was taken care of with the activating LSS and spinning reserve. Frequency increased before the unit 1 of Sampoor power plant was tripped at 55 s. Three stages of UFLS were operated

and totally 790 MW loads were shed. Load shed amount is greater than the loss but frequency has reached close to 50 Hz like in case 3.1. The peak in frequency was nearly 50 Hz but the frequency has settled at a value below 50 Hz and settling time was also higher than previous case 3.1. All three units of Pumped storage power plant were over loaded to 210 MW at 59 s.

Case 3.3: Tripping 200 MW, 150 MW Lakvijaya 3 Units and 140 MW Sampoor 1 Unit and 45 MW Pumped Storage 3 Units (835 MW) (Loosing 18% Generation – Tripping Three Plants)

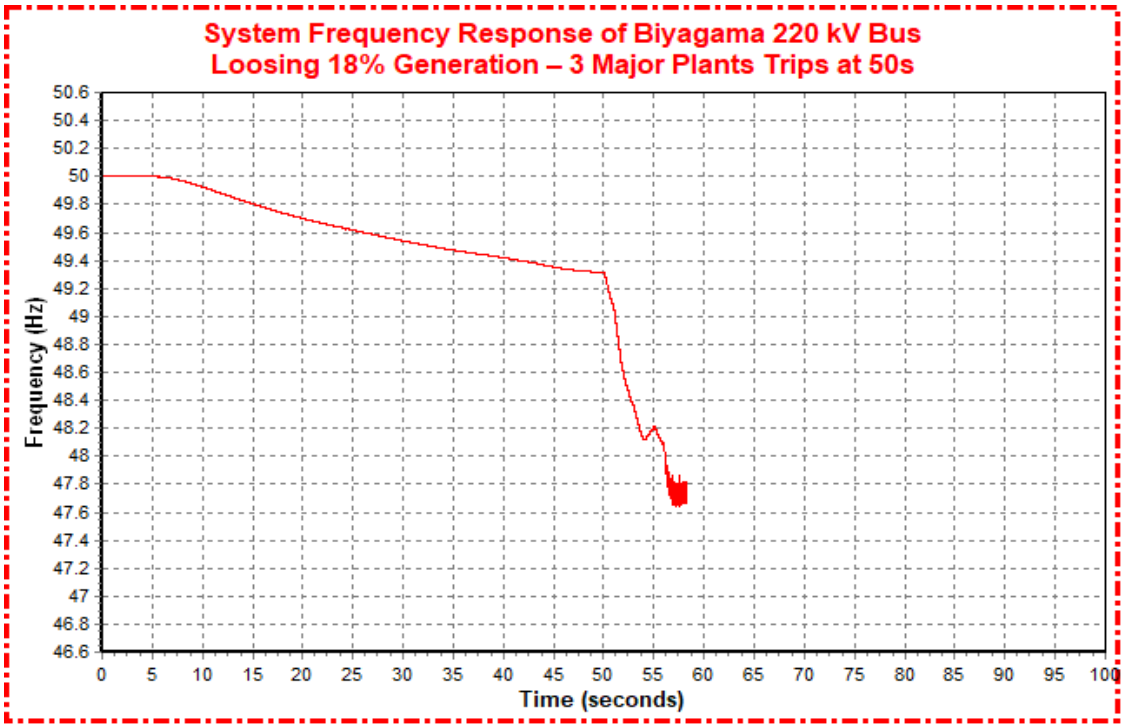

Figure 50: Frequency Response of Tripping 200 MW, 150 MW Loaded Lakvijaya 3 Units and 150 MW Loaded Sampoor 1 Unit and 45 MW Pumped Storage 3 Units at 50 s in RMDP scenario

Figure 50 illustrates the system frequency response of tripping three power plants including Lakvijaya coal power plant, Sampoor coal power plant and pumped storage power plant. Three generator units of Lakvijaya coal power plant were tripped at 50 s, 50.5 s and 51 s respectively. The generator unit 1 of Sampoor coal power plant was tripped at 52 s and all three units of pumped storage power plant were tripped at 53 s.

The total generation loss was 835 MW. The pumped storage is operated min load to cater power imbalances and provide free governor support to the system. By tripping the pumped storage power plant, the power system frequency behavior was simulated in this case. Similar to previous cases 3.1 and 3.2, frequency decreased gradually with the decrease in solar output. Three stages of UFLS were operated, but the frequency was not built up, which lead to system blackout situation. The load shedding was not capable enough to restore the system frequency due to tripping of pumped storage power plant, which supports the system by providing spinning reserve. The details of load shedding are mentioned in Table 51.

Table 51: Tabulated results of RMDP Scenario with existing LSS

Case	**Frequency before disturbance**	**Decaying Frequency**	**Load Shedding Scheme**	**Stabilizing Frequency**	**Settling Frequency**
3.1	49.3 Hz at 50 s	48.1 Hz at 56.4 s	Stage I at 54 s 377 MW df/dt -0.288 171MW Total Load shed 548 MW	50.2Hz at 90 s	50 Hz at 100 s
3.2	49.3 Hz at 50 s	48 Hz at 57.5 s	Stage I at 51.520 s 264.55 MW df/dt -0.940 Stage II at 52.752 s 176.45 MW Stage III at 53.8 s 78.76 MW df/dt -0.900 272.50 MW Total Load shed 790 MW	49.85 Hz at 87.5 s	49.68 Hz at 100 s
3.3	49.3 Hz at 50 s	47.85 Hz at 57.5 s	System Blackout		

CHAPTER 6

PROPOSED LOAD SHEDDING SCHEME

An effective LSS requires the knowledge about power system dynamics, disturbances and process constraints. In dynamic LSS system data is continuously monitored through real-time power system observing and simulation system. The total generation, total load demand, spinning reserve and load demand of each feeder in non-critical load shedding feeder list are the few of the most important system data which are required for dynamic LSS. The benefits of proposed dynamic LSS can be addressed as bellows.

1. Fast responses to disturbances
2. Optimal amount of load shed matches to the disturbance
3. Time to restore system frequency is lesser than existing LSS
4. No data training algorithms and operator training is required
5. Load shed from non-critical feeders accordance with the mismatch

In order to overcome the shortcomings identified in Static LSS, it is proposed to implement a dynamic load shedding scheme based on actual consumption data of feeders obtained through Supervisory Control and Data Acquisition (SCADA). The transmission and distribution system SCADA system collects real-time measurements from the grid and transfers them to the system control centre.

When designing this new LSS, the following assumptions were made:

1. There will be an increasing development of intelligent controllers and measuring monitors such as SCADA system and Phasor Measurement Units (PMU)
2. There will be protective relays installed at grid substations that respond to system disturbances within milliseconds to prevent the system

According to this algorithm it is possible to retrieve actual consumption data on real and reactive power by the feeders. The mechanism continuously observes generation of each unit, total generation, total load demand, list of low priority feeders and spinning reserve. This data retrieving is done by an advanced monitoring system in the power

system, which captures the real time system data of frequency, power generation and Load demand by means of data collection servers located at each of the grid substations and passes them to a centralized Data Collection Server, which is located at the system control centre. This server is a combination of knowledge base and computation base. The system uses these real time data and performs necessary calculations through power mismatch calculation module and frequency deviation and df/dt calculation module. This calculation model calculates load amount needs to be shed. Then is selects the non-critical feeders and create a list for load shedding to match the calculated load shedding amount. Load shedding PLC signal is then sent to activate load circuit breaker of the feeders in the list. The proposed LSS is illustrated in Figure 51.

According to Figure 51, the main components of the proposed LSS and their function in brief are as follows:

1. Data Collection Server – Generation Units: This server continuously collects real-time data of generation of each unit, total generation and spinning reserve. Sends collected real-time data to the Centralized Data Collection Server.

2. Data Collection Server – Grid Substations: This server continuously collects real-time data of load amount at each load bus, total load demand and list of low priority feeders. Sends collected real-time data to the Centralized Data Collection Server.

3. Centralized Data Collection Server – System Control Centre: This server uses real time data from Data Collection Server – Generation Units and Data Collection Server – Grid Substations to perform necessary calculations through power mismatch calculation module and frequency deviation and df/dt calculation module. This calculation model calculates load amount needs to be shed.

4. Power Mismatch Calculation module: This module calculates difference between total load demand and total power generation.

5. Frequency deviations and df/dt calculation Module: This module calculates deviations of system frequency and df/dt value.

6. Non-critical feeder list: Centralized Data Collection Server – System Control Centre updates this list with actual load amount of non-critical feeders and critical feeders which should avoid for load shedding.

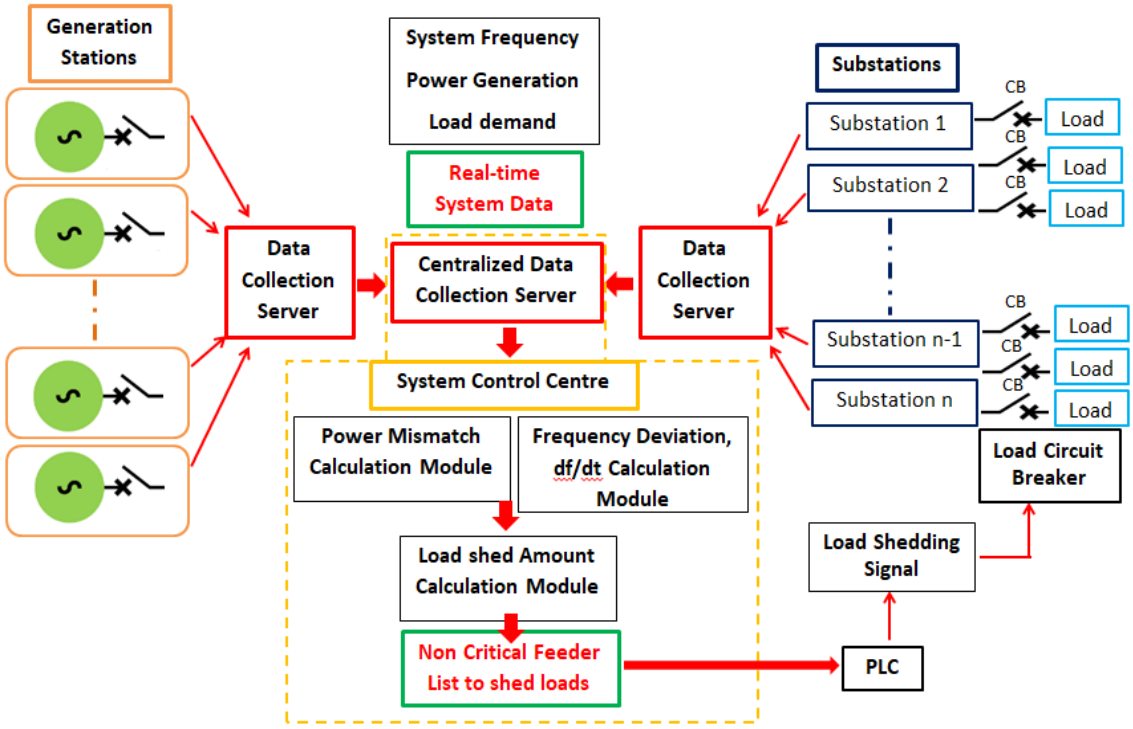

Figure 51: Basic implementation of proposed load shedding scheme

Following guidelines are considered for designing new load shedding scheme;

1. Load shedding would not occur as long as system frequency was above 49.4 HZ and df/dt is -0.65 Hz/s.
2. Adequate load amounts must be shed to avoid the system frequency decreasing below 47.5 Hz.
3. Load shedding must be considering frequency, df/dt and power mismatch to minimize the necessary load shedding amount at different levels of spinning reserves, and for different events of generation loss.

4. Load shedding must be avoid overshoot in system frequency. Therefore, it must not be allowed to increase higher than 52.5 Hz

6.1 Implementation of Proposed Load Shedding Scheme

In this study, power system of year 2030 was modeled and validated in PSS/E software. The Python Programming language was selected for implementation of proposed LSS in developed PSS/E power system model. The automated scripting is a latest technology introduced by PSS/E software, which allows user to retrieve real timed data using this Python automation code. Using these automated scripts, it enables users to automate power system studies such as power flow, modify saved case, create tripping events, clear tripping events, and write output to a file etc. The automation file which contain set of steps, or for batch operation, where PSS/E can run a defined set of procedures to complete the task without interaction with user. Therefore, this dynamic LSS was implemented using an automated Python code, which can retrieve data and change data during the process of dynamic simulations.

The proposed LSS algorithm is illustrated in Figure 52. System initialization is the first step of the algorithm as PSS/E simulation needs to initialize before performing dynamic analysis. It reads real time data for system frequency, power generation and demand for every 100 ms. These data are used to calculate power mismatch, frequency deviation, df/dt and load shedding amount by the Python code. The load shedding algorithm implemented through Python code can sense any load generation unbalance that may cause instability in system frequency. The programmed algorithm determines amount of power that is required for load shedding to restore frequency stability of the system. Then it defines the appropriate non-critical load buses from all load buses to match the load shedding amount and load amount needs to be shed from each selected candidate bus. Then, signals are sent to shed the correspondent load amount at the selected non-critical load buses.

The algorithm performs the following steps:

1. System Initialization Step - Given System Data: Equivalent inertia (H_t), Non-critical load bus list with available load amount in each bus (P_n, n is the non-critical bus number)

2. Real-time data monitoring Step - total mechanical power (P_{Mech}), total power generation (P_{Elec}), total load (P_{Load}), and system frequency (F_{Act}).

3. Calculation Step - Calculate frequency deviation (F_{Dev}), difference between electrical and mechanical power (P_{Diff}), absolute value of power mismatch (A_{PDiff}), rate of change of frequency (F_{DfByDt}), total load to be shed (P_{Shed}).

4. Decision Step 1 (Rapid Round) - Check $49.4 \geq F_{Act} > 49.0$ and $F_{DfByDt} > -0.85$ if this true, we have to shed loads. If false, go to step 6.

   If true, a part of load (P_n) shed at the 1st load bus in the Load shed bus list. Calculate P_{Remain} by subtracting the load amount (P_n) of 1st load bus in the load shed bus list from the P_{Shed}.

   Then check $P_{Remain} > 0$ if this true, shed load amount (P_n) from next load. Do this step until $P_{Remain} = 0$.

   If $P_{Remain} = 0$, then go to step 2.

5. Decision Step 2 (Basic Round I) - Check $49.0 \geq F_{Act} > 48.5$ and $-2.50 \geq F_{DfByDt} > -0.85$ if this true, we have to shed loads. If false, go to step 6.

   If true, a part of load (P_n) shed at the 1st load bus in the load shed bus list. Calculate P_{Remain} by subtracting the load amount (P_n) of 1st load bus in the load shed bus list from the P_{Shed}.

   Then check $P_{Remain} > 0$ if this true, shed load amount (P_n) from next load. Do this step until $P_{Remain} = 0$.

   If $P_{Remain} = 0$, then go to step 2.

6. Decision Step 3 (Basic Round II) - Check $48.5 \geq F_{Act} > 48.0$ and $-1.50 \geq F_{DfByDt} > -0.85$ if this true, we have to shed loads. If false, go to step 6.

   If true, a part of load (P_n) shed at the 1st load bus in the load shed bus list. Calculate P_{Remain} by subtracting the load amount (P_n) of 1st load bus in the load shed bus list from the P_{Shed}.

   Then check $P_{Remain} > 0$ if this true, shed load amount (P_n) from next load. Do this step until $P_{Remain} = 0$.

   If $P_{Remain} = 0$, then go to step 2.

7. Decision Step 4 (Basic Round III) - Check $48.0 \geq F_{Act} > 47.0$ and $0.85 \geq F_{DfByDt} > 0.65$ if this true, we have to shed loads. If false, go to step 6.

   If true, a part of load (P_n) shed at the 1st load bus in the load shed bus list. Calculate P_{Remain} by subtracting the load amount (P_n) of 1st load bus in the load shed bus list from the P_{Shed}.

   Then check $P_{Remain} > 0$ if this true, shed load amount (P_n) from next load. Do this step until $P_{Remain} = 0$.

   If $P_{Remain} = 0$, then go to step 2.

8. Load shedding Step – After deciding which amount to be shed to balance the mismatch and which amount to be shed from each load bus, the algorithm sends a trip signal to the selected non-critical load bus or feeder to trip the determined load amount which matches with the P_{Shed} amount calculated in Step 2.

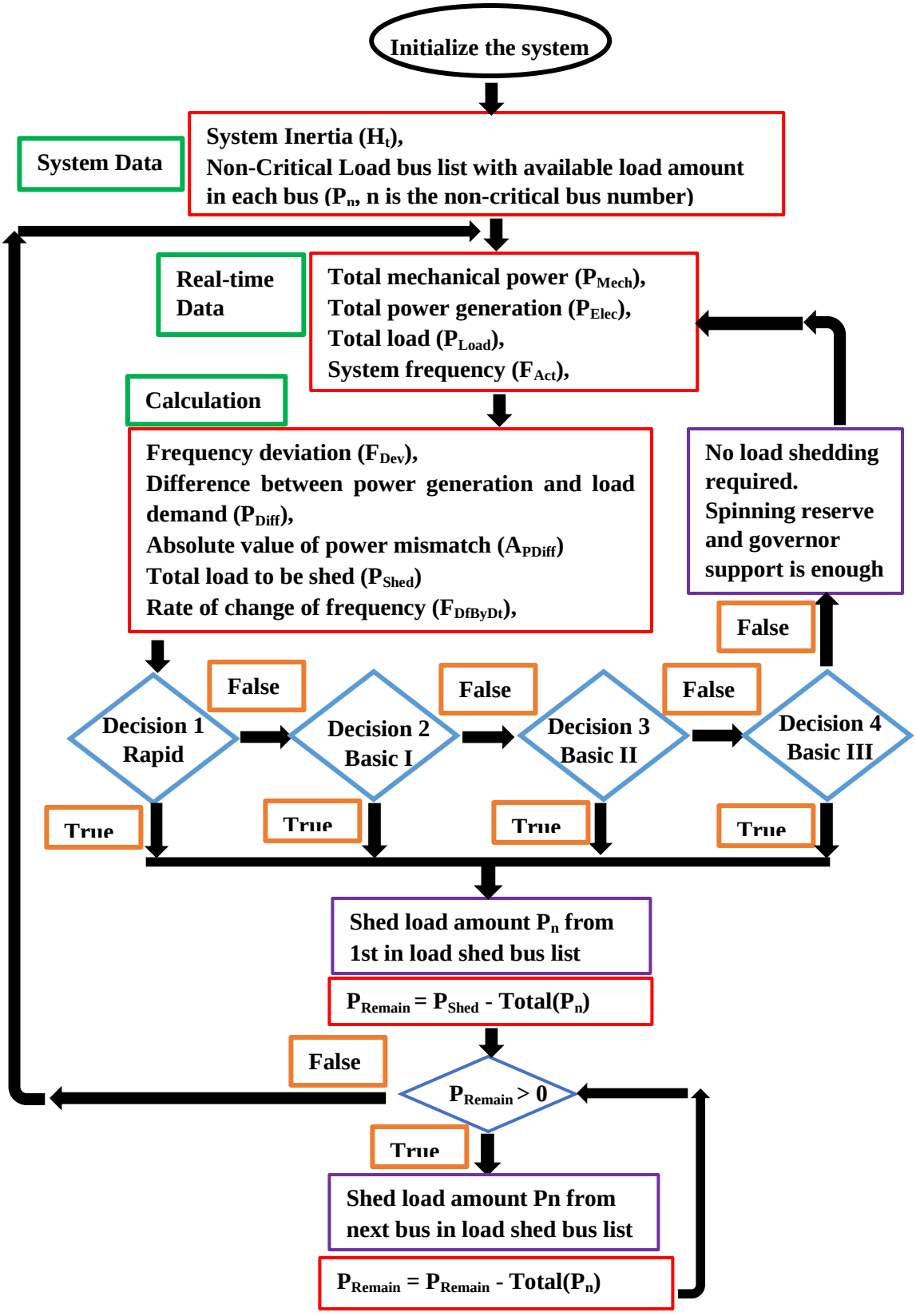

Figure 52: Algorithm of proposed load shedding scheme

6.2 Developing the Program Algorithm and Coding in PSS/E

Initially, the coding of the algorithm for operation of proposed dynamic LSS was done in Python programming language, which PSS/E allows user to create scripts for program automation.

Figure 53 illustrates starting of the algorithm by initializing all the variables used in the program and some basic steps in PSS/E dynamic simulations. It includes opening saved case, adding dynamic data or DYRE files, which contain all the dynamic simulation data as mentioned in the model dvelopment chapter, adding model library files or DLL files, which contain Vestas wind and solar models. Adding output response files to view all the output data progress are also included to the code.

```
import math
import psspy
# Library

t=0.05
x=1
z=1
Ht=0.2965495534 # Equivalent Inertia of system
f=49.50 # Minimum Frequency in SS
pRemain=0
Vbase=33
pMechlist=[]
pEleclist=[]
AccPlist=[]
pLoadlist=[]
ActFlist=[]
NCbusNumlist=[3150,3200,3240,3280,3340,3420,3440,3500,3510,3530,3550,3551,3560,3571,3581,3590,3620,3640,3650,3670,

psspy.case(r"""D:\Desktop New\HMDP N3\testcode\2030_HMDP edited.cnv""")
# Open the saved case and transfers its data into the PSSE working case

psspy.dyre_new(r"""D:\Desktop New\TMDP N3\testcode\2030v1.dyr""")
psspy.dyre_add(r"""D:\Desktop New\TMDP N3\testcode\2030 Solar - new ramp v2.dyr""")
psspy.dyre_add(r"""D:\Desktop New\TMDP N3\testcode\2030 Wind.dyr""")
# Add a dynamics data

psspy.addmodellibrary(r"""D:\Desktop New\HMDP N3\testcode\DLL\Vestas_GS_V8.2.0_PSSE33.dll""")
psspy.addmodellibrary(r"""D:\Desktop New\HMDP N3\testcode\DLL\Vestas_PPC_DF_A_1_3_1_K_PSSE33.dll""")
# Add dll files

psspy.progress_output(islct=2, filarg=r"""D:\Desktop New\HMDP N3\testcode\test1R1.txt""", options=2)
psspy.alert_output(islct=2, filarg=r"""D:\Desktop New\HMDP N3\testcode\test1R2.txt""", options=2)
psspy.prompt_output(islct=2, filarg=r"""D:\Desktop New\HMDP N3\testcode\test1R3.txt""", options=2)
# Add output reports
```

Figure 53: Developed Python Code in PSS/E – Code Initialization

Adding channels for frequency in each bus, voltage in each bus, machine data including machine speed, mechanical power, and electrical power and load bus data including active power and reactive power are illustrated in Figure 54. These are the real-time data used to detect system disturbances. These data were retrieved by real time channel

values of PSS/E Python coding during simulations, which is similar to collecting real time data using SCADA system and data collection servers installed at generation station and grid substations. Coding of PSS/E dynamic simulation initialization is shown in Figure 54.

```
36  psspy.delete_all_plot_channels()
37  # Delete all the plot channels in the working case
38
39  ## Add channels by subsystem
40  psspy.chsb(sid=0,all=1, status=[-1,-1,-1,7,0])
41  # Power totals for all buses
42  # BUS FREQUENCY
43  psspy.chsb(sid=0,all=1, status=[-1,-1,-1,1,12,0])
44  # BUS VOLTAGE
45  psspy.chsb(sid=0,all=1, status=[-1,-1,-1,1,13,0])
46  # MACHINE SPEED
47  psspy.chsb(sid=0,all=1, status=[-1,-1,-1,1,7,0])
48  # PMECH
49  psspy.chsb(sid=0,all=1, status=[-1,-1,-1,1,6,0])
50  # PLOAD
51  psspy.chsb(sid=0,all=1, status=[-1,-1,-1,1,25,0])
52  # QLOAD
53  psspy.chsb(sid=0,all=1, status=[-1,-1,-1,1,26,0])
54
55  psspy.strt(0,r"""D:\Desktop New\HMDP N3\testcode\test1.out""")
56  # Initialize
```

Figure 54: Developed Python Code in PSS/E – Adding Channels and Initialization

In PSS/E Python programming, a while loop is used to read and write real-time data for every 100 ms as shown in Figure 55. The system frequency, mechanical power, electrical power, accelerated power and load demand were retrieved by PSS/E channels into the declared arrays for each data for every cycle using the main while loop, which is ending in 100 s time frame.

The retrieved real-time data are inserted into the lists for further calculations in next steps. For each cycle, new data record is added from every variable into the relevant list of the variable. The Python code for inserting retrieved real-time data into lists for further calculations is illustrated in Figure 56.

```
while t<100.1 and x<2002:
    psspy.run(0,t,0,0,1)
    # Run to t seconds

    f=psspy.chnval(338)
    freq=f[1]
    ActF=50*(1+freq)
    # Actual Frequency value of Victoria Bus
    print("time",t)
    print("freq",ActF)

    pm=psspy.chnval(1)
    pMech=pm[1]
    print("mechanical power is",pMech)
    # Total Mechanical Power value for all Buses
    pe=psspy.chnval(2)
    pElec=pe[1]
    print("elec power is",pElec)
    # Total Electrical Power value for all Buses
    pa=psspy.chnval(3)
    AccP=pa[1]
    print("Accelerating Power is",AccP)
    # Total Accelerating Power value for all Buses
    pl=psspy.chnval(4)
    pLoad=pl[1]
    print("load power is",pLoad)
    # Total Load value for all Buses
```

Figure 55: Developed Python Code in PSS/E – Data Retrieval

```
    pMechlist.insert((x-1),pMech)
    print("pMech element is",pMechlist[(x-1)])
    # Insert pMech values to a list
    pEleclist.insert((x-1),pElec)
    print("pElec element is",pEleclist[(x-1)])
    # Insert pElec values to a list
    AccPlist.insert((x-1),AccP)
    print("AccP element is",AccPlist[(x-1)])
    # Insert AccP values to a list
    pLoadlist.insert((x-1),pLoad)
    print("pLoad element is",pLoadlist[(x-1)])
    # Insert pLoad values to a list
    ActFlist.insert((x-1),ActF)
    print("ActF element is",ActFlist[(x-1)])
    # Insert pLoad values to a list
```

Figure 56: Developed Python Code in PSS/E – Insert Retrieved Data into Lists

Figure 57 illustrates the python code of calculating diffrecne between mechanical power and electrical power and electrical power and load demand, which will be used in the swing equation to find df/dt. The power mismatch value obtained from the equation (2) and using real-time data values are compared to verify the power mismatch before the decision of load shedding is done.

```
126     pMechDiff=pMechlist[(x-2)]-pMechlist[(x-1)]
127     pElecDiff=pEleclist[(x-2)]-pEleclist[(x-1)]
128     pMechElecDiff=(pMechDiff-pElecDiff)
129     print("pMechDiff-pElecDiff is",pMechElecDiff)
130     # Calculate Power pMechDiff-pElecDiff
131
132     pElecDiff=pEleclist[(x-2)]-pEleclist[(x-1)]
133     pLoadDiff=pLoadlist[(x-2)]-pLoadlist[(x-1)]
134     pElecLoadDiff=(pElecDiff-pLoadDiff)
135     print("pElecDiff-pLoadDiff is",pElecLoadDiff)
136     # Calculate Power pElecDiff-pLoadDiff
137
138     pGenLoadDiff=(2*Ht*DfByDt)/ActF
139     print("pDiff using ROCOF is",pGenLoadDiff)
140     # Calculate Power Mismatch
141
```

Figure 57: Developed Python Code in PSS/E – Power Difference Calculation

$$\text{Total Load} - \text{Total generation} = \frac{2 \times Ht \times (df/dt)}{\text{Frequency}} \qquad (2)$$

The deviation of frequency is calculated and df/dt is obtained by using the frequency curve as shown in Figure 58.

```
123     fDev = 50.0 - ActF
124     print("Frequnecy deviation is",fDev)
125     # Calculate Frequnecy deviation
126
127     DfByDt = ((ActFlist[(x-2)]-ActFlist[(x-1)])*(-1))/0.05
128     print("ROCOF is",DfByDt)
129     # Calculate Rate of change of frequency
```

Figure 58: Developed Python Code in PSS/E –Frequency Deviation Calculation

The absolute value of the difference between load and generation is calculated in the calculation step as shown in Figure 59. The difference between load and generation was calculated in the real-time data monitoring step.

```
141     if pGenLoadDiff<0:
142         print("freq decreasing ")
143         ApDiff=pGenLoadDiff*(-1)
144         print("Power Absolute Mismatch  is",ApDiff)
145         # Power Absolute value of Power Mismatch
146 
147     else:
148         print("freq constant ")
149         ApDiff=pGenLoadDiff
150         print("Power Absolute Mismatch  is",ApDiff)
151         # Power Absolute value of Power Mismatch
```

Figure 59: Developed Python Code in PSS/E – Calculation Load generation is given

The load reduction factor and anticipated overload is calculated using the difference between load and generation value, which was calculated in the previous step. The load amount that need to be shed to match the power imbalance is calculated using the above calculated the load reduction factor and anticipated overload as is illustrated in Figure 60.

```
563 
564     d = pDiff/(ActF-50)
565     print("Load reduction factor is",d)
566     # Calculate Load reduction factor
567 
568     overL = (pLoad - pElec)/pElec
569     print("Anticipated overload",overL)
570     # Calculate Anticipated overload
571 
572     Pshed = ((overL/(1+overL))-(d(1-(f/50))))/(1-(d(1-(f/50))))
573     print("Load to be shed",Pshed)
574     # Calculate Load to be shed
575 
```

Figure 60: Developed Python Code in PSS/E – Calculation of Load amount to be shed

The load reduction factor is determined by the ratio between power mismatch and frequency deviation as mentioned in equation (3) as explained in [26].

$$\text{Load Reduction Factor (d)} = \frac{\text{Total Load} - \text{Total generation}}{\text{Frequency} - \text{Norminal Frequency (50 Hz)}} \quad (3)$$

The under frequency load shedding relays should shed loads similar to the maximum anticipated overload, which avoid system collapses. This factor is determined by equation (4) [26].

$$\text{Anticipated Overload (L)} = \frac{\text{Total Load} - \text{Total generation}}{\text{Total generation}} \tag{4}$$

The load amount need to be shed is determined by the overload factor, frequency factor and load reduction factor as shown in equation (5), equation (6), and equation (7) respectively [26].

$$\text{Overload Factor (LF)} = \frac{\text{Overload}}{1 + \text{ Overload}} \tag{5}$$

$$\text{Frequency Factor (FF)} = 1 - \frac{\text{Minimum premissible Frequency}}{\text{Norminal Frequency (50 Hz)}} \tag{6}$$

$$\text{Load to be Shed} = \frac{\text{LF} - \text{d} \times \text{FF}}{1 - \text{d} \times \text{FF}} \tag{7}$$

The "IF" loop is used to shed loads according to the calculated amounts in the calculation step. This is checking frequency value, power mismatch and df/dt to make load shedding command to the load bus to shed the selected amount of load to cater the power mismatch. Similar to the UFLS scheme used by CEB, a 100 ms time delay is used between load shedding steps to observe the frequency behavior.

Number of four decisions making, "IF" loops were used to check the frequency deviation and df/dt values. These four decisions making steps were named as Rapid round, Basic round I, Basic round II and Basic round III as described in decision step 1, 2, 3 and 4 respectively in algorithm to activate load shedding. During each step, the load amount is shed according to the calculated load shedding amount (P_{Shed}). The algorithm

checks the remaining the load shedding amount (P_{Remain}) by another decision making, inner “IF” loop. The Pyhton code for load shedding is illustrated in Figure 61.

```
155     if 48.50<ActF<=49.25 and -1.00<DfByDt<=-2.00:
156         if 375>=Pshed>275:
157             psspy.load_data_4(3571,r"""1""",[_i,_i,_i,_i,_i,_i],[ _f,_f, 37.728,_f,_f,_f])
158             pRemain=Pshed-21.222
159             print("P Remain",pRemain)
160             if pRemain>0:
161                 psspy.load_data_4(3640,r"""1""",[_i,_i,_i,_i,_i,_i],[ _f,_f, 39.632,_f,_f,_f])
162                 pRemain=pRemain-9.908
163                 print("P Remain",pRemain)
164                 if pRemain>0:
165                     psspy.load_data_4(3680,r"""1""",[_i,_i,_i,_i,_i,_i],[ _f,_f, 36.282,_f,_f,_f])
166                     pRemain=pRemain-24.3452
167                     print("P Remain",pRemain)
168                     if pRemain>0:
169                         psspy.load_data_4(3790,r"""1""",[_i,_i,_i,_i,_i,_i],[ _f,_f, 30.4329,_f,_f,_f])
170                         pRemain=pRemain-19.4571
171                         print("P Remain",pRemain)
172                         if pRemain>0:
173                             psspy.load_data_4(3240,r"""1""",[_i,_i,_i,_i,_i,_i],[ _f,_f, 6.4,_f,_f,_f])
174                             pRemain=pRemain-15.000
175                             print("P Remain",pRemain)
176                             if pRemain>0:
177                                 psspy.load_data_4(3420,r"""1""",[_i,_i,_i,_i,_i,_i],[ _f,_f, 40.08,_f,_f,_f])
178                                 pRemain=pRemain-30.00
179                                 print("P Remain",pRemain)
180                                 if pRemain>0:
181                                     psspy.load_data_4(3510,r"""1""",[_i,_i,_i,_i,_i,_i],[ _f,_f, 17.03,_f,_f,_f])
182                                     pRemain=pRemain-25.000
183                                     print("P Remain",pRemain)
184                                     if pRemain>0:
185                                         psspy.load_data_4(3620,r"""1""",[_i,_i,_i,_i,_i,_i],[ _f,_f, 10.4199,_f,_f,_f])
```

Figure 61: Developed Python Code in PSS/E – Load Shedding loop

CHAPTER 7

ANALYSIS OF PROPOSED LOAD SHEDDING SCHEME

7.1 Scenario 1 - Hydro Maximum Day Peak (HMDP)

Case 1.4: Tripping 275 MW Loaded Lakvijaya 3 Units (Loosing 17% Generation – Tripping Single Plant)

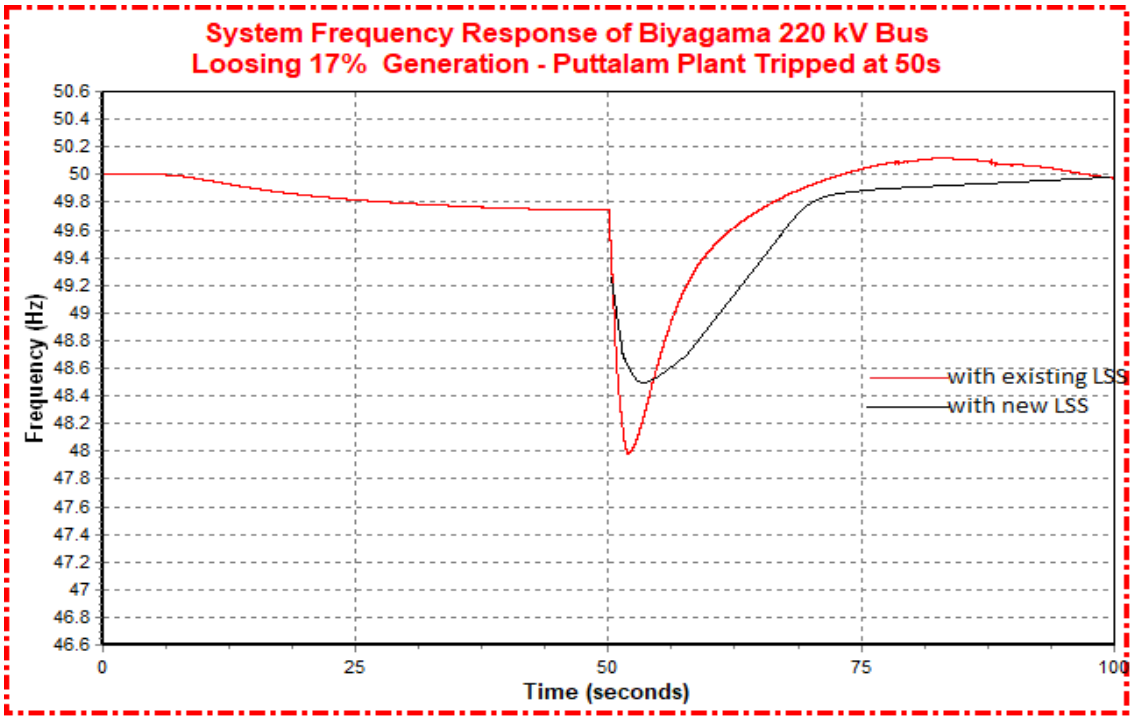

Figure 62: Tripping 275 MW Loaded Lakvijaya 3 Units in HMDP scenario

Figure 62 shows the frequency responses with existing CEB UFLS scheme and proposed LSC, when 825 MW power generation was lost by tripping all three generators of Lakvijaya coal plant which were in-service. Unit 1, 2 and 3 generators in Lakvijaya coal plant were tripped at 50 s, 50.5 s and 51 s respectively. With existing LSS, stage I of UFLS started at 50.857 s and three stages were operated. It has shed 663 MW from total available load amount. With the proposed LSS, only 480 MW load was shed at 49 Hz in the basic round I and II after 2nd generator tripped at 50.5 s.

Case 1.5: Tripping 275 MW Loaded Lakvijaya 3 Units and 140 MW Loaded Sampoor 1 Unit (965 MW) (Loosing 21% Generation – Tripping Two Plants)

Figure 63 shows the frequency responses with the existing CEB UFLS and with the proposed LSS, at a loss of 965 MW power generation by tripping all three in-service generators of Lakvijaya coal plant and one in-service generating unit of Sampoor power plant. Unit 1, 2 and 3 generators in Lakvijaya coal plant were tripped at 50 s, 50.5 s and 51 s respectively. Sampoor unit 1 was tripped at 51.5 s. Three stages of UFLS were operated and it has shed total 730 MW when simulating with existing LSS. It has shed only 530 MW from total available loads at 49 Hz in basic round I and II after 2nd generator tripped at 50.5 s when simulating with new LSS.

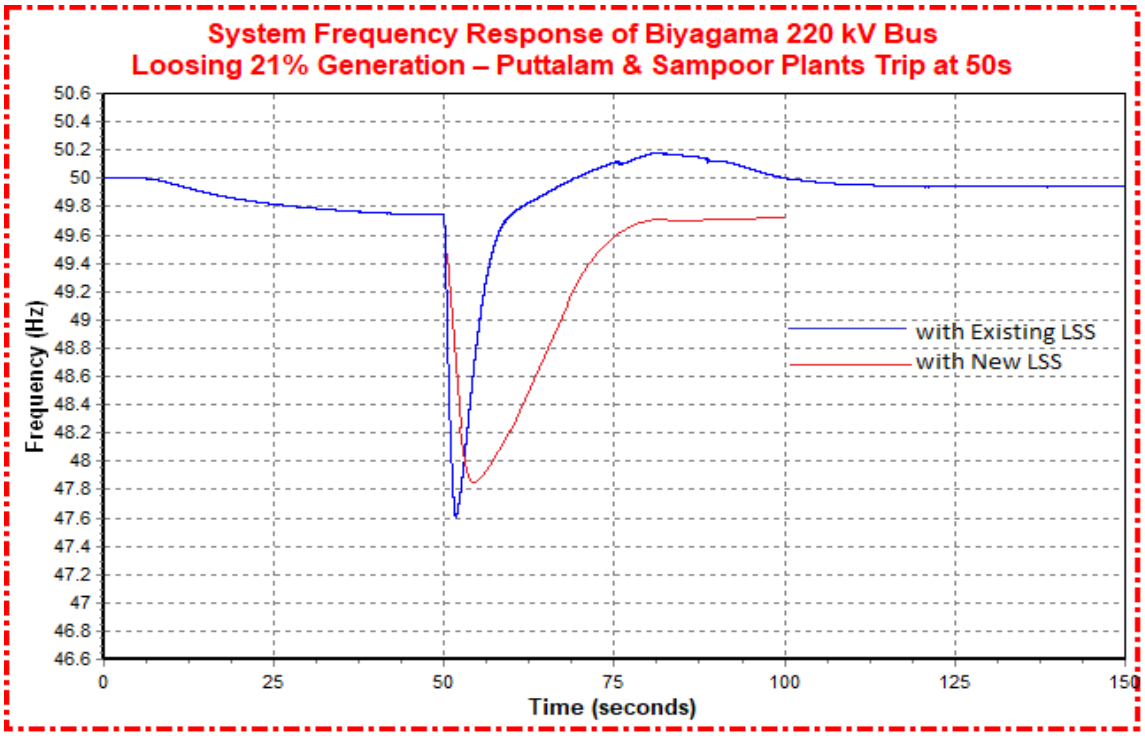

Figure 63: Tripping 275 MW Loaded Lakvijaya 3 Units and 140 MW Loaded Sampoor 1 in HMDP scenario

Case 1.6: Tripping Lakvijaya 3 Units, Sampoor 1 Unit and Upper Kothmale 2 Units and Samanalawewa 2 Units (1235 MW) (Loosing 27% Generation – Tripping Four Plants)

Figure 64 shows the frequency responses with the existing CEB UFLS and with the proposed LSS, at a loss of 975 MW power generation by tripping four major power plants. 275 MW loaded, all three in-service generators of Lakvijaya coal plant and one in-service generating unit of Sampoor power plant and 75 MW loaded two units in Upper Kothmale power plant, and 60 MW loaded two units in Samanala power plant were tripped at 50 s, 50.5 s and 51 s and 51.5 s respectively. The total generation loss was 1,245 MW. Three stages of UFLS were operated and it has shed total 1,056 MW load when simulating with existing LSS. With the proposed LSS, only 850 MW load was shed from total available loads at 49 Hz in basic round II and rapid round.

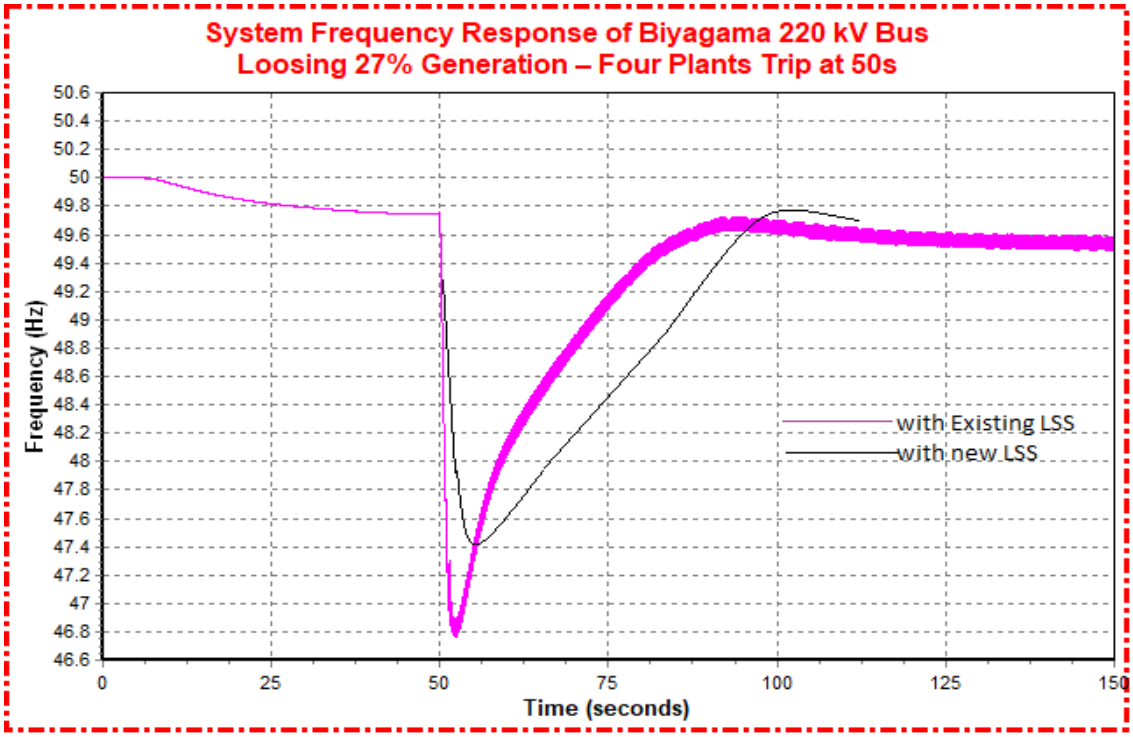

Figure 64: Tripping Lakvijaya 3 Units, Sampoor 1 Unit and Upper Kothmale 2 Units and Samanalawewa 2 Units

The details of load shedding for case 1.4, 1.5 and 1.6 are mentioned in Table 52. Aforementioned three cases show the system frequency response of Biyagama bus when

loosing 17%, 21% and 27% generation respectively. All three cases were simulated with both existing LSS and with new LSS. Both responses are shown in one plot per case for the comparison. In all three cases minimum frequency is less than when simulated with new LSS. All six curves show similar response before the disturbance. However, there was a slight decrease in frequency due to decrease in solar power generation until 50 s. Time taken to restore the system frequency with new LSS is a bit higher value when comparing with existing LSS. However, new LSS has shed fewer loads than existing LSS. It would be an economical advantage.

Table 52: Comparison of results of HMDP Scenario with both existing and new LSS

Case	Contingency	Load Shedding Scheme	Frequency before disturbance	Decaying Frequency	Load Shedding Scheme	Stabilizing Frequency	Settling Frequency
1.4	275 MW × 3 (17%) - Single Plant Outage	Existing	49.76 Hz at 50 s	47.98 Hz at 52.08 s	663 MW shed in 3 stages Highest df/dt -1.587	50.13 Hz at 84.37 s	49.93 Hz at 128.13 s
		New	49.76 Hz at 50 s	48.26 Hz at 53.78 s	480 MW shed in 2 stages Highest df/dt -1.787	49.85 Hz at 84.37 s	49.90 Hz at 128.13 s
1.5	975 MW (21%) - Two Plants Outage	Existing	49.76 Hz at 50 s	47.62 Hz at 52.06 s	730 MW shed 3 stages Highest df/dt -1.496	50.2 Hz at 81 s	49.86 Hz at 112.5 s
		New	49.76 Hz at 50 s	48.86 Hz at 50 s	530 MW shed in 2 stages Highest df/dt -1.687	49.76 Hz at 80.5 s	49.76 Hz at 100.5 s
1.6	1245 MW (26%) - Four Plants Outage	Existing	49.76 Hz at 50 s	46.57 Hz at 51.67 s	1056 MW shed in 4 stages Highest df/dt -2.892	49.68 Hz at 96.87 s	49.44 Hz at 146.5 s
		New	49.76 Hz at 50 s	47.46 Hz at 50 s	850 MW shed in 2 stages Highest df/dt -2.901	49.83 Hz At 100s	49.83 Hz At 100s

Case 1.7: Total Wind Power Plants Outage (976.9 MW) (Loosing 21% Generation – Tripping Single Plant)

Figure 65 shows the frequency responses with the existing CEB UFLS and with the proposed LSS, at a loss of 976.9 MW power generation by tripping the all wind power plants as a worst case simulation scenario. Stage I of UFLS was operated. However, existing LSS has failed to re-establish the system frequency and df/dt was a higher value. Therefore, the system was collapsed at 4 s when simulating with existing LSS. It has shed 640 MW at 49.4 Hz in rapid round and basic round I and II when simulating with new LSS. The new LSS has stabilized the frequency.

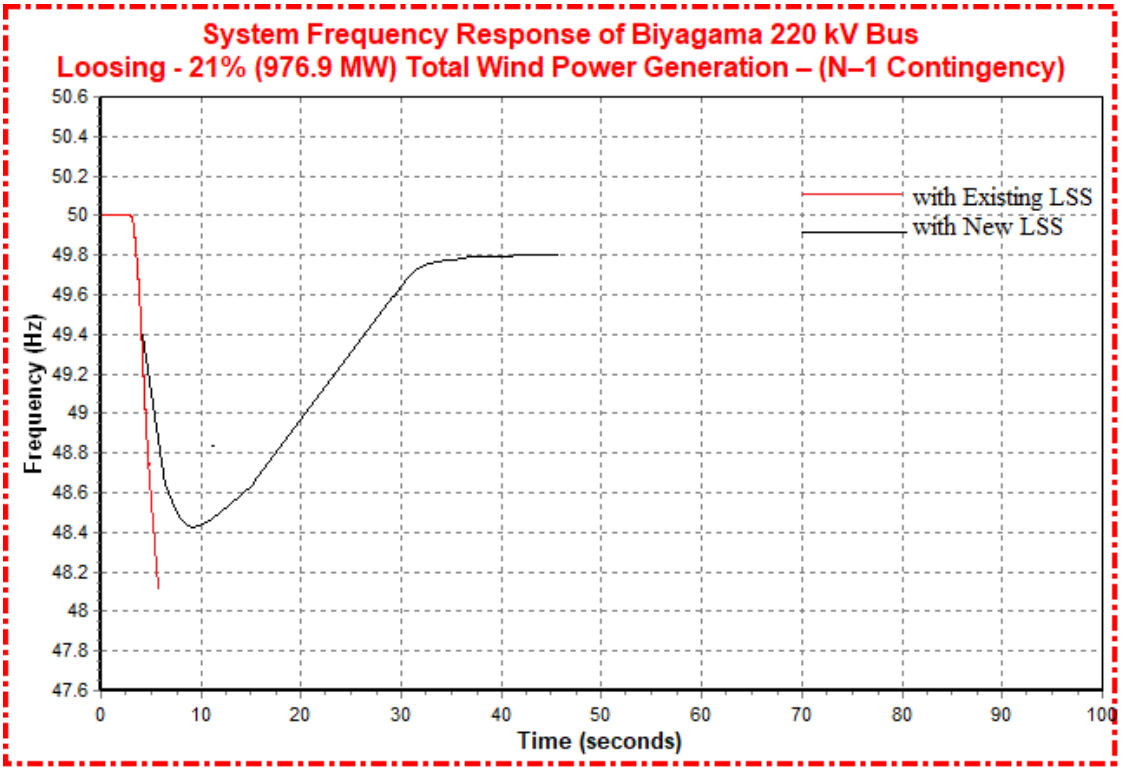

Figure 65: Total Wind Power Plants Outage in HMDP scenario

Case 1.8: Tripping Lakvijaya 3 Units and 50% of All Solar Power Plants (1,140 MW) (Loosing 25% Generation – Tripping Two Plants)

Figure 66 illustrates the frequency responses with the existing CEB UFLS and with the proposed LSS, at a loss of 1,140 MW of power generation by tripping bus 1 at

Lakvijaya coal power plant and by tripping 508 MW from total solar power plants. Three stages of UFLS were operated and shed total 910 MW, when simulating with existing LSS. With the new LSS 830 MW load was shed at 49 Hz in rapid round and basic round I. Similar to the case 1.7, time taken to stabilize the system with new LSS was a bit higher value when comparing with existing LSS. However, new LSS has shed lesser loads than existing LSS.

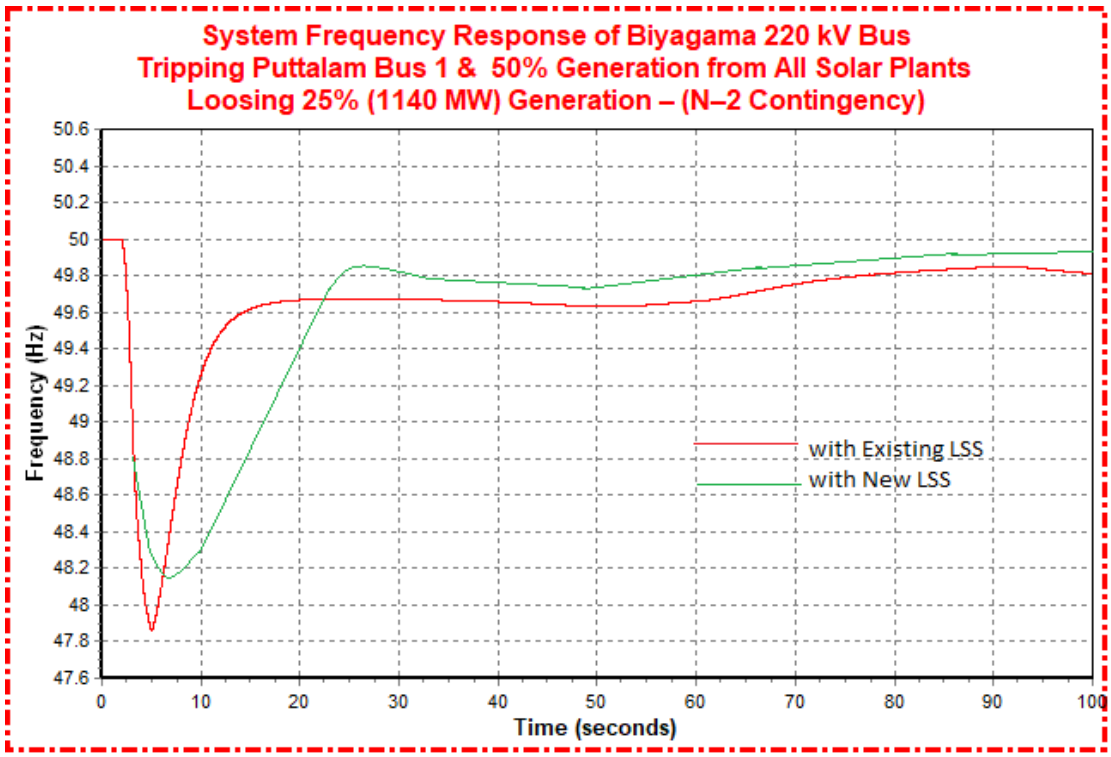

Figure 66: Tripping Lakvijaya 3 Units and 50% of All Solar Power Plants in HMDP scenario

Case 1.9: Tripping Lakvijaya 3 Units and 50% of All Wind Power Plants (1,375MW) (Loosing 29% Generation – Tripping Two Plants)

Figure 67 shows the frequency responses with the existing CEB UFLS and with the proposed LSS, at a loss of 1,375 MW of power generation by tripping bus 1 at Lakvijaya coal power plant and by tripping all wind power plants as a worst case. UFLS Stage I was operated when simulating with existing LSS. However, existing LSS has failed to re-establish the system frequency and df/dt was a higher value. Therefore, the system was collapsed at 4 s when simulating with existing LSS. With the new LSS,

1,540 MW of load was shed at 49.2 Hz in rapid round and all three basic rounds, and it has stabilized the frequency.

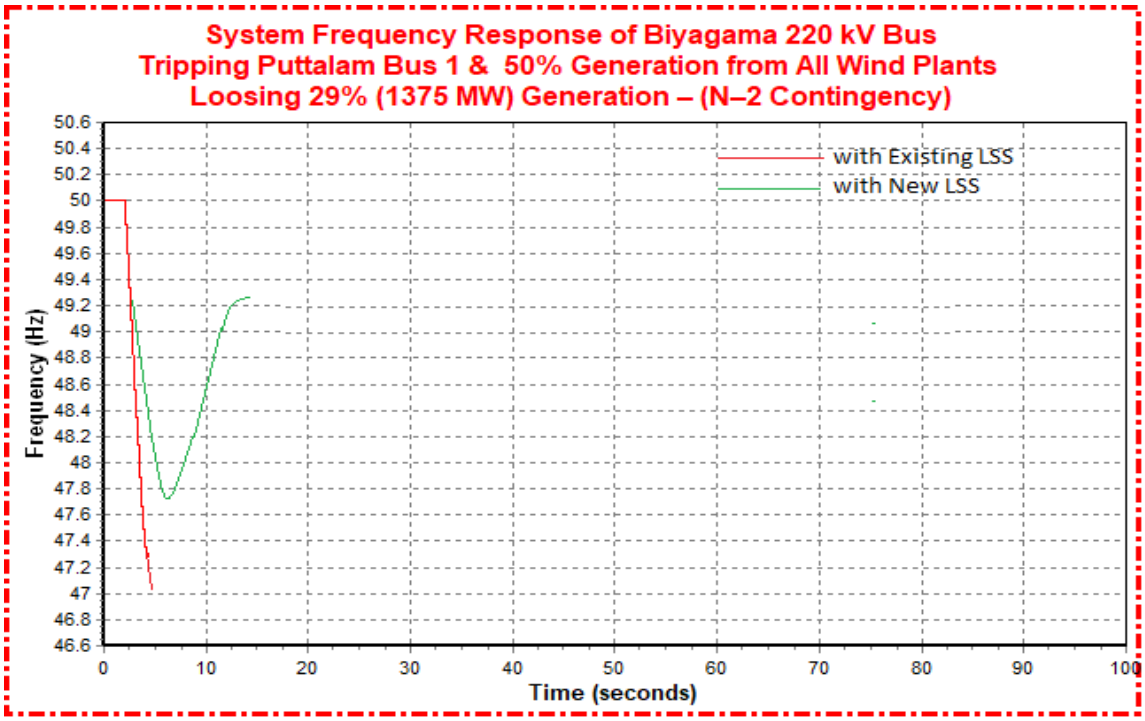

Figure 67: Tripping Lakvijaya 3 Units and 50% of All Wind Power Plants in HMDP scenario

Figure 65, 66, and 67 show the system frequency response of Biyagama bus when loosing 21%, 25% and 29% generation respectively. All three cases were used to simulate the system behavior of total solar generation tripped by a cloud cover or sudden loosing of total wind generation. The generators were tripped at 3 s, when the solar generation is maximum. This is to observe the behavior of high solar penetration. Case 1.7, 1.8, and 1.9 were simulated with existing LSS and with new LSS. Both graphs are shown in one plot per case for the comparison. In all three cases, minimum frequency with new LSS is greater than when simulated with existing LSS. All six curves show similar response before the disturbance at 3 s. The tabulated results of cases 1.7, 1.8, and 1.9 in HMDP Scenario with both existing and new LSS are provided in Table 53.

Table 53: Comparison of results of HMDP Scenario with both existing and new LSS

Case	Contingency	Load Shedding Scheme	Frequency before disturbance	Decaying Frequency	Load Shedding Scheme	Stabilizing Frequency	Settling Frequency
1.7	976.9 MW (21%) - Total Wind Plant Outage	Existing	49.9 Hz at 3s	47.98 Hz at 52.08 s	System Blackout		
		New	49.9 Hz at 3 s	48.43 Hz at 9.8 s	890 MW shed in rapid and basic I, II stages Highest df/dt -2.987	49.8 Hz at 32.5 s	49.8 Hz At 35 s
1.8	1140 MW (25%) - Puttalam Bus 1 and 50% of Total Solar Plant Outage	Existing	49.9 Hz at 3 s	47.84 Hz at 5.3 s	640 MW shed in rapid and basic I stages Highest df/dt -1.987	49.64 Hz at 20 s	49.82 Hz at 100.5 s
		New	49.9 Hz at 3 s	48.18 Hz at 7.02 s	830 MW shed in rapid and basic I, II stages Highest df/dt -2.997	49.82 Hz At 26s	49.85 Hz at 95 s
1.9	1375 MW (29%) - Puttalam Bus 1 and 50% of Total Wind Plant Outage	Existing	49.9 Hz at 3 s	47.02 Hz at 5.7 s	System Blackout		
		New	49.9 Hz at 3 s	47.76 Hz at 7 s	1540 MW shed in rapid and basic I, II and III stages Highest df/dt -2.97	49.29 Hz at 15.1 s	

7.2 Scenario 2 - Thermal Maximum Day Peak (TMDP)

Case 2.5: Total Solar Power Plants Outage (1,018 MW) (Loosing 23% Generation – Tripping Single Plant)

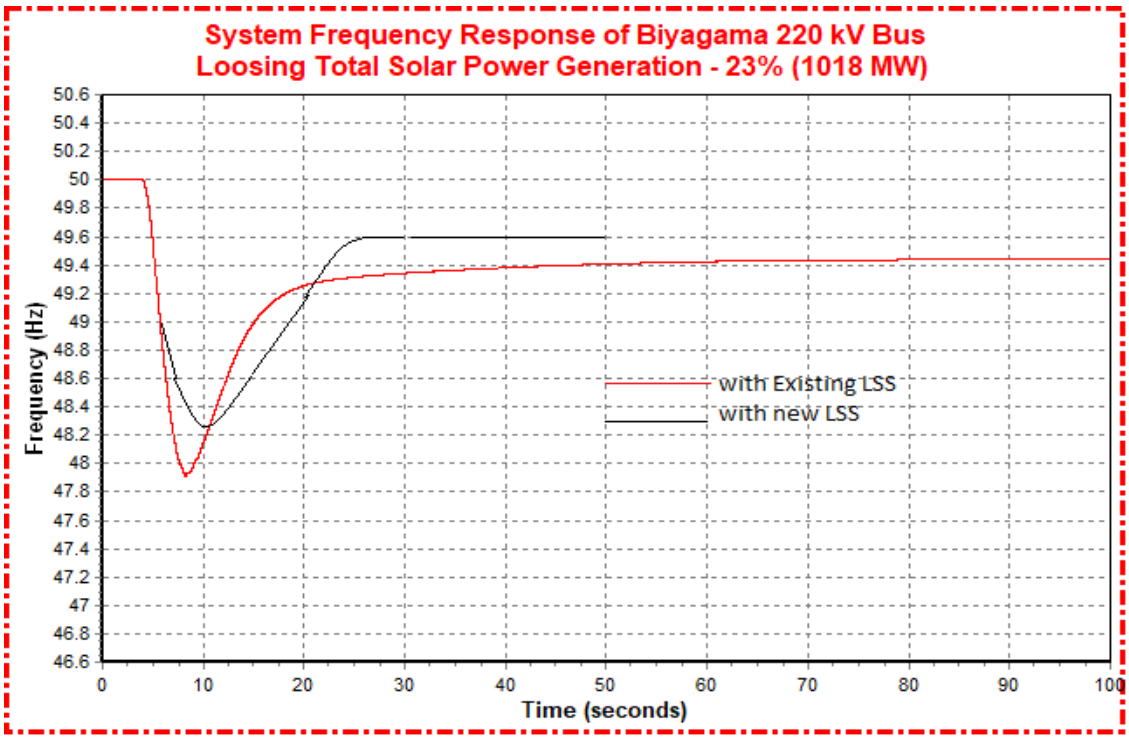

Figure 68: Total Solar Power Plants Outage in TMDP scenario

Figure 68 illustrates the frequency responses with the existing CEB UFLS and with the proposed LSS, at a loss of 1,018 MW power generation by tripping all solar generators at 3 s when solar generation is maximum. Three stages of UFLS were operated and it has shed total 990 MW, when simulating with existing LSS. However, it has stabilized the system at 49.28 Hz, which is not in the frequency band. With new LSS, total 850 MW load was shed at 49 Hz in rapid round and basic round I. It has stabilized at 49.6 Hz, which is in the frequency band.

Case 2.6: Tripping Lakvijaya 5 Units and 50% of All Wind Power Plants (1,375MW) (Loosing 29% Generation – Two Plants Trip)

Figure 69 illustrates the frequency responses with the existing CEB UFLS and with the proposed LSS, at a loss of 1,375 MW power generation by tripping the all five

generators of Lakvijaya coal power plant at 50s, 51s, 52s and 53 s. Three stages of UFLS with df/dt stage were operated and it has shed total 1,460 MW load when simulating with existing LSS. This load shed amount was greater than disturbance as spinning reserve and free governor generators support the system to arrest the frequency. New LSS has shed 1,200 MW in rapid round and basic round I and II, after 2nd generator tripped at 51 s. With both LSS, it has stabilized frequency at 49.51 Hz nearly.

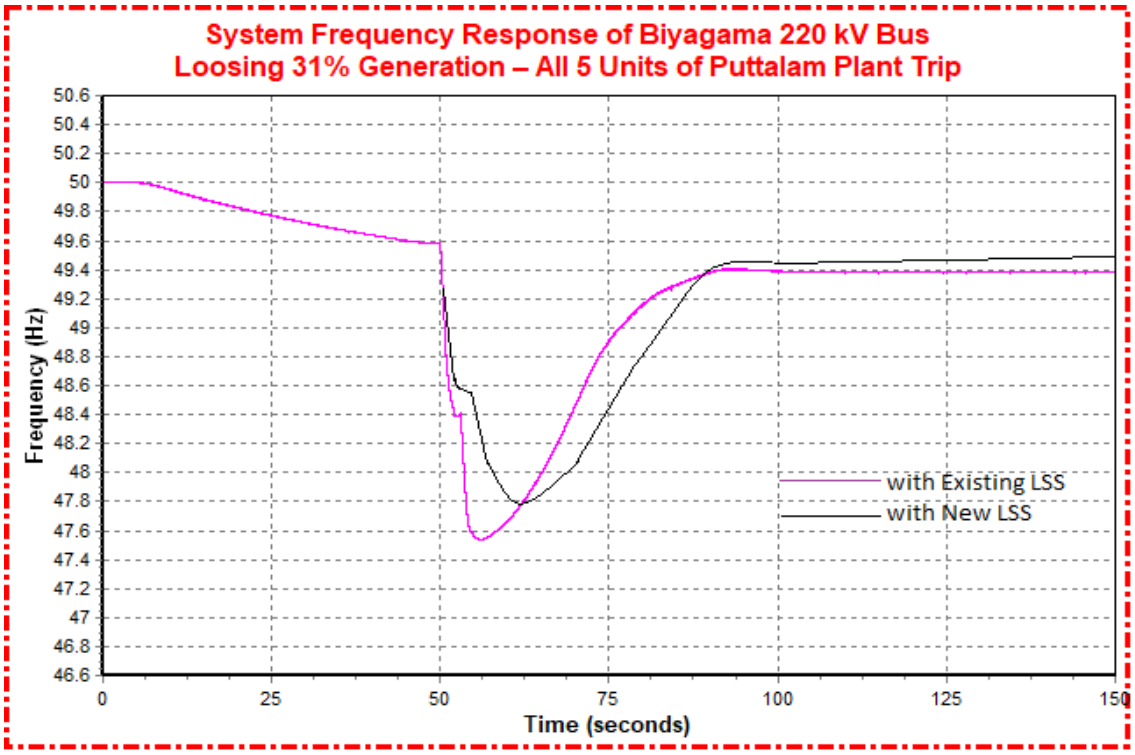

Figure 69; Tripping Lakvijaya 5 Units and 50% of All Wind Power Plants in TMDP scenario

Case 2.7: Tripping Lakvijaya 5 Units and Total Wind Power Plants Outage (1,933 MW) (Loosing 43% Generation – Two Plants Trip)

Figure 70 illustrates the frequency responses with the existing CEB UFLS and with the proposed LSS, at a loss of 1,933 MW power generation by tripping the all wind generators and bus 1 at Lakvijaya coal power plant, which contain 275 MW loaded five coal units. The generators were tripped at 3 s when solar generation is maximum. Two stages of UFLS were operated. However, the system was collapsed before restoring the

system frequency. New LSS has shed 1,650 MW at 49.2 Hz in rapid round and basic round I and II, after bus 1 at Lakvijaya was tripped at 3 s. It has stabilized at 44.5 Hz, which is not in the frequency band but it would be restored from manual LS

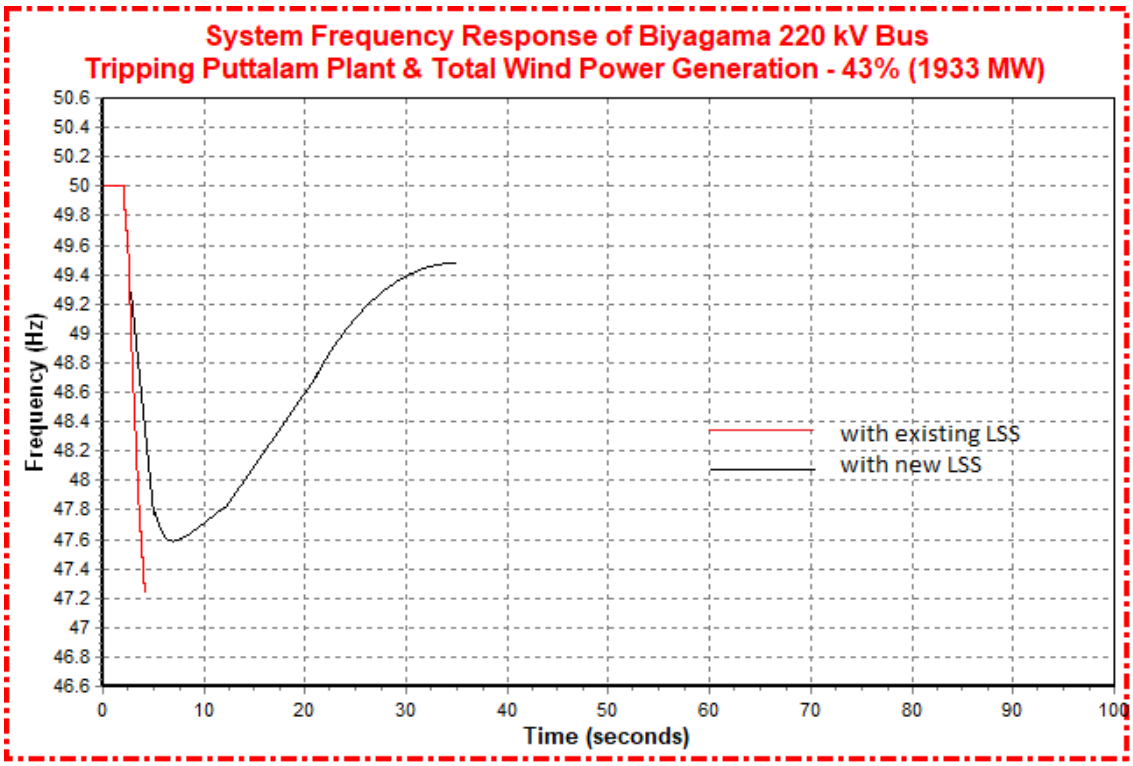

Figure 70: Tripping Lakvijaya 5 Units and Total Wind Power Plants Outage in TMDP scenario

Case 2.8: Tripping Lakvijaya 5 Units and Total Solar Power Plants Outage (2,463 MW) (Loosing 43% Generation – Two Plants Trip)

The frequency responses with the existing CEB UFLS and with the proposed LSS, at a loss of 2,463 MW power generation by tripping the all solar generators and bus 1 at Lakvijaya coal power plant is illustrated Figure 71. Bus 1 at Lakvijaya contains 275 MW loaded five coal units and it was tripped at 3 s when solar generation is maximum., Two stages of UFLS were operated. However, the system was collapsed before restoring the system frequency. The new LSS has shed 1,800 MW at 49.2 Hz in 3 rounds after bus 1 at Lakvijaya tripped at 3 s. It has stabilized at 49.09 Hz, which is not in the frequency band but it would be restored from manual LS.

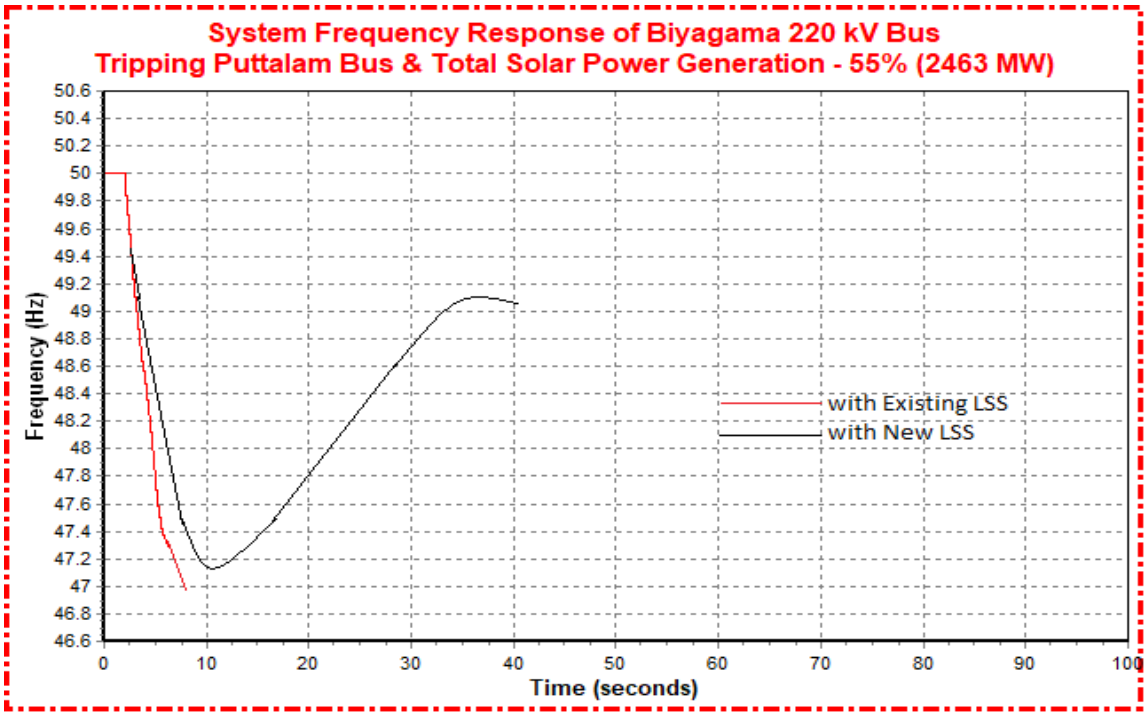

Figure 71: Tripping Lakvijaya 5 Units and Total Solar Power Plants Outage in TMDP scenario

Case 2.5, 2.6, 2.7 and 2.8 show the system frequency response of Biyagama bus when loosing 23%, 31%, 43%, and 55% generation respectively. All four cases were simulated with existing LSS and with new LSS, for the comparison both graphs are shown in one plot per case. In all four cases, minimum frequency with existing LSS is less than when simulated with new LSS. The curves in cases 2.5 and 2.6 show similar response before the disturbance occurred. There was a slight decrease in frequency in case 2.6 due to decrease in solar power generation until 50 s. Time taken to stabilize the frequency with new LSS was a bit higher value when comparing with existing LSS but it has shed less loads than existing LSS this is economically good. The comparison of case .5, 2.6, 2.7 and 2.8 is provided in Table 54.

Table 54: Comparison of results of TMDP Scenario with both existing and new LSS

Case	Contingency	Load Shedding Scheme	Frequency before disturbance	Decaying Frequency	Load Shedding Scheme	Stabilizing Frequency	Settling Frequency
2.5	1018 MW (23%) - Total Solar Plant Outage	Existing	49.9 Hz at 3 s	47.98 Hz at 7.67 s	990 MW shed in I, II and III stages	49.28 Hz at 20 s	49.24 Hz at 103 s
		New	49.9 Hz at 3 s	48.25 Hz at 10.05 s	850 MW shed in rapid round and basic round I	49.6 Hz at 24.9 s	49.6 Hz at 50 s
2.6	1375 MW (31%) - Puttalam Plants Outage	Existing	49.9 Hz at 3 s	47.5 Hz at 54.17 s	1460 MW shed in I, II and III, df/dt stages	49.5 Hz at 90.62 s	49.5 Hz at 103.25 s
		New	49.9 Hz at 3 s	47.8Hz at 62.5 s	1200 MW shed in rapid round and basic I, II rounds	49.51 Hz at 88.1 s	49.52 Hz at 150 s
2.7	1933 MW (43%) - Puttalam Plant and Total Wind Outage	Existing	49.9 Hz at 3 s	47.28 Hz at 4.5 s	System Blackout		
		New	49.9 Hz at 3 s	47.6Hz at 6.1 s	1650 MW shed in rapid round and basic I, II rounds	44.5 Hz at 35 s	
2.8	2463 MW (55%) - Puttalam Plant and Total Solar Outage	Existing	49.9 Hz at 3 s	46.99 Hz at 7.54 s	System Blackout		
		New	49.9 Hz at 3 s	47.6Hz at 6.1 s	1800 MW shed in rapid round and basic I, II rounds	49.11 Hz at 35.2 s	49.09 Hz at 40 s

7.3 Scenario 3 - Renewable Maximum Day Peak (RMDP)

Case 3.4: Tripping 200 MW and 150 MW Loaded Lakvijaya 3 Units (Loosing 11.5% Generation – Single Plant Trip)

Figure 72 shows the frequency responses with the existing CEB UFLS and with the proposed LSS, at a loss of 825 MW power generation by tripping the all three in-service generators out of five generators in Lakvijaya coal power plant. The all three generator were loaded to 275 MW and were tripped at 50 s when solar generation is minimum. When simulating with existing LSS, two stages of UFLS were operated and the system frequency was restored at 50.21 Hz and 81 s by shedding 679 MW load. New LSS has shed 550 MW at 49.2 Hz in two basic rounds after unit 2 of Lakvijaya coal power plant tripped at 51 s and it has stabilized at 49.8 Hz, which is very close to system nominal frequency.

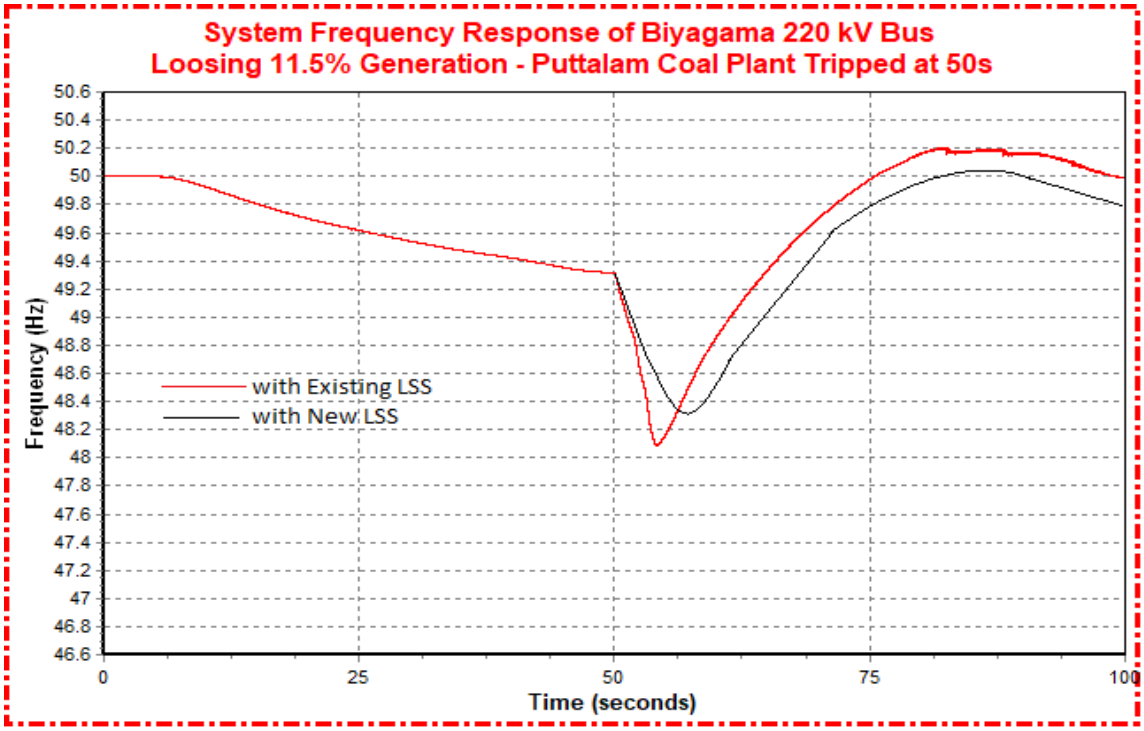

Figure 72: Tripping 200 MW and 150 MW Loaded Lakvijaya 3 Units in RMDP scenario

Case 3.5: Tripping 200 MW, 150 MW Lakvijaya 3 Units and 140 MW Sampoor 1 Unit and 45 MW Pumped Storage 3 Units (835 MW) (Loosing 18% Generation – Three Plants Trip)

Figure 73 shows the frequency responses with the existing CEB UFLS and with the proposed LSS, at a loss of 835 MW power generation by tripping three major power plants including Lakvijaya coal power plant, Sampoor coal power plant, and pumped storage power plant. 200 MW loaded two coal units and 150 MW loaded 1 unit in Lakvijaya coal power plant were tripped at 50 s, 51 s, and 52 s respectively. 150 MW loaded unit 1 in Sampoor power plant was tripped at 54 s. 45 MW loaded all three units in Pumped storage power plant were tripped at 56 s. Three stages of UFLS were operated but the system was collapsed before restoring the frequency, when simulating with existing LSS. With new LSS, only 800 MW load has shed at 49.2 Hz in 3 rounds. It has stabilized at 48.85 Hz, which is not in the frequency band.

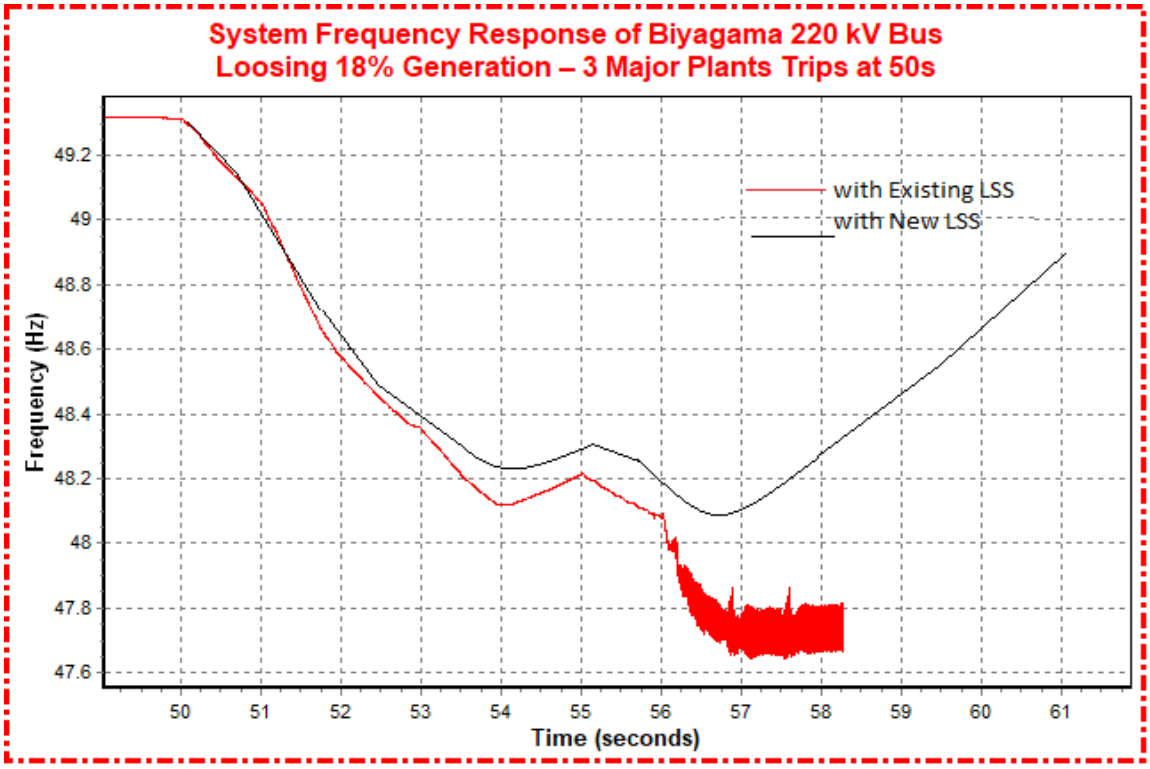

Figure 73: Tripping 200 MW, 150 MW Lakvijaya 3 Units and 140 MW Sampoor 1 Unit and 45 MW Pumped Storage 3 Units in RMDP scenario

Case 3.6: Tripping Lakvijaya 3 Units and Total Wind Power Plants Outage (1,527 MW) (Loosing 33% Generation – Two Plants Trip)

Figure 74 shows the frequency responses with the existing CEB UFLS and with the proposed LSS, at a loss of 1,527 MW power generation by tripping the all wind generators and Lakvijaya bus 1, which contain 275 MW loaded three coal units. Lakvijaya bus 1 was tripped at 3 s when solar generation is maximum. Three stages of UFLS were operated and df/dt stage was operated. However, the system was collapsed before restoring the frequency, when simulating with existing LSS. The new LSS has shed 1,350 MW at 49.2 Hz in 2 rapid rounds and 1 basic round after Puttalam bus 1 tripped at 3s and it has stabilized at 49.5 Hz, which is in the frequency band.

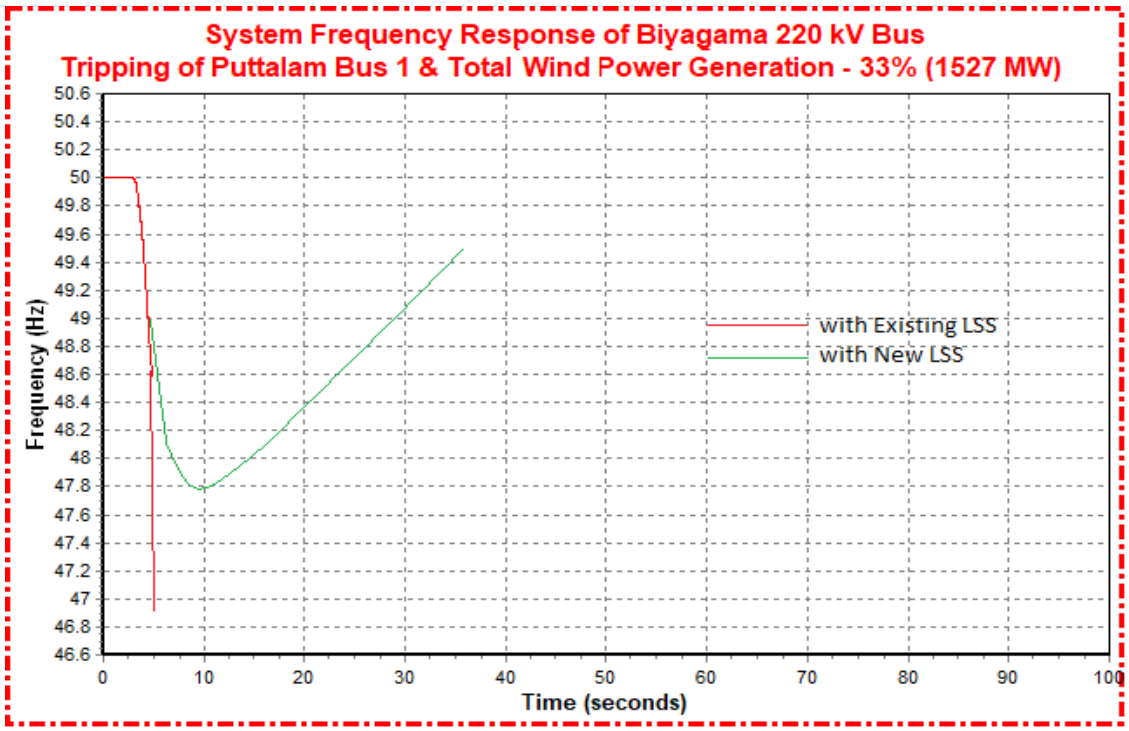

Figure 74: Tripping Lakvijaya 3 Units and Total Wind Power Plants Outage in RMDP scenario

Case 3.7: Tripping Lakvijaya 3 Units and Total Solar Power Plants Outage (1,628 MW) (Loosing 36% Generation – Two Plants Trip)

Figure 75 shows the frequency responses with the existing CEB UFLS and with the proposed LSS, at a loss of 1,628 MW power generation by tripping the all solar

generators and Lakvijaya bus 1 which contain 275 MW loaded three coal units. The generators were tripped at 3 s when solar generation is maximum. With existing LSS, three stages of UFLS and df/dt stage were operated. However, the system was collapsed before restoring the frequency. The new LSS has shed 1,420 MW at 49.4 Hz in 2 rapid rounds and 2 basic rounds after Lakvijaya bus 1 tripped at 3 s. It has stabilized at 49.6 Hz, which is very close to system nominal frequency.

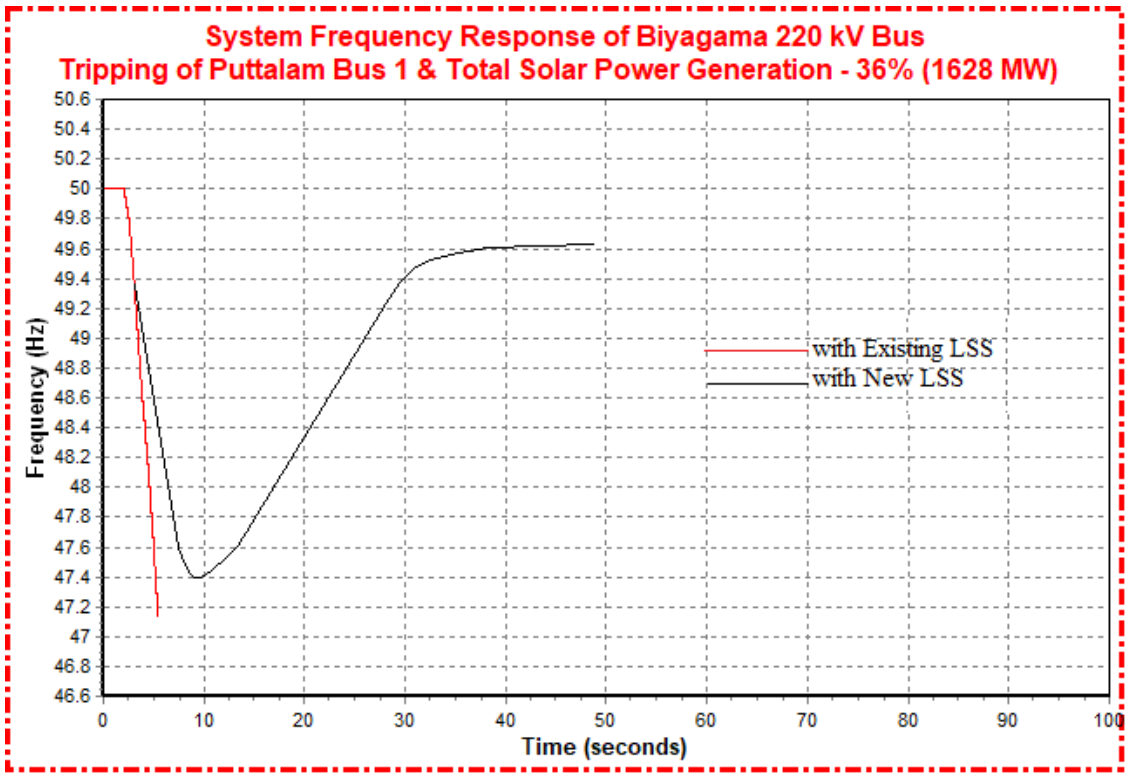

Figure 75: Tripping Lakvijaya 3 Units and Total Solar Power Plants Outage in RMDP scenario

Case 3.4, 3.5, 3.6 and 3.7 show the system frequency response of Biyagama bus when loosing 11.5%, 18%, 43%, and 55% generation respectively. These four cases were simulated with existing LSS and with new LSS, for the comparison both graphs were shown in one plot per case. In all four cases, minimum frequency with existing LSS was less than when simulated with new LSS. All curves show similar response before the disturbance and time taken to stabilize the frequency with new LSS was a bit higher value but it reestablished the frequency.

Table 55: Comparison of results of RMDP Scenario with both existing and new LSS

Case	Contingency	Load Shedding Scheme	Frequency before disturbance	Decaying Frequency	Load Shedding Scheme	Stabilizing Frequency	Settling Frequency
3.4	275 MW × 3 (11.5%) - Single Plant Outage	Existing	49.32 Hz at 50 s	48.08 Hz at 55.08 s	Stage I, II, operated and shed 679 MW	50.21 Hz at 81.37 s	50.0 Hz at 100 s
		New	49.32 Hz at 50 s	48.32 Hz at 56.78 s	550 MW shed in 2 rapid rounds	50.02 Hz at 87.8 s	49.8 Hz at 100 s
3.5	975 MW (18%) - Three Plants Outage	Existing	49.32 Hz at 50 s	47.63 Hz at 57.02 s	System Blackout		
		New	49.32 Hz at 50 s	48.1 Hz at 56.78 s	800 MW shed 2 rapid and 2 basic rounds	48.85 Hz at 61 s	
3.6	1527 MW (33%) - Puttalam Bus 1 and Total Wind Plant Outage	Existing	49.9 Hz at 3 s	46.91 Hz at 5.62 s	System blackout		
		New	49.9 Hz at 3 s	47.79 Hz At 9.9 s	1350 MW shed in 2 rapid rounds and 1 basic round	49.51 Hz at 36.09 s	
3.7	1628 MW (36%) - Puttalam Bus 1 and Total Solar Plant Outage	Existing	49.9 Hz at 3 s	47.18 Hz at 5.62 s	System blackout		
		New	49.9 Hz at 3 s	47.42 Hz At 9.8 s	1370 MW shed 2 rapid and 2 basic rounds	49.6 Hz at 40 s	49.62 Hz at 48 s

CHAPTER 8

CONCLUSION AND FUTURE WORKS

8.1 Conclusion

According to the least cost long term generation expansion plan 2018 – 2037 of CEB, a strong renewable energy development has been expected for the next twenty years as compared to the past two decades. In order to maintain renewable portfolio in the generation mix, and to facilitate the harnessing of indigenous natural resources, it has been proposed to integrate 1,218 MW of solar capacity and 976.9 MW wind capacity into the Sri Lankan power network by year 2030. However, solar and wind energy are non-dispatchable capacities, which contains no rotational inertia. Increased penetration level of solar PV generation, which is intermittent by nature, introduces more variability into the system starting from finer time scale. During the day peak time wind and solar generation will be high.

System variations of a power grid during operation conditions are normal to every power system. Contingency situations may occur by sudden increase of electrical load demand, forced outage of a transmission line or generator. Load shedding provides the ultimate guard to protect power system from contingency situations. At present in Sri Lanka, a static Under Frequency Load Shedding (UFLS) scheme is used, which is initiated through a rate of change of frequency (ROCOF) value. The pre-determined load amount shed at each stage according to the frequency value and ROCOF value. The weaknesses of the present load shedding were identified during the simulation studies.

In this research, a new load shedding scheme was proposed, which uses a dynamic load shedding method to overcome the weakness of the existing scheme discussed in detail in the thesis. The simulations were performed in forecasted power system model for 2030, which was simulated in PSS/E. The simulation results demonstrated how the proposed dynamic load shedding scheme adaptively shed loads relevant to power mismatch calculated by using real-time data. The performance of proposed load shedding scheme is higher than the conventional static UFLS used by Sri Lanka.

According to the simulation results the frequency decay with the proposed load shedding scheme is lower than that with the existing load shedding scheme. However the proposed load shedding scheme has taken slightly higher time to restore system frequency than existing load shedding scheme. The reason behind that is the new load shedding scheme has implemented to shed equal or less load amount correspond to the power mismatch. The existing load shedding scheme was designed to shed pre-defined load amount which is larger than the power mismatch. According to the equation (1), the frequency falling rate increases with power mismatch value increases. Similarly, the frequency rising rate will decrease by shedding equal or less amount to the power mismatch. The proposed load shedding scheme has increased the system frequency gradually by checking real-time system parameters of power generation, load demand and frequency for every 100 ms and by checking load shedding amount for every 100 ms, which is not shed more than the power mismatch. Therefore, the time taken to restore system frequency is less value with existing load shedding scheme.

Although the time taken to restore system frequency was slightly higher than with existing load shedding scheme, all the other weaknesses, such as excessive amount of load shedding and inadequate amount of load shedding, which may lead to power system blackout can be avoided using the proposed dynamic load shedding scheme.

The benefits that can be achieved from the proposed load shedding scheme can be concluded as follows,

1. Restore the system frequency for larger disturbances
2. No excessive amount of load shedding occurred
3. Frequency decay with the proposed load shedding scheme is lower than that with the existing load shedding scheme
4. Restore the system frequency even with higher penetration of solar and wind energy in the system under disturbances where existing load shedding scheme failed to restore

8.2 Future Works and Limitations

It is recommend applying dynamic load shedding scheme for Sri Lankan power system, which avoid system collapsing from larger disturbances due to the effect of high penetration of large solar and wind power generation. After the implementation of SCADA system for real-time data measuring, the proposed algorithm will provide the system frequency stability for severe disturbances avoiding system collapses as shown in the analysis of new load shedding scheme. The data collection servers are required to be installed at grid substation and generation units, and a centralized data collection server is required to be installed at system control center of CEB to obtain real-time data to detect disturbances. For accurate data acquisition Ethernet-equipped, intelligent, high efficient, fiber optic network data transmission system is required to be installed for the implementation of proposed load shedding scheme. Frequency relays with PLC for shedding selected load buses and selected load amounts are also required to be remained in the system for implementation of the proposed load shedding scheme. As all calculations are performed in a processor installed in the centralized data collection server of CEB system control center, a data storing module can be also installed to record all previous disturbance data. This modification will provide data training system, which provides storing past disturbance data for future manipulation.

The proposed load shedding scheme does not consider the disturbance location and selection of load shedding buses among non-critical load buses. This proposed algorithm considered non-critical feeders, but the tripping priority for each load bus was not considered. By calculating a voltage stability index using real time data of voltage magnitude and phase angle of each load bus, a priority load buses list can be obtained for each disturbance. This modification will improve voltage stability of a power system. Calculation of frequency sensitivities is another method for the selection of priorities from non-critical load buses but the implantation would be complex for a larger power system. Also selection of load buses for load shedding can be performed through the disturbance location by calculating severity factors for each load bus as mentioned in some literature.

The proposed load shedding scheme is required a precise real-time data monitoring and data retrieving system like SCADA or PMU to augment it into the 2019 Sri Lankan power system. Currently, real-time system data of 2019 Sri Lankan power system is available for every 1 second. Therefore, the proposed scheme is not possible to implement to the current network. However, this research is recommended to implement this proposed load shedding scheme for future power system to achieve the benefits mentioned above with the future development of power system real-time monitoring.

REFERENCE LIST

[1] Ceyloan Electricity Board, "CEB Statistical Digest Report 2019"[Online]. Available: https://ceb.lk/publication-media/statistical-reports/88/en.

[2] L. N. W. Arachchige, J. R. Lucas and M. S. Nakandala, "Generation Cost Optimization through a Network Stability Study-Final Report-," July 2016. [Online]. Available: http://www.pucsl.gov.lk/english/wp-content/uploads/2017/03/Final-report-stability-study-to-PUCSL-07-07-2016.pdf.

[3] Ceylon Electricity Board, "Long term generation expansion plan 2020-2039 Draft," March 2020. [Online]. Available: https://ceb.lk/publication-media/planing-documents/77/en.

[4] Ceylon Electricity Board, "Long term generation expansion plan 2018-2037," June 2018. [Online]. Available: http://www.ceb.lk/index.php?aam_media=4464.

[5] Transmission Division Ceylon Electricity Board, "Grid Code Ceylon Electricity Board," January 2018. [Online]. Available: https://ceb.lk/front_img/img_reports/1532500179Grid_Code_of_Transmission_Division.pdf.

[6] P. Kundur, Power System Stability and Control, McGraw Hill., 1994.

[7] G. Kishokumar, "Designing Automatic Load-Frequency Control Scheme For Sri Lankan Power System," 2018.

[8] A. A. M. Zin, H. M. Hafcz and W. K. Wong, "Static and Dynamic Under-frequency Load Shedding: A Comparison," in *2004 Intematlonal Conference on Power System Technology - POWERCON*, Singapore, 2004.

[9] A. Saffarian and M. Sanaye-Pasand, "Enhancement of Power System Stability Using Adaptive Combinational Load Shedding Methods," *IEEE Transactions on PowerSystems*, vol. 26, no. 3, p. 1010 1019, 2011.

[10] B. Jie, T. Tsuji and K. Uchida, "Analysis and modelling regarding frequency regulation of power systems and power supply–demand-control based on penetration of renewable energy sources," *The Journal of Engineering*, vol. 2017, no. 13, p. 1824–1828, Nov 2017.

[11] S. Kazemlou and S. Mehraeen, "Novel Decentralized Control of Power Systems With Penetration of Renewable Energy Sources in Small-Scale Power Systems," *IEEE Transactions on Energy Conversion*, vol. 29, no. 4, pp. 851-861, Dec 2014.

[12] M. Gunawardena, C. Hapuarachchi, D. Haputhanthri, I. Harshana, J. R. Lucas and W. A. D. S. Wiyayapala, "Use of Load Shedding Scheme to Increase the Capacity limit on the Single Largest Generator," *ENGINEER Institute of Engineers, Sri Lanka,* vol. 46, no. 1, p. 31 36, 2013.

[13] H. Chamikara, K. T. M. U. Hemapala and M. N. S. Ariyasinghe, "New load shedding scheme for reliability improvement of an existing transmission network: A Case study," *2013 3rd International Conference on Instrumentation Control and Automation (ICA),* pp. 180-186, 2013.

[14] s. Bambaravanage, S. Kumarawadu and A. Rodrigo, "Comparison of three Under-Frequency Load Shedding Schemes referring to the Power System of Sri Lanka," vol. XLIX, no. No.01, pp. 41-52, 2016.

[15] C. P. Reddy, S. Chakrabarti and S. C. Srivastava, "A Sensitivity-Based Method for Under-Frequency Load-Shedding," *IEEE TransactionS on Power Systems,* vol. 29, no. 2, p. 984 985, 2014.

[16] J. A. Laghari, H. Mokhlis, M. Karimi, A. H. A. Bakar and A. Monti, "A New Under-Frequency Load Shedding Technique Based on Combination of Fixed and Random Priority of Loads for Smart Grid Applications," *IEEE TransactionS on Power Systems,* vol. 30, no. 5, pp. 2507 - 2515, 2015.

[17] H. Seyedi and M. Sanaye-Pasand, "New centralised adaptive load-shedding algorithms to mitigate power system blackouts," *IET Generation, Transmission & Distribution,* vol. 3, no. 1, pp. 99 - 114, January 2009.

[18] T. Shekari, F. Aminifar and M. Sanaye-Pasand, "An Analytical Adaptive Load Shedding Scheme Against Severe Combinational Disturbances," *IEEE TransactionS on Power Systems,* vol. 31, no. 5, pp. 4135 - 4143, 2016.

[19] C. Xin, W. Zengping and Z. Zhichao, "A load shedding method for two-area power system," *The International Conference on Advanced Power System Automation and Protection,* vol. 2, pp. 1080-1083, 2011.

[20] S. Eftekharnejad, G. T. Heydt and V. Vittal, "Optimal Generation Dispatch With High Penetration of Photovoltaic Generation," *IEEE Transactions on Sustainable Energy,* vol. 6, no. 3, p. 1013 1020, July 2015.

[21] T. L. C. A. N. O. C. W. W. M. P. Musau, "Effects of Renewable Energy on Frequency Stability: A Proposed Case Study of the Kenyan Grid," *2017 IEEE PES-IAS PowerAfrica,* pp. 12-15, June,2017.

[22] C. S. L. L. L. a. F. X. H.T. Zhang, "A Novel Load Shedding Strategy Combining Undervoltage and Underfrequency with Considering of High Penetration of Wind

Energy," *2015 IEEE International Conference onSystems, Man, and Cybernetics*, pp. 659-664, Oct. 2015.

[23] S. A. Energy Management Division, "High-performance Transmission Planning and Operations Software for the Power Industry," Siemens AG 2017, Germany, 2017.

[24] Siemens Industries, Inc. , "PSSE 33.5 Model Library," Siemens Power Technologies International, New York, USA, 2013 Oct.

[25] Subcommittee, NERC Model Validation Task Force of the Transmission Issues, "Power System Model Validation," North American Electric Reliability Corporation - NERC, Princeton, 2010.

[26] A. V. Kulkarni, W. Gao and J. Ning, "Study of Power System Load Shedding Scheme Based On Dynamic Simulation," in *IEEE PES Transmission and Distribution Conference and Exposition*, New Orleans, LA, USA, 2010.

APPENDIX A - The Map of Transmission System in Sri Lanka in year 2019

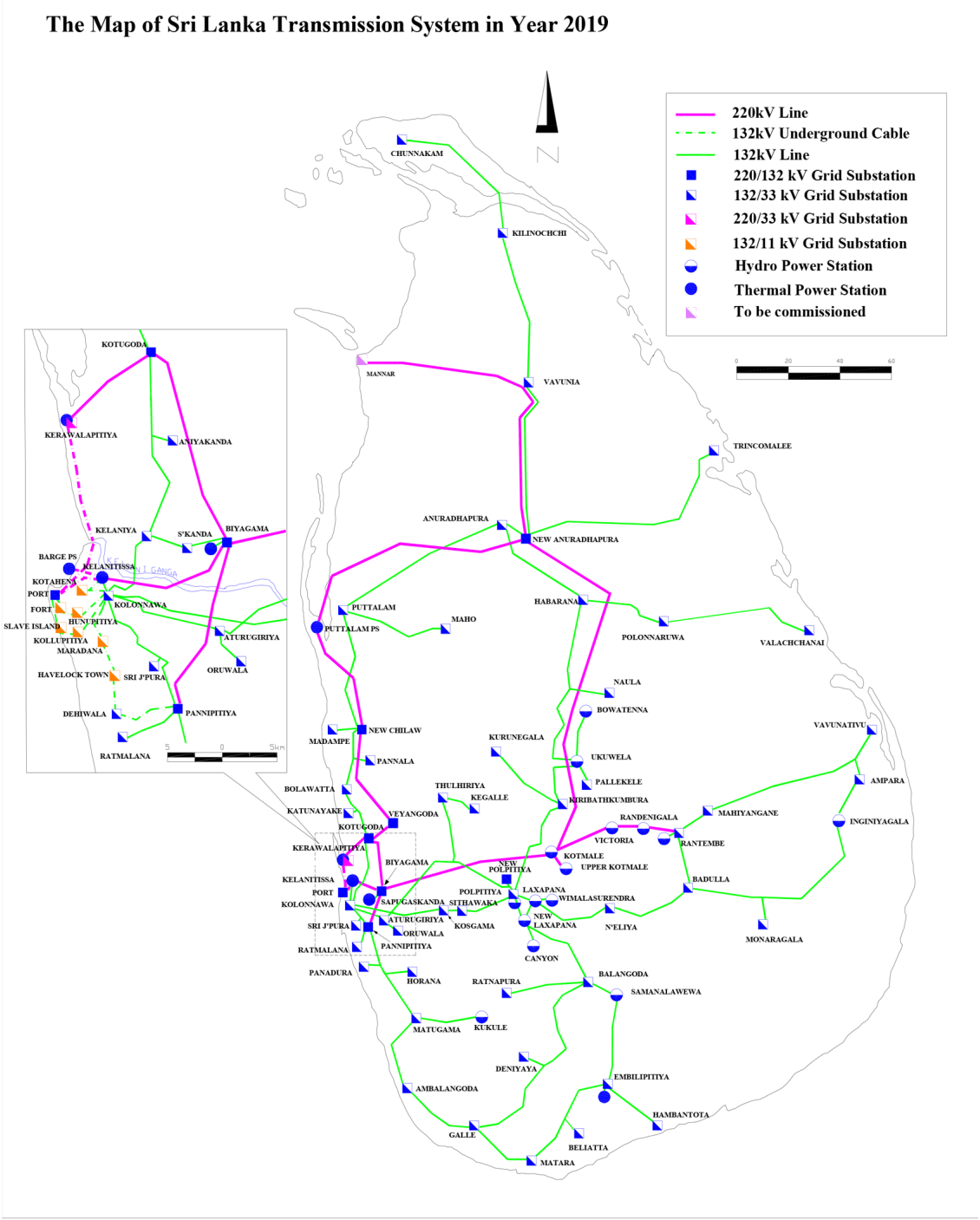

APPENDIX B

Table B-1: Power Flow Data for Load modeling [24]

Parameter	Description
PL	Active Power Component of Constant MVA load (MW)
QL	Reactive Power Component of Constant MVA load (Mvar)
IP	Active Power Component of Constant Current Load (MW)
IQ	Reactive Power Component of Constant Current Load (Mvar)
YP	Active Power Component of Constant Admittance Load (MW)
YQ	Reactive Power Component of Constant Admittance Load (Mvar)

Table B-2: Power Flow Data for Generator modeling [24]

Parameter	Description
PGen	Generator active power output (MW)
QGen	Generator reactive power output (Mvar)
PMax	Maximum Generator active power output (MW)
QMax	Maximum Generator reactive power output (Mvar)
PMin	Minimum generator active power output (MW)
QMin	Minimum generator reactive power output (Mvar)
Mbase	Total MVA base (MVA)
ZR, ZX	Complex machine impedance (pu)
RT, XT	Step-up transformer impedance (pu)
GENTAP	Off-nominal turns ratio of step-up transformer (pu)
ISG	Machine status of one for in-service and zero for out-of-service
QPCT	Percent of the total Mvar required to hold the voltage at the bus controlled by bus (%)

Table B-3: Power Flow Data for Step up transformer [24]

Parameter	Description
Z_T positive	Transformer positive sequence impedance in p.u. based on 100 MVA
Z_T negative	Transformer negative sequence impedance in p.u. based on 100 MVA
Z_T zero	Transformer zero sequence impedance in p.u. based on 100 MVA
Tap ratio	Transformer tap position
Connection Code	Transformer connection code (Y-Y, Y-delta,….etc.)

APPENDIX C

Power Plant Name in 2030 PSS/E Model	PGen (MW)
LAX-1 132.00	12.9996
LAX-1 132.00	4.0895
WIMAL-1 132.00	10
WIMAL-1 132.00	15
POLPI-1 132.00	20
POLPI-1 132.00	14.9994
CANYO-1 132.00	15
CANYO-1 132.00	0
SAMAN-1 132.00	40
SAMAN-1 132.00	60
UKUWE-1 132.00	17.9999
UKUWE-1 132.00	17.9999
BOWAT-1 132.00	11
KELAN-1 132.00	0
KUKULE-1 132.00	36.9998
KUKULE-1 132.00	36.9998
KHD -1 132.00	47.6999
EMBIL-1 132.00	82.9987
PUTTA-1 132.00	0
BARGE-2 220.00	44.9999
RANDE-2 220.00	36
RANDE-2 220.00	56
WIMAL-3 33.000	0
UKUWE-3 33.000	0
RANTE-3 33.000	0
KELAN-3A 33.000	0
KELAN-3B 33.000	32
HORANA_3 33.000	0
SITHA-33 33.000	0
NUWAR-3 33.000	0
SAPUG-3A 33.000	0
BADUL-3 33.000	0
BALAN-3 33.000	0
MATARA-3 33.000	19.9998
CHUNNAKAUM 333.000	0
CHUNNAKAUM 333.000	23.4
RATNAP-3 33.000	0
KIRIB-3 33.000	0

PUTTA-3 33.000	0
WIND 33.000	7
WIND NOR 33.000	22
NLAX-1 12.500	39.9994
NLAX-2 12.500	30
KOTH GEN1 13.800	52.2295
KOTH GEN2 13.800	0
KOTH GEN 3 13.800	0
UPPER-KOTH 13.800	0
UPPER-KOTH 13.800	44.9999
VIC GEN-1 12.500	0
VIC GEN 2 12.500	60
VIC GEN 3 12.500	0
RANTE-G1 12.500	14.9999
RANTE-G2 12.500	0
GT 07 15.000	115.003
KCCP GT 15.000	99.9998
KCCP ST 11.500	56
AES GT 10.500	102.9998
AES ST 10.500	55.9999
KERAWALA-G 14.500	87.1
KERAWALA-G 14.500	100.6392
KERAWALA-S 14.500	55.9986
SAPUG-P 11.000	31.9999
SAPUG-P2 11.000	36.0499
SAPUG-P2 11.000	46.7699
PUTT COAL-1 20.000	201.8297
PUTT COAL-2 20.000	269.9998
PUTT COAL-3 20.000	270.9998

Load Bus Name	P (MW)	Q (MVar)
WIMAL-3 33.000	11.43	3.31
AMPA-3 33.000	39.88	21.59
INGIN-3 33.000	0	0
UKUWE-3 33.000	35.15	12.87
VAVUN-33 33.000	10.11	5.88
RANTE-3 33.000	0	0
MAHIYANGE 3 33.000	9.38	2.93
KELAN-3A 33.000	21.04	4.85
KELAN-3B 33.000	0	0
NAULA-3 33.000	27.94	13.13
MONARA-3 33.000	3.64	1.04
BELIATT-3 33.000	6.61	-2.76
HAMBA-33 33.000	12.62	4.99
HAMBA-33 33.000	23.77	14.65
HORANA_3 33.000	15.27	13.87
KATUNA-3 33.000	47.3	4.96
MAHO-3 33.000	16.83	6.6
POLON-3 33.000	11.76	6.16
VAUNA-3 33.000	13.85	1.98
PALLEK-3 33.000	18.8	7.6
KOSGA-3 33.000	41.54	19.46
SITHA-33 33.000	24.33	9.22
NUWAR-3 33.000	22.11	4.25
THULH-3 33.000	28.88	21.45
ORUWA-3 33.000	2.82	0.43
KOLON-3A 33.000	51	-3.77
KOLON-3B 33.000	21.88	7.47
PANNI-3 33.000	35.77	16.43
BIYAG-3 33.000	65.67	14.28
KOTUG-3 33.000	35.29	11.7
KOTU_NEW-3 33.000	43.88	21.35
SAPUG-3A 33.000	67.86	37.59
BOLAW-3 33.000	41.57	21.57
BADUL-3 33.000	17.15	3.77
BALAN-3 33.000	13.52	5.7
DENIY-3 33.000	8.87	2.33
GALLE-3 33.000	0	0
NEW_GALLE 33.000	46.1	13.08
EMBIL-3 33.000	14.95	4.81
MATARA-3 33.000	44.09	4.13

KURUN-3 33.000	43.66	17.74
HABAR-3 33.000	32.39	11.85
ANURA-3A 33.000	18.64	0
ANURA-3B 33.000	0	0
NEWANU-3 33.000	24.04	13.96
TRINC-3 33.000	20.4	4.31
KILINOCH-3 33.000	9.89	-2.01
CHUNNAKAUM 333.000	36.56	11.35
RATNAP-3 33.000	8.06	0.98
KIRIB-3 33.000	38.42	16.12
VALACH_3 33.000	12.9	1.54
VALA 3 33.000	0	0
RATMA-3A 33.000	51.38	28.68
MATUG-3 33.000	32.04	23.74
PUTTA-3 33.000	19.91	3.11
CEMENT 33.000	13.07	2.81
ATURU-3 33.000	39.49	15.94
VEYAN-33 33.000	45.17	24.58
JPURA_3 33.000	59.51	25.62
PANAD-3 33.000	62.11	37.16
MADAM-3 33.000	37.41	19.03
K-NIYA-3 33.000	26.59	15.68
AMBALA 33.000	26.78	12.12
DEHIW_3 33.000	32.6	14.86
PANNAL 33.000	32.76	16.44
ANIYA 33.000	26.55	13.62
COL_I_11 11.000	37.09	12.66
COL_A_11 11.000	37.15	11.1
COL_E-11 11.000	50	0
COL_F-11 11.000	43.89	20.45
PUTT COAL-1 20.000	0	0
PUTT COAL-2 20.000	0	0
PUTT COAL-3 20.000	0	0
SUB C-11 11.000	19.61	9.13

APPENDIX D

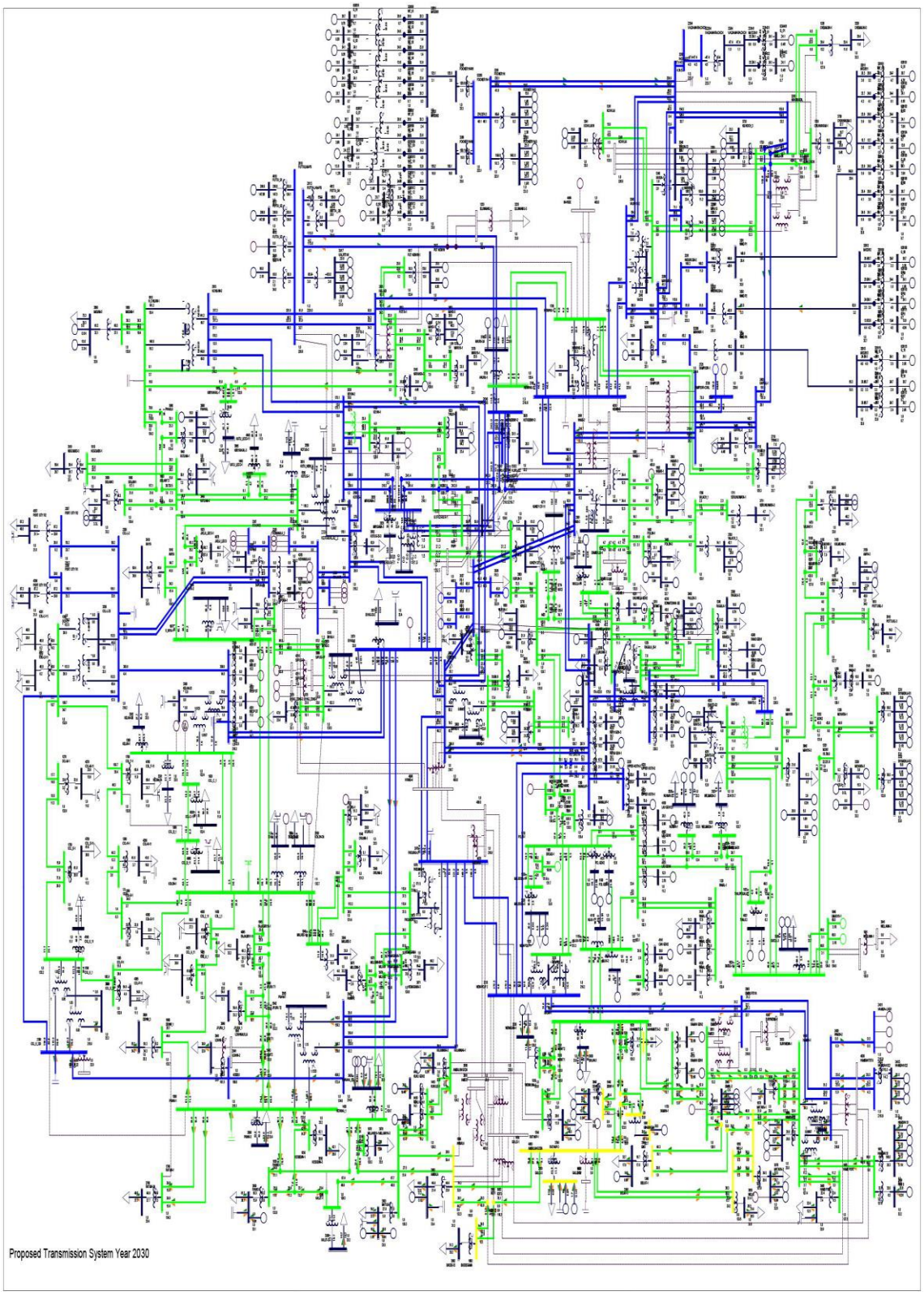

APPENDIX E

Power Plant Name in 2030 PSS/E Model	PGen (MW)	PMax (MW)	Mbase (MVA)	Inertia (H)	Damping (D)	Droop (R)
BROADLAND-1 132.00	35	35	41.18	2.83	0.5	0.05
MORAGOLLA 132.00	0	27	31.76	2.83	0.5	0.05
UMAOYA-1 132.00	60	60	70.59	3.02	0.5	0.05
UMAOYA-1 132.00	60	60	70.59	3.02	0.5	0.05
Pumped Storage 1 220.00	45.0001	206	217	3.67	0.5	0.045
Pumped Storage 2 220.00	45.0001	206	217	3.67	0.5	0.045
Pumped Storage 3 220.00	45.0001	206	217	3.67	0.5	0.045
MALIBODA-3 33.000	20	20	23.53	2.83	0.5	0.05
GIN3 33.000	20	20	23.53	2.83	0.5	0.05
Laxapana GEN123 11.000	28.5	28.5	33.53	3	0.5	0.05
Laxapana GEN4 11.000	12.5	12.5	14.71	3	0.5	0.05
Laxapana GEN5 11.000	12.5	12.5	14.71	3	0.5	0.05
New Laxapana-1 12.500	50	50	58.82	3.9	0.05	0.059
New Laxapana -2 12.500	50	50	58.82	3.9	0.05	0.059
WIMAL GEN1 11.000	25	25	29.41	3	0.5	0.05
WIMAL GEN2 11.000	25	25	29.41	3	0.5	0.05
POL GEN1 12.500	38	38	44.71	2.83	0.5	0.05
POL GEN2 12.500	38	38	44.71	2.83	0.5	0.05
CAN GEN1 12.500	30	30	35.29	3.8	0.5	0.05
CAN GEN2 12.500	30	30	35.29	3.8	0.5	0.05
SAMAN GEN1 10.500	60	60	70.59	3.75	0.05	0.043
SAMAN GEN2 10.500	60	60	70.59	3.75	0.05	0.043
UKUWELA GEN112.500	19	19	22.35	3.2	0.5	0.05
UKUWELA GEN212.500	19	19	22.35	3.2	0.5	0.05
BOWATENNA GE11.000	40	40	47.06	4	0.5	0.05
KOTM GEN-1 13.800	67.0001	67	78.82	3.02	0.5	0.05
KOTH GEN-2 13.800	0.0001	67	78.82	3.02	0.5	0.05
KOTH GEN-3 13.800	0.0001	67	78.82	3.02	0.5	0.05
UPPER KOTH-113.800	75.0001	75	88.24	4.3	0.5	0.05
UPPER KOTH-213.800	75.0001	75	88.24	4.3	0.5	0.05
VIC GEN-1 12.500	30.4629	70	82.35	3.45	0.05	0.016
VIC GEN-2 12.500	0	70	82.35	3.45	0.05	0.016
VIC GEN-3 12.500	0	70	82.35	3.45	0.05	0.016
RAND GEN1 12.500	60.0001	60	70.59	3.65	0.5	0.05
RAND GEN2 12.500	60.0001	60	70.59	3.65	0.5	0.05
RANTE-G1 12.500	27	27	31.76	2.62	0.5	0.05
RANTE-G2 12.500	27	27	31.76	2.62	0.5	0.05

KUKU GEN1 13.800	38	38	44.71	2.84	0	
KUKU GEN2 13.800	38	38	44.71	2.84	0	
THAL6.3 6.3000	7.5	7.5	8.82	2.83	0.5	0.05
THAL6.3 6.3000	7.5	7.5	8.82	2.83	0.5	0.05
ING GEN 6.9000	10	10	11.76	5.084	0.5	0.05
GT7				8	0.5	0.05
KCCP GT 15.000	100	104	122	8	0.5	0.05
KCCP ST 11.500	45	61	72	4	0.5	0.05
AES GT 10.500	100	109	122	4	0.5	0.05
AES ST 10.500	45	54	72	4	0.5	0.05
KERAWALA-G 14.500	113	113	133	7.253	0.5	0.05
KERAWALA-G 14.500	113	113	133	7.253	0.5	0.05
KERAWALA-S 14.500	54	54	64	4.469	0.5	0.05
SAPUG-P 11.000	0	72	85	2.5	0.13	0.053
SAPUG-P2 11.000	0	36	42	2.5	0.13	0.053
SAPUG-P2 11.000	0	36	42	2.5	0.13	0.053
KELAN-1 132.00	45	45	52.94	4.5	0.5	0.05
KELAN-1 132.00	45	45	52.94	4.5	0.5	0.05
CHUNNAKAM-3 33.000	24	24	28.24	4.5	0.5	
CO-LNG1 220.00	100	100	126	7.253	0.5	0.05
CO-LNG1 220.00	100	100	126	7.253	0.5	0.05
CO-LNG1 220.00	80	100	126	4.469	0.5	0.05
CO-LNG2 220.00	100	100	126	7.253	0.5	0.05
CO-LNG2 220.00	100	100	126	7.253	0.5	0.05
CO-LNG2 220.00	80	100	126	4.469	0.5	0.05
CO-LNG3 220.00	100	100	126	7.253	0.5	0.05
CO-LNG3 220.00	100	100	126	7.253	0.5	0.05
CO-LNG3 220.00	80	100	126	4.469	0.5	0.05
HAMBA-LNG1 220.00	100	100	126	7.253	0.5	0.05
HAMBA-LNG1 220.00	100	100	126	7.253	0.5	0.05
HAMBA-LNG1 220.00	80	100	126	4.469	0.5	0.05
BIYAG-2 220.00	0	9999	150			
SAMPOOR-COAL220.00	150.0001	270	353	4.376	0.5	0.05
SAMPOOR-COAL220.00	200	270	353	4.376	0.5	0.05
PUTTA_G1 20.000	200.0002	275	353	4.376	0.5	0.05
PUTTA_G2 20.000	200.0002	275	353	4.376	0.5	0.05
PUTTA_G3 20.000	2	275	353	4.376	0.5	0.05
PUTTA_G4 20.000	150.0002	275	353	4.376	0.5	0.05
PUTTA_G5 20.000	275	275	353	4.376	0.5	0.05
GALLE-1 132.00	100	100	117.65	3.2	0.5	
EMBIL-1 132.00	100	100	117.65	3.2	0.5	

HORANA_3 33.000	24	24	28.24	2.5	0.13	0.053
MONARA-3 33.000	24	24	28.24	2.5	0.13	0.053
PALLEK-3 33.000	24	24	28.24	2.5	0.13	0.053
MATARA-3 33.000	20	20	23.53	2.5	0.13	0.053
HABAR-3 33.000	24	24	28.24	2.5	0.13	0.053